NCAT Report 09-05

EVALUATION OF MIXTURE PERFORMANCE AND STRUCTURAL CAPACITY OF PAVEMENTS USING SHELL THIOPAVE®

Phase I: Mix Design, Laboratory Performance Evaluation and Structural Pavement Analysis and Design

By
David Timm
Nam Tran
Adam Taylor
Mary Robbins
Buzz Powell

August 2009

National Center for Asphalt Technology
NCAT
at AUBURN UNIVERSITY

277 Technology Parkway ■ Auburn, AL 36830

EVALUATION OF MIXTURE PERFORMANCE AND STRUCTURAL CAPACITY OF PAVEMENTS UTILIZING SHELL THIOPAVE®

Phase I:
Mix Design, Laboratory Performance Evaluation and Structural Pavement Analysis and Design

By

David Timm
Nam Tran
Adam Taylor
Mary Robbins
Buzz Powell

National Center for Asphalt Technology
Auburn University, Auburn, Alabama

Sponsored by

Shell Oil Products, USA

August 2009

ACKNOWLEDGEMENTS

This project was sponsored by Shell Oil Products, USA. The project team appreciates and thanks Shell Oil Products, USA for their sponsorship of this project.

DISCLAIMER

The contents of this report reflect the views of the authors who are responsible for the facts and accuracy of the data presented herein. The contents do not necessarily reflect the official views or policies of Shell Oil Products, USA or the National Center for Asphalt Technology, or Auburn University. This report does not constitute a standard, specification, or regulation. Comments contained in this paper related to specific testing equipment and materials should not be considered an endorsement of any commercial product or service; no such endorsement is intended or implied.

TABLE OF CONTENTS

1. BACKGROUND

The utilization of sulfur as an extender of asphalt binder properties in hot mix asphalt (HMA) was tried in the 1970s and continued into the early 1980s until the price of sulfur was too high for use in road paving (*1*). In addition, during this period, sulfur-extended asphalt mixtures were produced using hot liquid sulfur that emitted a significant amount of fumes and odors unpleasant to workers. The transportation and supply of hot liquid sulfur was also problematic.

To replace the use of hot liquid sulfur for asphalt mixture production, solid sulfur pellets, known as Sulfur Extended Asphalt Modifier (SEAM) which was recently renamed Shell Thiopave®, were further improved by Shell in the late 1990s (*1*). Thiopave, as shown in Figure 1.1, is both a binder extender and an asphalt mixture modifier. The manufacturer reports that Thiopave can improve the performance of sulfur-extended asphalt mixtures, reduce construction costs and production temperatures, and provide more friendly conditions for sulfur-extended mixture production (*2*).

FIGURE 1.1 Shell Thiopave for Sulfur-Extended Asphalt Mixtures.

This study was planned to evaluate the performance of a Thiopave asphalt mixture and predicted structural capacity of a pavement constructed with Thiopave mix layers. This information is useful for future implementation of this product in perpetual pavement and mechanistic empirical (ME) pavement design methods.

2. OBJECTIVE AND SCOPE

This study was divided into two phases. Phase I included laboratory testing as well as theoretical structural pavement analysis and design. Phase II is a field study at the NCAT Pavement Test Track. A set of objectives was defined below for each phase.

The objectives of Phase I were to:

- Perform Thiopave mix designs using the Superpave mix design method;
- Measure mechanistic and performance properties of the Thiopave asphalt mixture in the laboratory for use in structural pavement analysis and design as well as laboratory performance evaluation; and
- Perform theoretical structural pavement analysis, using mechanistic analysis, and design to determine appropriate structural pavements for the field study in Phase II.

The objectives of Phase II are to:

- Evaluate the mixture performance and structural capacity of the pavement structure designed in Phase I through the field study at the NCAT Pavement Test Track; and
- Incorporate any needed modifications and/or additional information to the findings in Phase I.

Phase I of this study has been completed as documented in this report. At the writing of this report, Phase II has begun.

3. LITERATURE REVIEW

3.1 Development of Sulfur-Extended Mix

The use of sulfur as an asphalt mixture modifying agent (known as SEA, or sulfur-extended asphalt) was originally tried in the 1970s and continued into the 1980s. The added sulfur was used both as a binder extender (replacing a percentage of the asphalt binder) and to modify the properties of the resulting asphalt mixture. This original testing utilized sulfur in a hot liquid phase, which generated a significant amount of fumes that were problematic for construction personnel. In the 1980s, a sharp rise in the price of sulfur made its use uneconomical in highway paving (*3*).

Recent technological improvements in sulfur production, coupled with an increase in sulfur abundance, have led to resurgence in the exploration of the use of sulfur as an asphalt mixture modifier. In the late 1970s, processes were developed that allowed for the handling of sulfur in a solid, dust-free format. However, this technology was not used in conjunction with the original SEA studies (*3*). In the late 1990s, this technology was further developed by the Shell Corporation. This technology was referred to as SEAM (Sulfur Extended Asphalt Modifier), which has recently been renamed to Shell Thiopave. The Thiopave modifier consists of small pellets of sulfur modifier that are added to the asphalt mixture during the mixing process. The Thiopave melts rapidly on contact with the hot mix and is dispersed throughout the asphalt mixture during the mixing process (*1*).

While the Thiopave pellets contain some additives designed to reduce odor and fumes during mixing, temperature control of the mixture and good ventilation practices are still required. Thiopave mixtures are typically produced at a target mixing temperature of 140 ± 5°C. The mixtures must be produced above a temperature of 120°C so that the sulfur pellets will melt and the sulfur will be dispersed throughout the asphalt mixture. Above mixing temperatures of

145°C, the potential for harmful emission generation greatly increases and could be problematic for workers involved in both the mixing and compaction processes (*1*).

3.2 Effects of Thiopave on Asphalt Mixture Performance

In addition to lowering the virgin binder requirement for a given asphalt mixture, the addition of Thiopave can significantly alter the performance properties of the mix. The change in these performance properties is dependent both on (1) the percentage of virgin binder that is substituted with Thiopave; and (2) the amount of time the specimen is allowed to cure prior to performance testing (*1,3*).

The most notable impact of the addition of Thiopave to an asphalt mixture is an increase in the stiffness of the mixture. This behavior has been quantified through laboratory studies. The consensus of literature is that an increase in Thiopave percentage will correspondingly increase the Marshall Stability value of the mixture, as shown in Figure 3.1 (*1,3).* Strickland et al. (*1*) state that this increase in mixture stability has the effect of increasing the high PG grade of the mix binder by between 1 and 3 PG grades. However, for the full mixture stiffening properties of the Thiopave to be realized, it must be tested after an appropriate curing period. Deme and Kennedy (*3*) allowed all of their specimens to cure on a shelf at room temperature for a minimum of 14 days prior to performance testing.

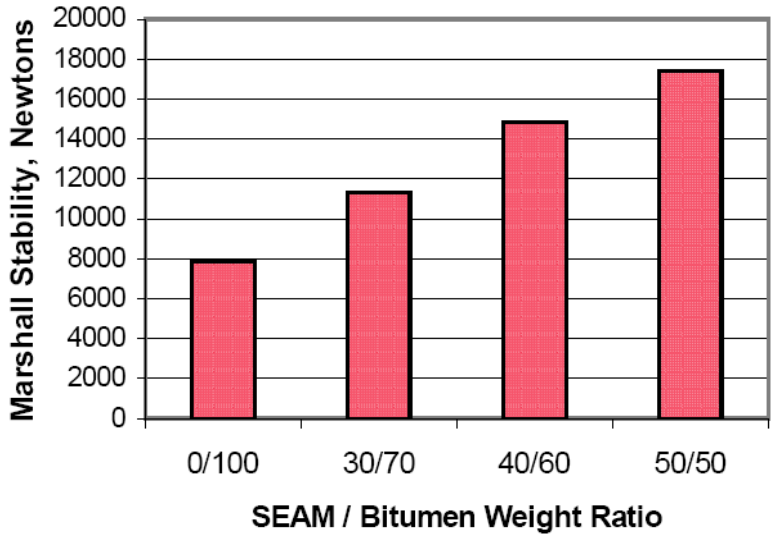

FIGURE 3.1 Effect of Thiopave/Bitumen Weight Ratio on Mixture Marshall Stability.

The increase in stiffness of the Thiopave mixtures is also tangible in laboratory tests that quantify resistance to deformation. Strickland et al. (*1*) reported that the addition of more Thiopave product caused an upward shift of the dynamic modulus master curve when compared to a control mixture. This increase was most notable in the range of testing that involved high temperatures and longer loading times. This increase in stiffness is a positive attribute in the sense that it gives asphalt mixtures higher resistance to permanent deformation. This increased resistance to deformation has been quantified in the lab with APA rutting data. Both Deme and Kennedy (*3*) and Strickland et al. (*1*) report increased rutting resistance of Thiopave mixtures to control mixtures in laboratory testing.

A potential downside of increased mixture stiffness could be higher susceptibility to cracking, notably fatigue cracking and low temperature cracking. Strickland et al. (*1*) reported that the Thiopave mixture showed a 5% reduction in fatigue life when compared with a control mixture, but this reduction was not enough to be detrimental for pavement design purposes. Conversely, Deme and Kennedy (*3*) reported that the Thiopave mixtures actually increased the fatigue life of asphalt mixtures when the mixtures were tested at constant stress. The consensus of the laboratory studies performing thermal stress-restrained specimen testing (TSRST) was that the addition of the Thiopave material did not affect the temperature at which low temperature cracking occurred (*1,3,4)*.

The final mixture property that could potentially be impacted by the addition of Thiopave is moisture susceptibility. Strickland et al. (*1*) reported that the addition of Thiopave could cause up to a 10% reduction in the tensile strength ratio (TSR) of the Thiopave mixtures in comparison with a control mixture. This trend was also witnessed in Hamburg Wheel-Tracking (Hamburg) testing. However, the authors believed the addition of an anti-stripping agent could help counter this effect.

3.3 Summary

Literature has shown that the addition of Thiopave materials can have a positive impact on laboratory mixture performance. The addition of Thiopave has been shown to significantly increase the Marshall Stability and deformation resistance of asphalt mixtures in the laboratory after a two week curing period. The Thiopave material also had little negative impact in areas that were thought to be problematic, such as fatigue cracking resistance, low temperature cracking resistance, and moisture susceptibility.

4. LABORATORY TESTING PLAN AND METHODOLOGY

This section describes testing conducted in the NCAT laboratory to assess the laboratory performance of asphalt mixtures with varying percentages of Thiopave to that of a control asphalt mixture (without Thiopave) that has been used at the NCAT Pavement Test Track.

4.1 Testing Plan

A wide array of testing was utilized for this project to quantify the laboratory behavior of the asphalt mixtures with varying amounts of Thiopave additive versus the properties of a control asphalt mixture. The control mixture was based on a mix design used in construction of layers 3 and 4 of section S11 during the 2006 research cycle at the NCAT Pavement Test Track. The testing plan was designed so that there would be multiple tests, if possible, used to assess the performance characteristics of the sulfur-extended asphalt mixtures. The relevant performance characteristics, along with the relevant testing procedures, are listed below. Table 4.1 shows the complete testing plan for this project.

TABLE 4.1 Laboratory Testing Plan for Phase I

%Thiopave	Design Air Voids	Test	Number of Specimens
0% (Control mix)	Mix Design	G_{mb} (3 binder contents)	6
		G_{mm} (3 binder contents)	6
	4%	TSR	6
		E* at 1 day (@ 21C and 0.01 Hz to 10 Hz)	2
		E* after 14 days (@ 21C and 0.01 Hz to 10 Hz)	2
		E* using the same samples tested at 14 days (10, 5, 1, 0.5, 0.1, 0.01 Hz at each of 4, 20, 46C)	2
		F_n using the same E* samples (58C, 70 psi for deviator and 10 psi for confinement)	2
		APA after 14 days (@ 64C)	6
		BBF tested after 14 days (@ 20C and three strain levels of 200, 400 and 600 microstrain)	6
		Hamburg (wet test, @ 50C)	2
		TSRST	3
Each of 30% and 40%	Mix Design	G_{mb} (4 binder contents)	8
		G_{mm} (4 binder contents)	8
	4%	TSR	6
	3.5%	E* at 1 day (@ 21C and 0.01 Hz to 10 Hz)	2
		E* after 14 days (@ 21C and 0.01 Hz to 10 Hz)	2
		E* using the same samples tested at 14 days (10, 5, 1, 0.5, 0.1, 0.01 Hz at each of 4, 20, 46C)	2
		F_n using the same E* samples (58C, 70 psi for deviator and 10 psi for confinement)	2
		APA after 14 days (@ 64C)	6
		BBF tested after 14 days (@ 20C and three strain levels of 200, 400 and 600 microstrain)	6
		Hamburg (wet test, @ 50C)	2
		TSRST	3
	2%	E* at 1 day (@ 21C and 0.01 Hz to 10 Hz)	2
		E* after 14 days (@ 21C and 0.01 Hz to 10 Hz)	2
		E* using the same samples tested at 14 days (10, 5, 1, 0.5, 0.1, 0.01 Hz at each of 4, 20, 46C)	2
		F_n using the same E* samples (58C, 70 psi for deviator and 10 psi for confinement)	2
		BBF tested after 14 days (@ 20C and three strain levels of 200, 400 and 600 microstrain)	6
		APA after 14 days (@ 64C)	6
		Hamburg (wet test, @ 50C)	2
		TSRST	3

- Moisture susceptibility
    - Tensile Strength Ratio (TSR) Testing (ALDOT 361-88)

  - Tensile Strength Ratio (TSR) Testing (AASHTO T283-07)
  - Hamburg Wheel-Track (Hamburg) Testing (AASHTO T 324-04)
- Determination of laboratory fatigue limits
  - Bending Beam Fatigue (BBF) Testing (ASTM D 7460-08)
- Rutting and deformation susceptibility
  - Asphalt Pavement Analyzer (APA) Testing (AASHTO TP 63-07)
  - Hamburg Wheel-Track Testing (AASHTO T 324-04)
  - Flow Number (F_n) Testing (NCHRP 9-29 and 9-30A)
- Low Temperature Cracking Susceptibility
  - Thermal Stress-Restrained Specimen Tensile Strength (AASHTO TP 10-00)
- Mixture Stiffness
  - Dynamic Modulus (E*) Testing (AASHTO TP 62-07)

A total of five asphalt mixtures were tested during this phase of the study. Each of these mixtures had the same gradation and base binder type (details of which will be discussed in Section 4.2). The differences in these mixtures were in both the percentage of Thiopave utilized as a replacement of the virgin binder and in the design air void content. The control mixture contained 0% Thiopave and was compacted to 4% design air voids. Two of the mixtures contained 30% Thiopave as a replacement of the virgin binder. One of these mixes was compacted to a design air void content of 3.5%. The other was designed as a fatigue-resistant rich bottom layer with a design air void content of 2%. The final two mixes contained 40% Thiopave and had design air void levels of 3.5% and 2%, respectively. In this report, the mixtures with a design air void level of 2% are referred to as 'rich bottom' mixtures. The mixtures with 4% or 3.5% design air voids are referred to as 'base' layer mixtures. The change in base layer air void content from 4% for the control mix to 3.5% for the Thiopave mixes was done in order to offset the increased brittleness of the stiffer Thiopave mixtures as well as to provide additional moisture and fatigue resistance in these mixes. The tests listed above were conducted on each of the five mixtures, with one exception--moisture susceptibility testing via the determination of a TSR was not performed on the rich bottom mixes. Reasons are given later with a discussion of the test results.

4.2 Mix Design

For this project, a mix design was conducted for each of the control and sulfur-extended asphalt mixtures with 30 and 40 percent of Thiopave. These mix designs were conducted in accordance with AASHTO M323-07, *Standard Specification for Superpave Volumetric Mix Design,* and AASHTO R35-04, *Standard Practice for Superpave Volumetric Design for Hot-Mix Asphalt.*

For the control mix, the optimum binder content was determined corresponding to 4 percent air voids. For each Thiopave mix, the optimum content of combined Thiopave and asphalt binder was determined according to Equation 4.1, to account for the presence of Thiopave materials in the mixture. For each Thiopave percentage level, two optimum contents of combined Thiopave and asphalt binder were determined for mixtures that would be used in the base and rich bottom layers. The optimum Thiopave and asphalt content for the base layer mix was determined at 3.5 percent air voids and the optimum Thiopave and asphalt content for the rich bottom mix was

determined at 2 percent air voids. The mix designs were carried out using a spreadsheet provided by Shell, being modified for use with this project.

$$Thiopave + Binder\% = A * \frac{100R}{[100R - P_s(R - G_{binder})]} \quad (4.1)$$

where:

A = weight percentage of binder in conventional mix design
R = Thiopave to binder substitution ratio
R = $G_{Thiopave}/G_{Binder}$ (R = 1.90 for this study)
P_s = weight percentage of Thiopave in Thiopave-blended binder
G = specific gravity of the unmodified binder

As mentioned earlier, the mix design with Thiopave was based on the mix design used for the bottom lift of section S11 (S11-4). This was a 19.0 mm mix consisting of four aggregate stockpiles. The coarse aggregate used in the mix designs was a limestone obtained from stockpiles at Martin-Marietta Quarry in Auburn, Alabama. Two different stockpiles (#57 and #78) of this limestone were used. The fine granite (M10) was obtained from Vulcan Materials Barin Quarry in Columbus, Georgia. Finally, the natural sand used was from Martin Marietta Sand and Gravel in Shorter, Alabama. The percentages of each stockpile were generated from the original laboratory mix design used at the NCAT Pavement Test Track. The gradations of individual stockpiles, the gradation of the total blend, and the percentages of each stockpile used in the final blend are shown in Table 4.2. Figure 4.1 shows a plot of the design gradation curve. The aggregate specific gravities, absorptions, and consensus properties (crushed face count, uncompacted voids in fine aggregate, sand equivalency, and flat and elongated particle percentages) for each of the four stockpiles are shown in Table 4.3. The weighted average of each of the four consensus properties fell within the specification for an acceptable mix design set forth in AASHTO M323.

TABLE 4.2 Aggregate Gradations

Sieve Size (mm)	Sieve Size (Inches)	Percent Passing				
		EAP Limestone #78	EAP Limestone #57	Columbus Granite M10	Shorter Natural Sand	Total Blend
50.0	2.0"	100.0	100.0	100.0	100.0	100.0
37.5	1.5"	100.0	100.0	100.0	100.0	100.0
25.0	1.0"	100.0	98.0	100.0	100.0	99.6
19.0	3/4"	100.0	63.0	100.0	100.0	92.6
12.5	1/2"	92.0	23.0	100.0	100.0	82.1
9.5	3/8"	61.0	15.0	100.0	100.0	70.9
4.75	# 4	10.0	3.0	99.0	99.2	52.2
2.36	# 8	4.0	2.0	86.0	91.6	44.8
1.18	# 16	3.0	1.0	65.0	75.2	34.9
0.600	# 30	2.0	1.0	47.0	46.1	23.7
0.300	# 50	1.0	1.0	31.0	11.6	12.0
0.150	#100	1.0	1.0	19.0	3.6	6.9
0.075	#200	0.4	1.0	10.6	2.2	3.9
Cold Feed		**31%**	**20%**	**30%**	**19%**	

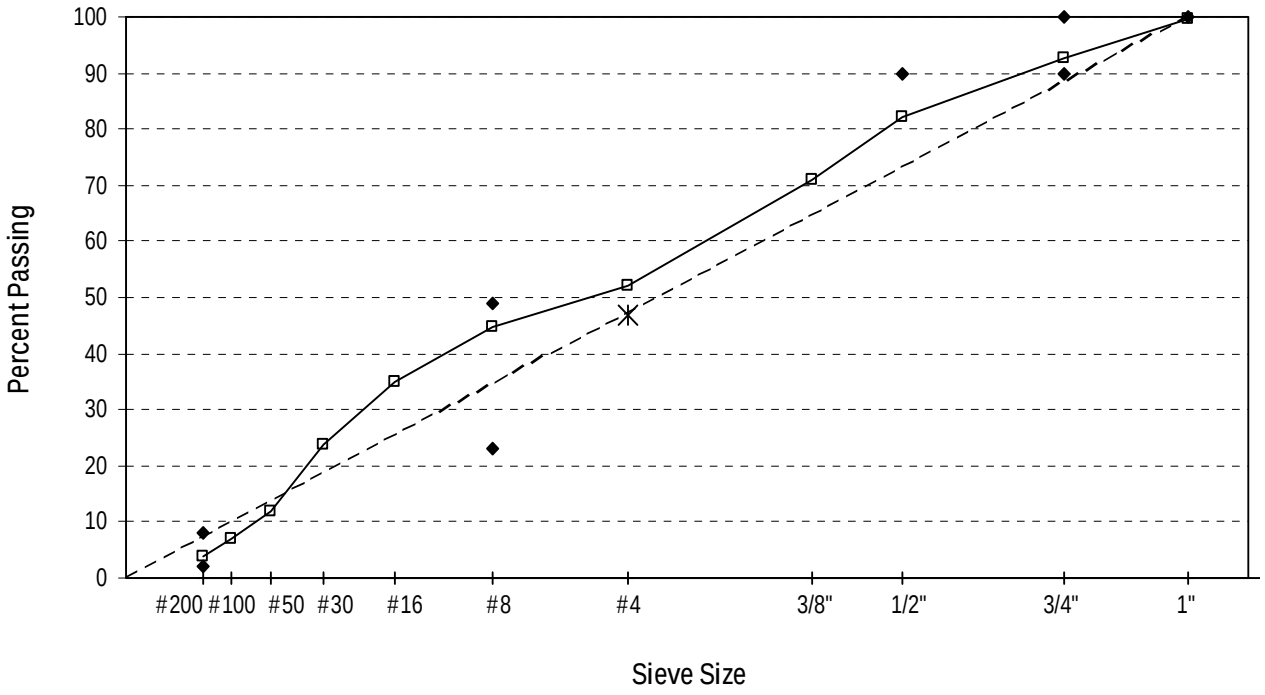

FIGURE 4.1 Shell Aggregate Gradation Curves.

TABLE 4.3 Aggregate Properties

Consensus Property	EAP Limestone #78	EAP Limestone #57	Columbus Granite M10	Shorter Natural Sand	Total Blend (Weighted Average)
Bulk Specific Gravity (Gsb)	2.819	2.833	2.707	2.614	2.746
Absorption (%)	0.5	0.4	0.3	0.2	0.3
Crushed Face Percentage*	100/100*	100/100*	N/A	N/A	100/100
FAA (Uncompacted Void Content)	N/A	N/A	50.2	45.8	48.4
Sand Equivalency Value	N/A	N/A	72	81	75.2
Flat and Elongated Particle Percentage**	<1	<1	N/A	N/A	<1

* - Blasted and Crushed Limestone Material
** - Weighted Average Based on Gradation (5:1)

A PG grade 67-22 binder with 0.5 percent (by weight of the binder) AD-here 1500 anti-stripping agent was used for all the mixes evaluated in this study. For the Thiopave mixes, a compaction additive was also added at 1.52 percent (by the binder weight), as shown in Figure 4.2. This compaction additive (CA), consisting of fine wax crystals, aids in the compaction of Thiopave mixes to the target air voids at the lower compaction temperatures that are necessary to control sulfur emissions.

To mix the Thiopave samples in the laboratory, the Thiopave additive was added to the hot aggregate and asphalt binder immediately after the start of the mixing process. The mixing process using the Thiopave materials, as shown in Figure 4.3, was conducted in a well-ventilated mixing room. All the samples were short-term aged in the oven at a temperature of 140^{o}C for two hours before compaction. The design pills were compacted to an N_{des} level of 60 gyrations and a target height of 115 ±5 mm. The control mixtures for this project were short-term aged for two hours at 157^{o}C to achieve a compaction temperature between 149^{o}C and 152^{o}C.

The loose mixes and compacted specimens were cooled down in the laboratory. Then, the bulk specific gravity of the compacted specimens was determined according to AASHTO T166, and the maximum theoretical specific gravity of the loose mixtures was determined in accordance with AASHTO T209. The specific gravity information was used to determine the volumetric properties of the mixes that are presented later in this report.

FIGURE 4.2 Compaction Aid Used for Thiopave Mixtures.

FIGURE 4.3 Mixing of Thiopave Mixture.

4.3 Mechanistic and Performance Testing

4.3.1 Moisture Susceptibility

Moisture susceptibility testing was performed according to two different methods (ALDOT 361 and AASHTO T283). For each of the following mixtures, two sets of three specimens were used to determine the tensile strength ratio (TSR): control mix at 4 percent design air voids, 30 percent Thiopave with 4 percent design air voids, and 40 percent Thiopave with 4 percent design air voids. Testing by the ALDOT method was performed for two sets of specimens with

different curing times (less than 14 days and greater than 14 days) at room temperature. AASHTO TSR testing was performed on specimens that had been allowed to cure at room temperature for 14 days.

For the ALDOT method, all of the specimens were compacted to a height of 95 mm and an air voids level of 7 ± 1 percent. Within each set of specimens, three specimens were tested with no moisture conditioning while the other three were conditioned. The conditioned specimens were vacuum saturated to the point at which 55 to 80 percent of the internal voids were filled with water. These specimens were then conditioned in 60 ± 1°C water bath for 24 ±1 hours. All samples, conditioned and unconditioned, were brought to room temperature in a 25 ± 0.5°C water bath to equilibrate the sample temperature just prior to testing. The indirect tensile strength was then calculated using Equation 4.2 based on the failure loading and measured specimen dimensions. The tensile strength ratio was then calculated for each set by dividing the average tensile strength of the conditioned specimens by the average tensile strength of the unconditioned specimens. ALDOT 361 recommends a TSR value of 0.8 and above for moisture resistant mixes. The Pine Instruments Marshall Stability Press used for determining indirect tensile strength is shown in Figure 4.4.

$$S_t = \frac{2 * P}{3.14 * D * t} \tag{4.2}$$

where:

S_t = tensile strength (psi)
P = average load (lb)
D = specimen diameter (in.)
t = specimen thickness (in.)

FIGURE 4.4 Pine Instruments Marshall Stability Press.

For the AASHTO TSR method, the sample preparation was the same as the ALDOT method except that the specimens had to adhere to a tigher air void control (± 0.5 percent air voids). The specimens were vacuum saturated so that 70 to 80 percent of the internal voids were filled with water. These specimens were then wrapped in plastic wrap and placed in a leak-proof plastic bag with 10 mL of water prior to being placed in the freezer for a minimum of 16 hours. After the freezing process, the conditioned samples were placed in a 60 ± 1°C water bath for 24 ±1 hours to thaw. All samples, conditioned and unconditioned, were brought to room temperature in a 25 ± 0.5°C water bath to equilibrate the sample temperature for two hours just prior to testing. Calculation of the failure load, splitting tensile strength, and TSR value is done by the same procedure as the ALDOT method.

4.3.2 Dynamic Modulus

Dynamic modulus testing was conducted in accordance with AASHTO TP62. This testing was performed using an IPC Global Asphalt Mixture Performance Tester (AMPT), shown in Figure 4.5. Dynamic modulus testing was performed for each of the five mix designs listed in Section 4.1. A Pine Instruments gyratory compactor was used to compact specimens to 150 mm in diameter and 170 mm in height. These samples were then cored using a 100 mm core drill and trimmed to 150 mm in height. The air voids for these cut specimens were 7 ± 0.5 percent.

FIGURE 4.5 IPC Global Asphalt Mixture Performance Tester.

For each mix design, a set of two specimens was tested at two different curing times to assess the effect of aging on the mixtures. The first set of specimens was tested with 1 day between compaction and testing to quantify the strength parameters of the mix post-compaction. The second set of specimens was tested after 14 days of room-temperature curing had passed to assess the effects of curing time on the modulus of the different mixtures. For the evaluation of

the effects of aging, the specimens were tested at a chamber temperature of 21.1°C and the following frequencies: 25, 10, 5, 1, 0.5, 0.1, and 0.01 Hz.

To provide the necessary information for M-E pavement analyses, the five sets of dynamic modulus test specimens used for "14-day" testing (referring to the curing time), were re-tested using three temperatures (4.4, 21.1, and 46.1°C) and six frequencies (10, 5, 1, 0.5, 0.1, and 0.01 Hz). This testing produced a data set for generating master curves for the control and Thiopave mixtures using the procedure outlined in NCHRP Report 614 (*5*).

To ensure quality of the measured data, the coefficient of variation (COV) between measured moduli when tested at the same temperatures and frequencies was required to be less than 15 percent. If a high level of variation was determined between specimens, the specimens were re-tested. Equations 4.3 and 4.4 were used to generate the master curve for each mix design. Equation 4.3 is the master curve equation, while Equation 4.4 shows how the reduced frequency is determined. The regression coefficients and shift factors, which are used to shift the modulus data at various test temperatures to the reference temperature of 21.1°C, are determined simultaneously during the optimization process using the Solver function in an Excel® spreadsheet.

$$\log|E^*| = \delta + \frac{\alpha}{1 + e^{\beta + \gamma \log f_r}} \tag{4.3}$$

$$\log f_r = \log f + \log a(T) \tag{4.4}$$

where:

- $|E^*|$ = dynamic modulus, psi
- f = loading frequency at the test temperature, Hz
- f_r = reduced frequency at the reference temperature, Hz
- $\alpha, \delta, \beta, \gamma$ = regression coefficients
- $a(T)$ = temperature shift factor

4.3.3 Flow Number

The determination of the F_n for the mixtures was performed using the AMPT. Flow number testing was performed using the specimens that were tested for E* for each of the five mix designs listed in Section 4.1. Fn tests were conducted at a temperature of 58°C. The specimens were tested at a deviator stress of 70 psi and a confining pressure of 10 psi, and the tests were terminated when the samples reached 10 percent axial strain. For the determination of tertiary flow, two model forms were utilized. The first model form is the classical power model in Equation 4.5. The second model form was the Francken model in Equation 4.6 (*6*). The non-linear regression analysis used to fit both models to the test data was performed within the testing software (Universal Testing Systems (UTS) SPT Flow Software – Version 1.37).

$$\varepsilon_p(N) = aN^b \tag{4.5}$$

$$\varepsilon_p(N) = aN^b + c(e^{dN} - 1) \quad (4.6)$$

where:

$\varepsilon_p(N)$ = permanent strain at 'N' cycles
N = number of cycles
a,b,c,d = regression coefficients

4.3.4 Asphalt Pavement Analyzer

The rutting susceptibility of all five mix designs (listed in Section 4.1) was evaluated using the APA, as shown in Figure 4.6. Testing was performed in accordance with AASHTO TP 63. The samples used for this testing were prepared to a height of 75 mm and an air void level of 7 ± 0.5 percent. Six replicates were tested for each mix. All specimens were cured at room temperature 14 days prior to testing to allow for development of the time-dependent stiffness properties of the Thiopave-asphalt mixtures. The samples were tested at a temperature of 64°C (the 98 percent reliability temperature for the high PG grade of the binder). The samples were loaded by a steel wheel (loaded to 100 lbs) resting atop a pneumatic hose pressurized to 100 psi for 8,000 cycles. Manual depth readings were taken at two locations on each sample before and after the loading was applied to determine the specimen rut depth.

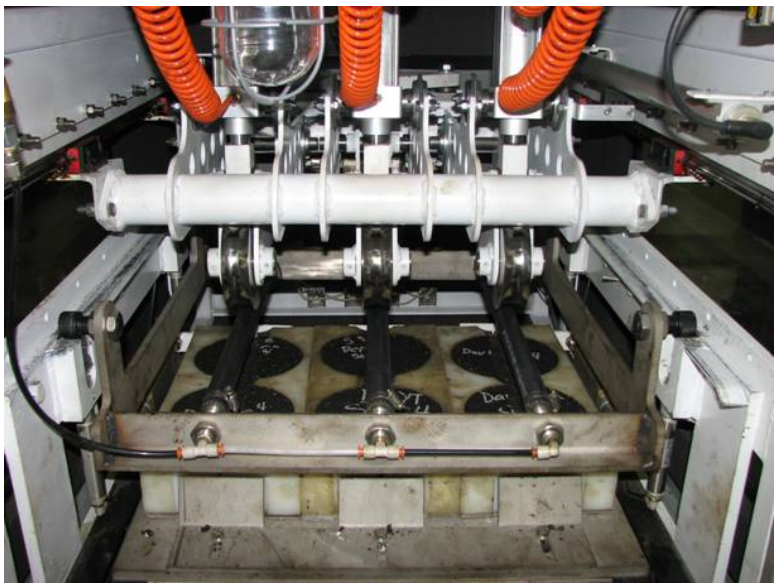

FIGURE 4.6 Asphalt Pavement Analyzer.

4.3.5 Hamburg Wheel Tracking Device

Hamburg wheel-track testing, shown in Figure 4.7, was performed to determine both the rutting and stripping susceptibility of the five mixture listed in Section 4.1. Testing was performed in accordance with AASHTO T 324. For each mix, a minimum of two replicates were tested. The specimens were originally compacted to a diameter of 150 mm and a height of 115 mm. These

specimens were then trimmed so that two specimens, with a height between 38 mm and 50 mm, were cut from the top and bottom of each gyratory-compacted specimen. The air voids on these cut specimens were 7 ± 2%, as specified in AASHTO T 324. All specimens were cured at room temperature for 14 days prior to testing.

The samples were tested under a 158 ± 1 lbs wheel load for 10,000 cycles (20,000 passes) while submerged in a water bath which was maintained at a temperature of 50°C. While being tested, rut depths were measured by an LVDT which recorded the relative vertical position of the load wheel after each load cycle. After testing, these data were used to determine the point at which stripping occurred in the mixture under loading and the relative rutting susceptibility of those mixtures. Figure 4.8 illustrates typical data output from the Hamburg device. These data show the progression of rut depth with number of cycles. From this curve two tangents are evident, the steady-state rutting portion of the curve and the portion of the curve after stripping. The intersection of these two curve tangents defines the stripping inflection point of the mixture. The slope of the steady-state portion of the curve is also quantified and multiplied by the number of cycles per hour (2520) to determine the rutting rate per hour. Comparing the stripping inflection points and rutting rates of the five different mixtures gives a measure of the relative moisture and deformation susceptibility of these mixtures.

FIGURE 4.7 Hamburg Wheel-Tracking Device.

4.3.6 Bending Beam Fatigue

Bending beam fatigue testing was performed in accordance with ASTM D7460 to determine the fatigue limits of the five asphalt mixtures listed in Section 4.1. Six beam specimens were tested for each mix. Within each set of six, two beams each were tested at 200 microstrain, 400 microstrain, and 600 microstrain. The specimens were originally compacted in a kneading beam compactor, shown in Figure 4.9, then were trimmed to the dimensions of 380 ± 6 mm in length,

63 ± 2 mm in width, and 50 ± 2 mm in height. Additionally, the orientation in which the beams were compacted (top and bottom) was marked and maintained for the fatigue testing as well.

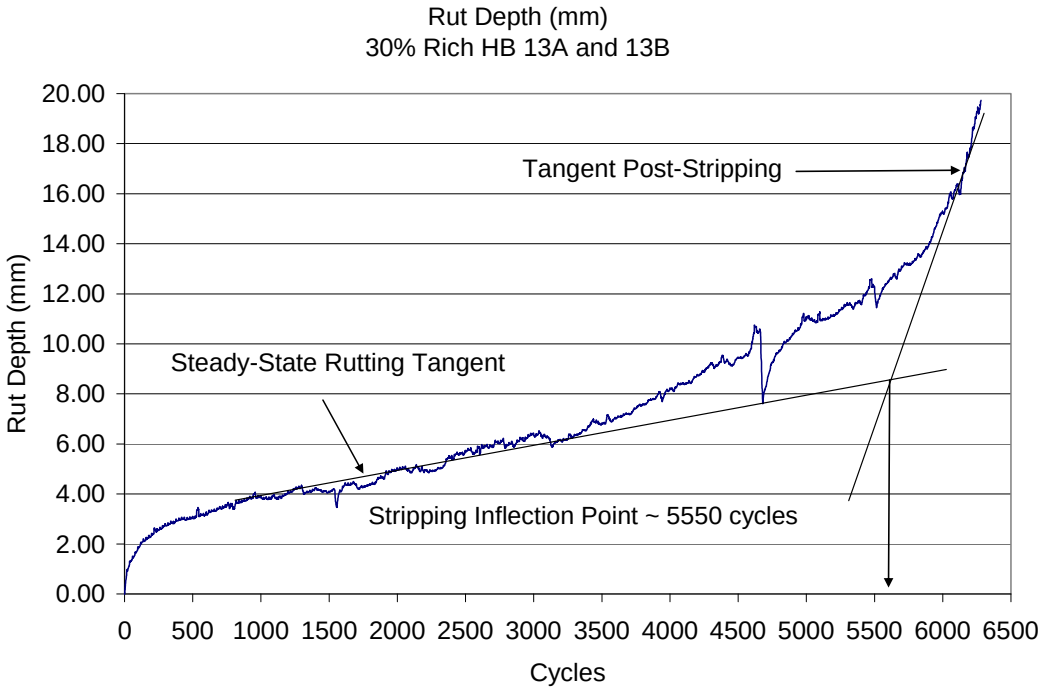

FIGURE 4.8 Example of Hamburg Raw Data Output.

FIGURE 4.9 Kneading Beam Compactor.

The beam fatigue apparatus, shown in Figure 4.10, applies haversine loading at a frequency of 10 Hz. During each cycle, a constant level of strain is applied to the bottom of the specimen. The loading device consists of 4-point loading and reaction positions which allow for the application of the target strain to the bottom of the test specimen. Testing was performed at 20 ± 0.5°C. The data acquisition software was used to record load cycles, applied loads, beam deflections. The software also computed and recorded the maximum tensile stress, maximum tensile strain, phase angle, beam stiffness, dissipated energy, and cumulative dissipated energy at user specified load cycle intervals.

FIGURE 4.10 IPC Global Beam Fatigue Testing Apparatus.

At the beginning of each test, the initial beam stiffness was calculated by the data acquisition software after 50 conditioning cycles. ASTM D 7460 recommends the test be terminated when the beam stiffness is reduced to 40 percent of the initial stiffness. As a factor of safety and to ensure a complete data set, the beams for this project were allowed to run until the beam stiffness was reduced to 30 percent of the initial stiffness. Based on the collected data, the value of Normalized Modulus × Cycles was calculated using Equation 4.7 to help interpret the point of failure. According to ASTM D 7460, the failure point of the beam occurs at the maximum point on a plot of Normalized Modulus × Cycles versus number of testing cycles. An example of this type of plot is shown in Figure 4.11. This also corresponds to a sudden reduction in stiffness of the specimen. Given the cycles to failure for three different strain levels, the fatigue limit was then calculated for each mix design.

$$NM = \frac{S_i x N_i}{S_o x N_o} \tag{4.7}$$

where:

NM = Normalized Modulus × Cycles
S_i = flexural beam stiffness at cycle i
N_i = cycle i

S_o = initial flexural beam stiffness (estimated at 50 cycles)
N_o = actual cycle number where initial flexural beam stiffness is estimated

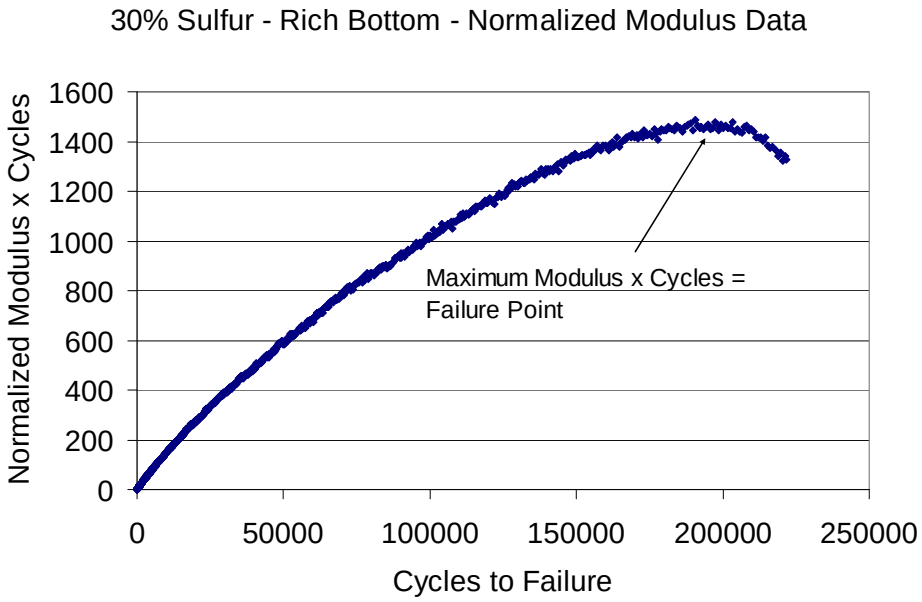

FIGURE 4.11 Sample Plot of Normalized Modulus × Cycles versus Number of Cycles.

Using a proposed procedure developed under NCHRP 9-38 (*7*), the endurance limit for each of the five mixes was estimated using Equation 4.8 based on a 95 percent lower prediction limit of a linear relationship between the log-log transformation of the strain levels (200, 400, and 600 microstrain) and cycles to failure. All the calculations were conducted using a spreadsheet developed under NCHRP 9-38.

$$\text{Endurance Limit} = \hat{y}_0 - t_\alpha s\sqrt{1+\frac{1}{n}+\frac{(x_0-\bar{x})^2}{S_{xx}}} \tag{4.8}$$

where:

$\hat{y}_o$ = log of the predicted strain level (microstrain)
t_α = value of *t* distribution for n-2 degrees of freedom = 2.131847 for n = 6 with α = 0.05
s = standard error from the regression analysis
n = number of samples = 6
S_{xx} = $\sum_{i=1}^{n}(x_i-\bar{x})^2$ (Note: log of fatigue lives)
x_o = log (50,000,000) = 7.69897
$\bar{x}$ = log of average of the fatigue life results

4.3.7 Thermal Stress Restrained Specimen Test

The TSRST testing, shown in Figure 4.12, was conducted at the Western Regional Superpave Center at the University of Nevada at Reno. The testing was conducted in accordance with AASHTO TP10. The test specimens were prepared in the NCAT laboratory. For this testing, five beams for each of the five mix designs listed in Section 4.1 were compacted. The specimens were compacted to 7 ± 1 percent air voids and were trimmed to be 10 inches in length and 2 inches square in cross-section. The specimens were compacted using the same kneading beam compactor used for the compaction of the bending beam fatigue test specimens. Only three beams from each mix design were tested at UNR, the extra beams were compacted in the event some of the specimens were damaged during shipping.

FIGURE 4.12 Thermal Stress Restrained Specimen Test.

5. LABORATORY TEST RESULTS AND ANALYSIS

This section details the results of the laboratory testing conducted for this project. The results of the mix design process show how the optimum binder contents used for this project were obtained. Additionally, this section includes the results of the mechanistic and performance testing on both the control and Thiopave modified mixes. These test results show how the Thiopave mixes performed relative to the control mix in terms of moisture susceptibility, fatigue resistance, rutting and deformation resistance, resistance to low temperature cracking, and overall mixture stiffness.

5.1 Mix Design

Mix designs were conducted for this project using three different percentages of Thiopave for replacing a part of the asphalt binder—without Thiopave, 30 percent Thiopave, and 40 percent

Thiopave. Details regarding the methodology and materials used for this process were presented in Section 4.2. A summary of test results for the mix designs is shown in Appendix A.

Figures 5.1, 5.2, and 5.3 show the air voids versus binder content plots for the control (without Thiopave), 30 percent Thiopave, and 40 percent Thiopave mix designs, respectively. For the control mix, the design binder content was obtained at 4 percent air voids. For the 30 percent and 40 percent Thiopave mixes, an optimum binder content was determined for both a "base" and a "rich bottom" mix. The binder content for a "base" mix was determined at 3.5 percent air voids while the binder content for a "rich bottom" mix was determined at 2 percent air voids. For the Thiopave mixes, the optimum binder content was determined as the binder content of combined Thiopave and asphalt binder (defined in Section 4.2).

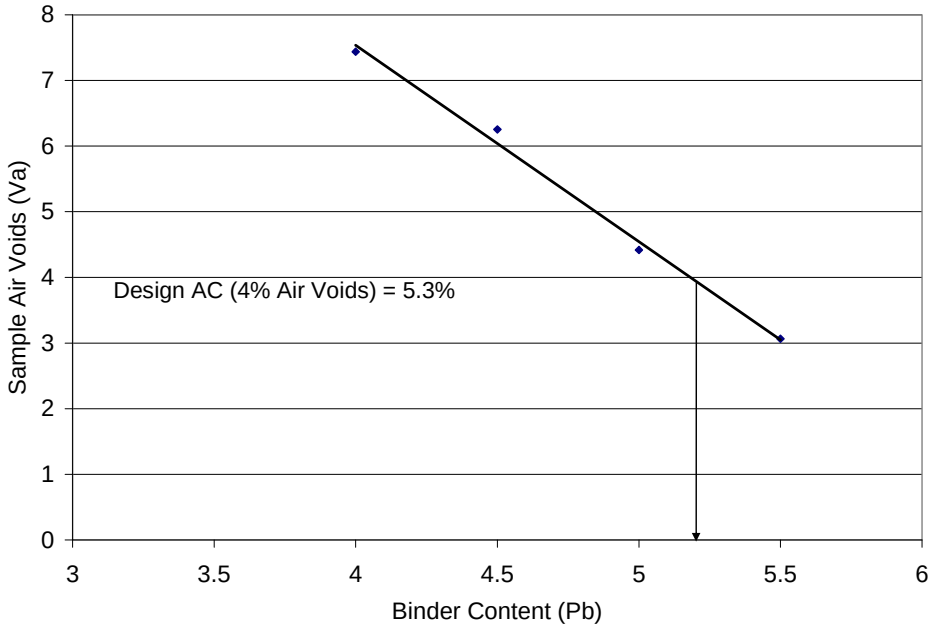

FIGURE 5.1 Optimum Binder Content for Control Mix.

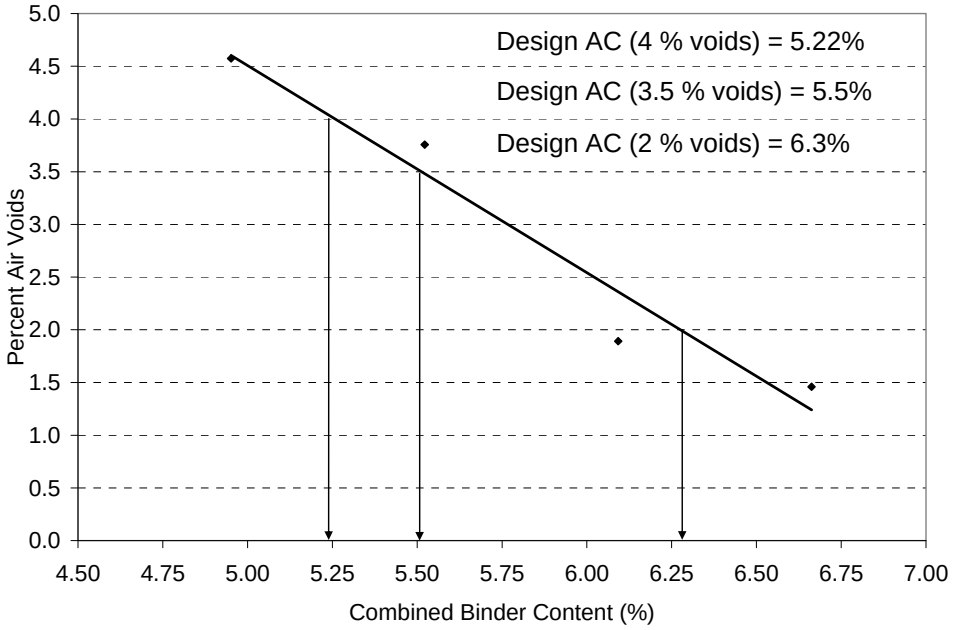

FIGURE 5.2 Optimum Binder Contents for 30 Percent Thiopave Mixes.

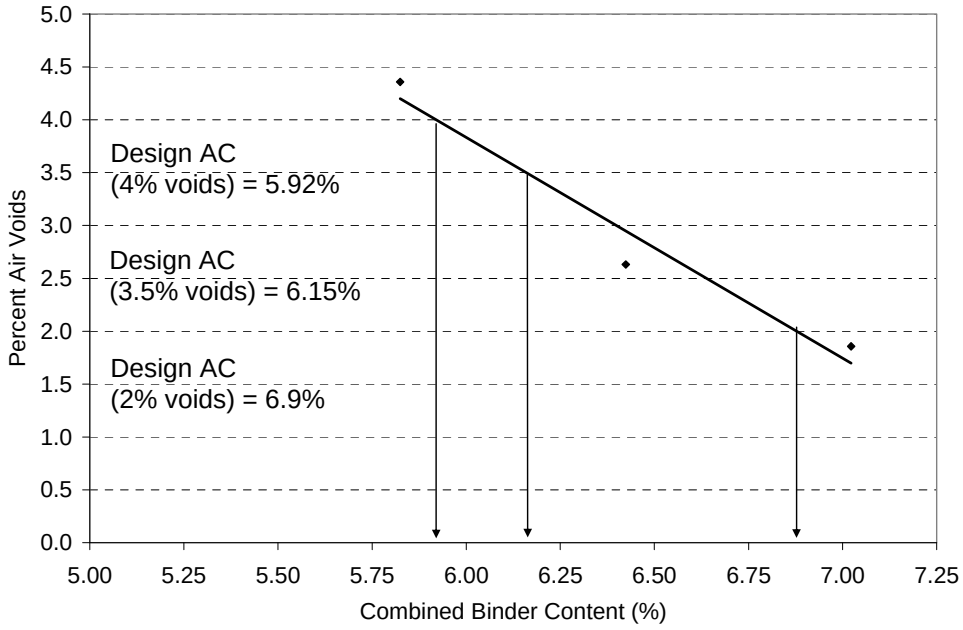

FIGURE 5.3 Optimum Binder Contents for 40 Percent Thiopave Mixes.

A summary of the volumetric properties is given in Table 5.1. The volumetric properties were calculated using the modified design spreadsheet provided by Shell. According to AASHTO M323, the minimum VMA (Voids in Mineral Aggregate) requirement for a 19mm NMAS mix is 13.0. However, the specification states that mixes with VMA higher than 2 percent above the minimum value may be prone to flushing and rutting. It can be seen from Table 5.1 that the only

mixture with a higher VMA is the control mixture. The AASHTO M323 VFA (Voids Filled with Asphalt) requirement for a 19mm NMAS mix with a design traffic level of higher than 3 million ESAL is between 65 and 75 percent. The only mixes that strictly adhere to this requirement are the control mix and the 30 percent Thiopave base layer mix. The 40 percent Thiopave base layer mix has a VFA that is less than 1 percent above the specified upper limit. The high VFA of the rich bottom mixes was expected due to the low design air void levels. Each of the five mix designs fell within the AASHTO M323 required range for dust proportion (0.6-1.2).

TABLE 5.1 Mix Design Optimum Binder Contents

Percent Thiopave by Binder Weight	Design Air Voids (%)	Content of Thiopave + Bitumen (%)	Equivalent Binder (%)	VMA	VFA	Dust Proportion
0	4.0	N/A	5.30	15.3	74.2	0.82
30	3.5	5.50	4.78	14.0	74.5	0.80
30	2.0	6.30	5.48	13.9	86.0	0.69
40	3.5	6.15	5.07	14.5	75.9	0.71
40	2.0	6.90	5.70	14.5	86.5	0.62

5.2 Mechanistic and Performance Testing

5.2.1 Moisture Susceptibility

5.2.1.1 Moisture Susceptibility with Less Than 14 Days of Curing

Initially, moisture susceptibility testing was performed on three different mix designs for this project (control mix, 30 percent Thiopave mix with 4 percent design air voids, and 40 percent Thiopave mix with 4 percent design air voids). This was done with the belief that the strength gain with curing time would be the same for both the conditioned and unconditioned specimens, thus having no effect on the tensile strength ratio value (TSR). Testing was performed in accordance with ALDOT 361-88 and was described in detail in Section 4.3.1. A detailed summary of the TSR testing results is presented in Table B.1 of Appendix B. Both the saturation and air void requirements specified in ALDOT 361 were met for each specimen tested.

Table 5.2 gives a summary of results from the TSR testing on the base layer mixes. Table 4 shows that the TSR values for each of the three mix designs were very high, with 0.99 being the lowest value exhibited by the control mix. The TSR values for the sulfur-modified materials were all greater than 1.0, with the TSR value increasing with an increasing percentage of Thiopave being used as virgin binder replacement. Table 5.2 also shows the average splitting tensile strength of the specimen subsets. The average splitting tensile strength was lower when sulfur materials were added. The average tensile strength of control mixes was on the order of 130 psi, while the average tensile strength of sulfur mixes ranged between 90 and 105 psi. It should be noted that the increase in the splitting tensile strength after conditioning could be a consequence of testing the sulfur-modified mixtures prior to allowing them to cure for 14 days.

Hence, there could be a curing effect of the specimens in the hot water bath that has a greater impact than the conditioning procedure. Therefore, it was deemed prudent to test these specimens for moisture susceptibility after allowing all the specimens to cure at room temperature for 14 days. If there was a potential curing effect of the conditioned specimens in the hot water bath, this effect would be minimized by testing specimens that had already been allowed the full 14 days of curing and achieved most of their time-dependent strength gain.

TABLE 5.2 Summary of TSR Testing for Base Layer Mixes (ALDOT Method – Less than 14 Days of Curing)

Mix ID	Treatment	Air Voids (%)	Saturation (%)	Splitting Strength (psi)	TSR
Control	Conditioned	6.7	64.6	132.0	0.99
	Unconditioned	6.9	N/A	133.0	
30% Thiopave	Conditioned	7.0	62.3	98.4	1.04
	Unconditioned	7.0	N/A	94.6	
40% Thiopave	Conditioned	6.8	61.4	104.6	1.16
	Unconditioned	6.9	N/A	90.4	

Figure 5.4 shows some photographs of TSR specimens that have been broken for closer inspection of the mix. This was done to observe any stripping or moisture damage in the conditioned specimen in reference to the unconditioned specimens. Figure 5.4 shows that there was no visible moisture damage or stripping in any of the specimens, regardless of Thiopave usage or conditioning.

FIGURE 5.4 Broken TSR Specimens.

5.2.1.2 Moisture Susceptibility after 14 Days of Curing

After the initial testing was performed on Thiopave-modified specimens with less than 14 days of curing, moisture susceptibility testing was performed on three base layer mix designs (control mix, 30 percent Thiopave mix with 3.5 percent design air voids, and 40 percent Thiopave mix with 3.5 percent design air voids) after the specimens were allowed to cure 14 days at room temperature. The Thiopave-modified mixtures were tested at 3.5 percent design air voids for this round of testing to be more representative of the materials tested in the remainder of the study.

Testing was performed in accordance with both ALDOT 361-88 and AASHTO T283-07 (both are described in detail in Section 4.3.1). A detailed summary of the TSR testing results for the ALDOT method with 14 days of curing is presented in Table B.2 of Appendix B. A detailed summary of the TSR testing results for the AASHTO method with 14 days of curing is presented in Table B.3 of Appendix B. Both the saturation and air void requirements specified in ALDOT 361 and AASHTO T283 were met for each specimen tested.

Table 5.3 lists a summary of the TSR results for these mixes using the ALDOT method after the specimens were allowed to cure for 14 days. Table 5.4 lists a summary of the TSR testing results for these mixes using the AASHTO method after the specimens were allowed to cure for 14 days. Figure 5.5 shows a summary plot of both the AASHTO and ALDOT TSR values for the specimens that were allowed to cure for 14 days. Figure 5.5 shows that the Thiopave-modified mixes had a lower TSR value than the control mixture using both the ALDOT method and the AASHTO method. For both the ALDOT and AASHTO methods, the TSR value for this mix fell below the commonly accepted failure threshold of 0.8. As such, it appears that the amount of time the specimens are allowed to cure at room temperature has a significant impact on the moisture susceptibility results. For both the ALDOT and AASHTO results, the 30 percent Thiopave mix has a lower TSR value than the 40 percent Thiopave mix. As such, it does not appear that replacing more than 30 percent of the virgin binder with Thiopave has any additional adverse affect on the moisture susceptibility of the mix. It also appears that the gap in the TSR values between the control mix and the Thiopave-modified mixes is greater for those specimens tested with the ALDOT method rather than with the AASHTO method.

TABLE 5.3 Summary of TSR Testing for Base Layer Mixes (ALDOT Method – More than 14 Days of Curing)

Mix ID	Treatment	Air Voids (%)	Saturation (%)	Splitting Strength (psi)	TSR
Control	Conditioned	6.7	64.6	132.0	0.99
	Unconditioned	6.9	N/A	133.0	
30% Thiopave	Conditioned	7.1	56.5	73.0	0.60
	Unconditioned	7.1	N/A	122.1	
40% Thiopave	Conditioned	7.6	59.7	74.8	0.67
	Unconditioned	7.0	N/A	111.6	

TABLE 5.4 Summary of TSR Testing for Base Layer Mixes (AASHTO Method – More than 14 Days of Curing)

Mix ID	Treatment	Air Voids (%)	Saturation (%)	Splitting Strength (psi)	TSR
Control	Conditioned	6.6	73.1	115.0	0.87
	Unconditioned	6.8	N/A	133.0	
30% Thiopave	Conditioned	7.0	71.4	86.5	0.71
	Unconditioned	7.1	N/A	122.1	
40% Thiopave	Conditioned	7.1	74.5	81.6	0.73
	Unconditioned	7.0	N/A	111.6	

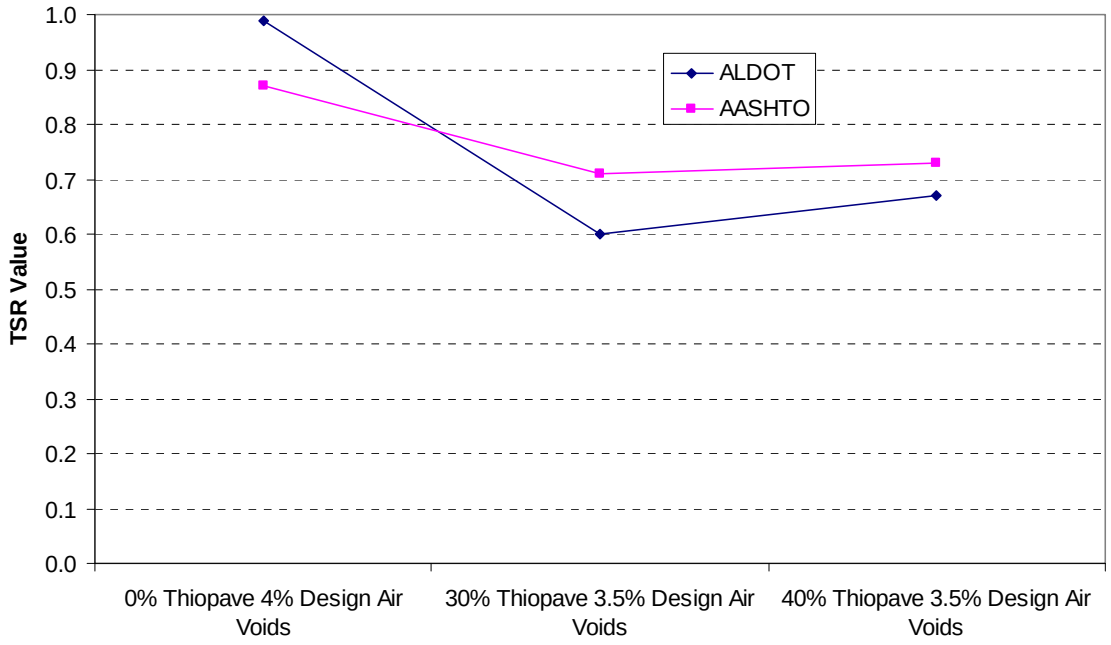

FIGURE 5.5 Summary of TSR Results (after 14 Days of Curing).

Given the results of this testing, it is advisable to conduct a more comprehensive moisture susceptibility evaluation. This evaluation would better quantify the potential reduction in laboratory moisture resistance of Thiopave-modified mixes in certain cases and better explore ways to mitigate this negative impact through the use of more effective anti-stripping agents, other additives, or mix design modifications. Shell is currently studying this perceived limitation in more detail, and the Thiopave-modified field mixes that will be paved on the NCAT Test Track will be thoroughly examined for this distress in Phase II.

5.2.2 Dynamic Modulus Testing Results

The first phase of the dynamic modulus investigation involved testing specimens after both 1 day and 14 days of curing. This was done to assess the time-dependent strength properties of the Thiopave mixtures. A description of the test procedure was outlined in Section 4.3.2. A detailed summary of the E* results is included in Appendix C.

Figures 5.6 and 5.7 show the dynamic modulus values (over the full range of testing frequencies at 21^{o}C) of each of the five mix designs after 1 day and 14 days of curing, respectively. In Figure 5.6, the 1-day E* results of the Thiopave mixes were comparable or greater than the respective 1-day E* values for the control mix. The 14-day E* results for the Thiopave mixes shown in Figure 5.7 increased significantly compared to the 1-day E* results of all the mixes evaluated and the 14-day E* results of the control mix at every testing frequency.

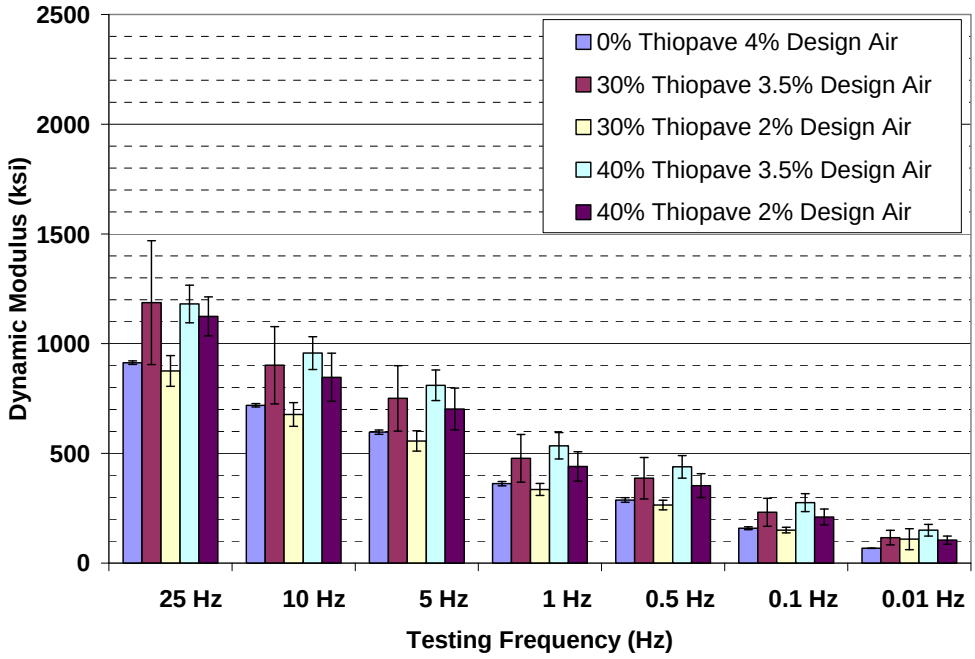

FIGURE 5.6 Dynamic Modulus Results at 21°C and 1 Day of Curing.

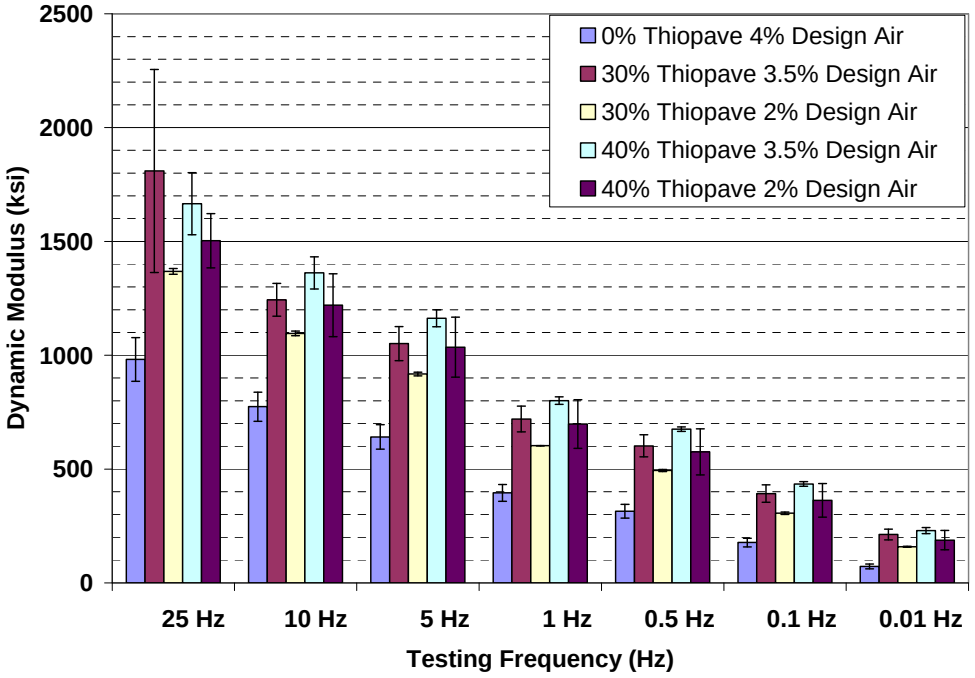

FIGURE 5.7 Dynamic Modulus Results at 21°C and 14 Days of Curing.

Figure 5.8 shows the average dynamic moduli for each of the five mix designs at 10 Hz and 21°C after both 1 day and 14 days of curing. Stiffness of the Thiopave mixes increased 300 to 400 ksi

over the two week curing period. In contrast, the control mixture showed no tangible increase in stiffness.

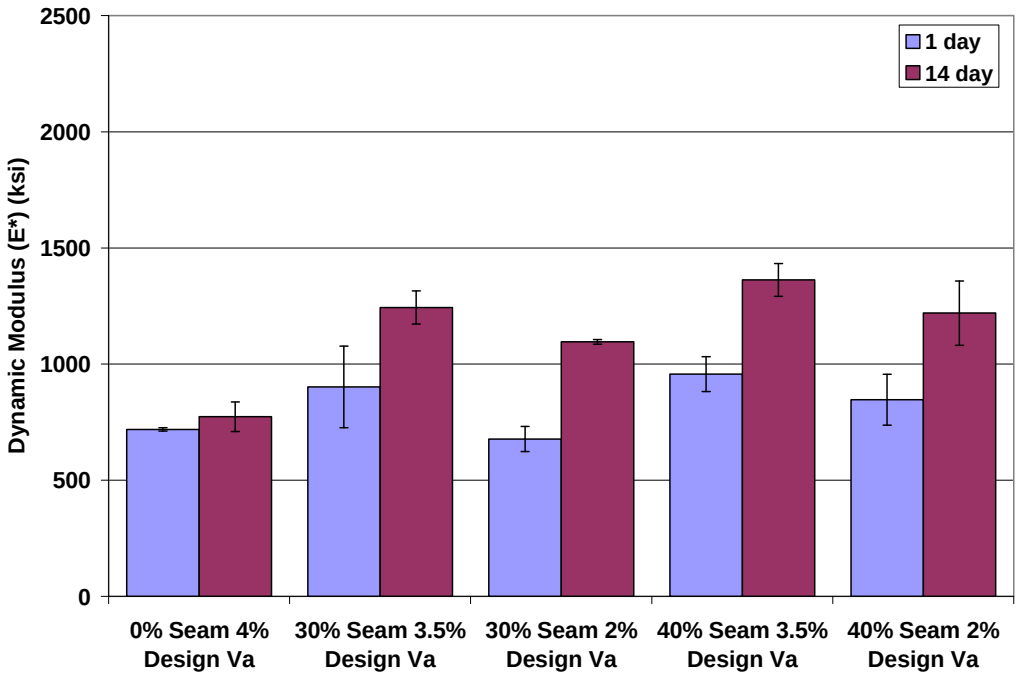

FIGURE 5.8 E* Results at 10 Hz and 21°C for All Mixtures After 1 and 14 Days of Curing.

The second phase of the dynamic modulus investigation involved laboratory E* testing at three temperatures and six frequencies to develop a master curve for each of the five mix designs. Detailed E* test results are presented in Appendix C. The procedure for developing the master curves was explained in detail in Section 4.3.2.

Figure 5.9 shows the master curves that were developed for each of the five mix designs. There was a distinct separation between the curves of the control mix and those of the Thiopave mixtures. This separation is evident across the range of testing frequencies. The most notable separation is at the higher temperatures (lower frequencies), but this difference is exaggerated somewhat by the presence of the log scale.

At the lower temperatures (higher frequencies), the 40 percent Thiopave mixtures (both 3.5 percent and 2 percent design air voids) exhibited higher stiffness values than the 30 percent Thiopave mixtures. As the testing temperature increased (frequency decreased), the mixes with 3.5 percent design air voids (both 30 and 40 percent Thiopave) began to display stiffer behavior than the mixtures with 2 percent design air voids for rich bottom layers. This behavior was anticipated because the rich bottom mixes were designed with more asphalt for improving fatigue cracking resistance. Table 5.5 gives a summary of the master curve regression coefficients that were generated using the models presented in Section 4.3.2.

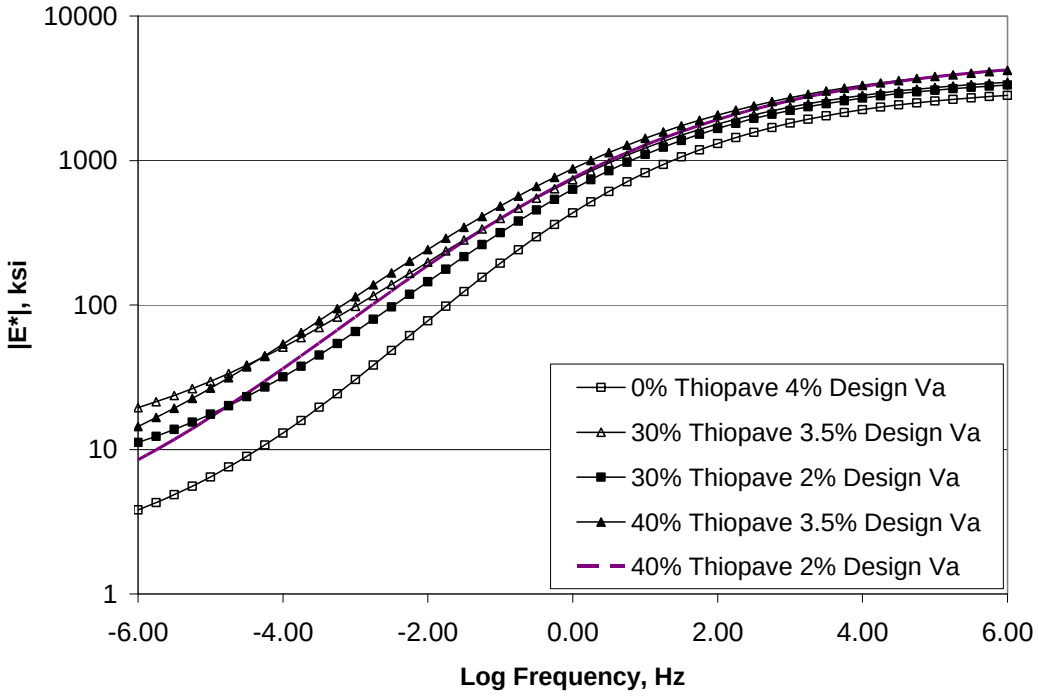

FIGURE 5.9 Dynamic Modulus Master Curve for All PG 67-22 Mixtures.

TABLE 5.5 Master Curve Regression Coefficients

Parameters	Control Mix 4% Design Va	30% Thiopave 3.5% Design Va	30% Thiopave 2% Design Va	40% Thiopave 3.5% Design Va	40% Thiopave 2% Design Va
Delta	0.1249	0.8884	0.6449	0.3627	0.0025
Alpha	3.3887	2.7164	2.9378	3.3519	3.7308
Beta	-1.0541	-0.9881	-1.0152	-1.2084	-1.2133
Gamma	0.4851	0.4567	0.4753	0.3955	0.3868

5.2.3 Flow Number Test Results

Flow number testing was performed on the specimens that had been used for 14-day dynamic modulus testing discussed in section 5.2.2. Flow number testing was performed in accordance with the procedure outlined in Section 4.3.3, and the flow number for each of these specimens were determined using two different model forms—the Power and Francken models. Figure 5.10 shows a graph of the plastic strain versus the number of loading cycles for each test specimen. Figures 5.11 and 5.12 compare all the flow number results and average flow number values, respectively, for the five mixes evaluated in this study. More results of the flow number testing, including the permanent strain values at the flow point, are presented in Appendix D.

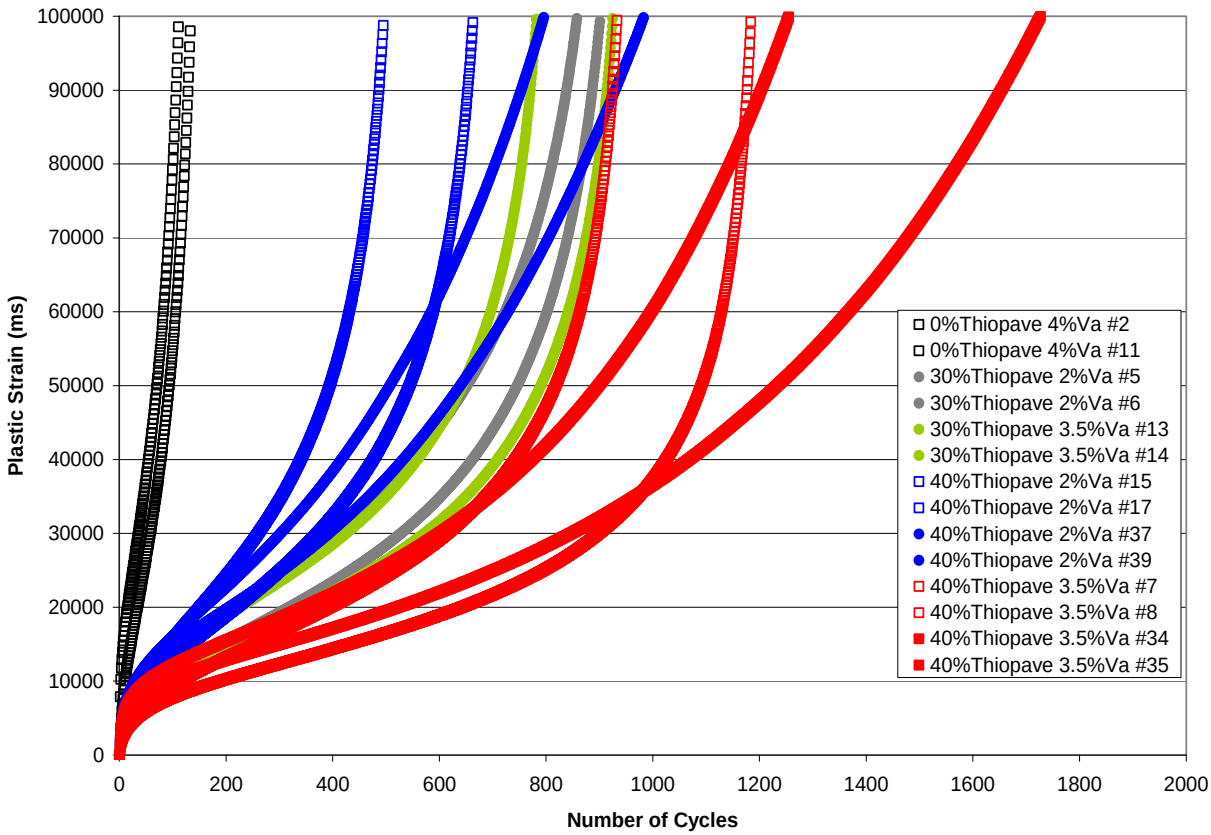

FIGURE 5.10 Plastic Strain versus Number of Cycles for Flow Number Test.

From these results, it appeared that the 40 percent Thiopave mix with 3.5 percent air voids had the highest resistance to rutting, given these specimens took the greatest number of cycles to fail. The 30 percent Thiopave mixtures with 3.5 and 2 percent design air voids had similar deformation resistance. These mixes took longer to fail than the 40 percent Thiopave mix with 2 percent design air voids but showed less deformation resistance than the 40 percent Thiopave mix with 3.5 percent design air voids. All of the Thiopave mixtures showed significant improvement in deformation resistance over the control mixture. This finding is consistent with the results of the dynamic modulus testing showing the Thiopave mixes to have a much stiffer behavior under loading than the control, especially at higher temperatures. In summary, the 40 percent Thiopave mix with 3.5 percent design air voids showed the highest resistance to deformation of the five mix designs tested. There was seemingly no relationship between the relative deformation susceptibility of the mixes and the Thiopave percentage or the combined Thiopave and asphalt content.

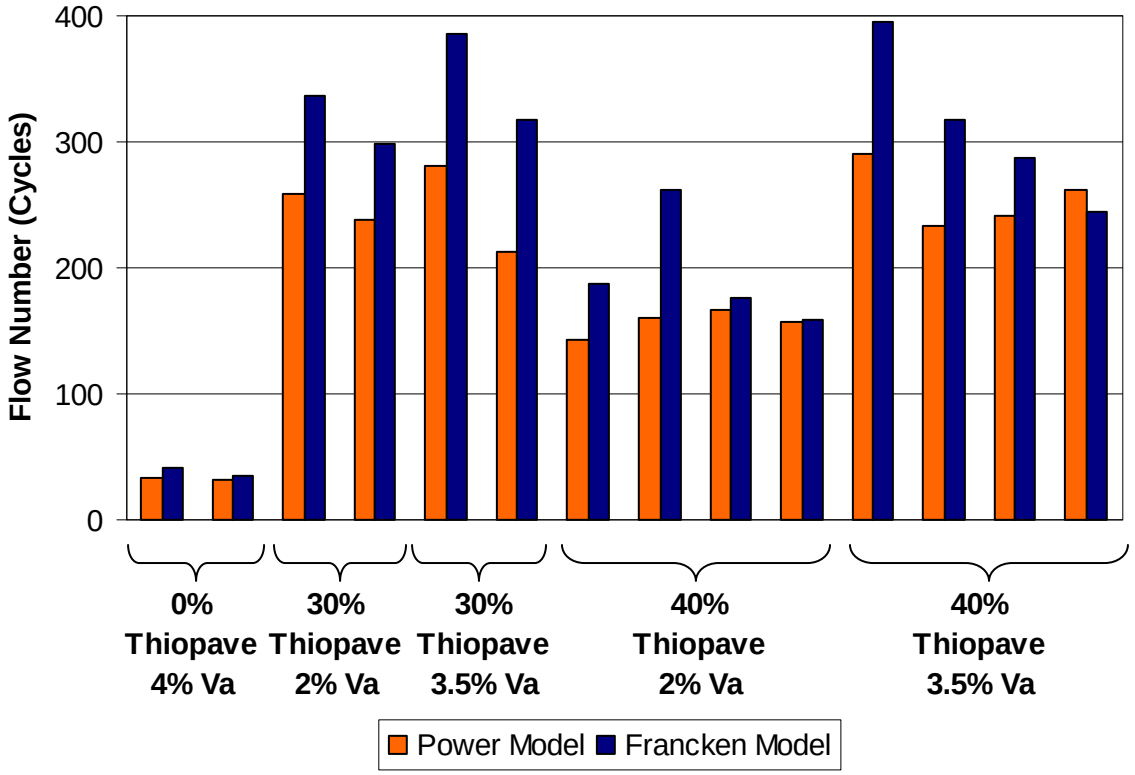

FIGURE 5.11 Comparison of Flow Number Results using Power and Francken Models.

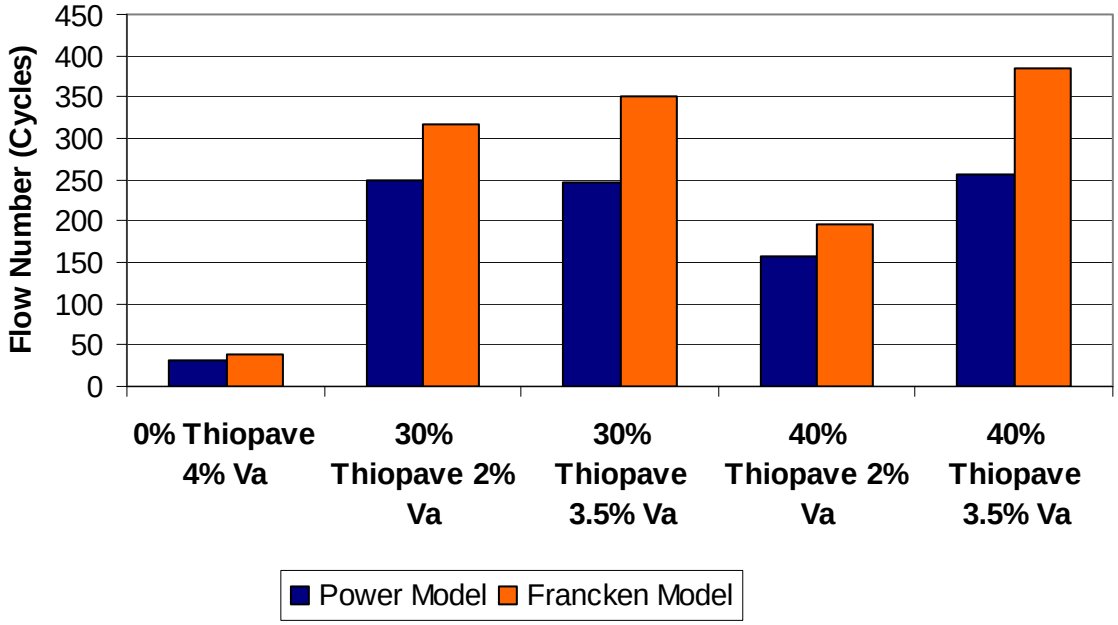

FIGURE 5.12 Comparison of Average Flow Numbers using Power and Francken Models.

5.2.4 APA Test Results

Asphalt Pavement Analyzer (APA) testing was performed on each of the five mix designs used for this project in accordance with AASHTO TP 63. More details regarding the test procedure can be found in Section 4.3.4. For each mix, a total of six specimens were tested. It should be noted that for the control mix, one of the hoses failed during the testing owing to only four data points being available. A summary of test results is included in Appendix E.

Figure 5.13 shows a plot of the manually and automatically measured rut depths for each grouping of specimens versus the percent Thiopave of the mixes. It can be seen that the Thiopave mixes had significantly reduced APA rutting from that of the control mix. The control mix had an average rut depth of 9.9 mm while the 30 percent Thiopave and 40 percent Thiopave mixes with 3.5 percent design air voids had an average manual rut depth of 5.4 mm and 5.8 mm, respectively. While the 40 percent Thiopave mix had a slightly higher average rut depth, there was no statistical difference between the rutting behavior of 30 percent Thiopave and 40 percent Thiopave mixes (one-way ANOVA p-value = 0.42 > critical p-value = 0.05). The 30 percent Thiopave rich bottom mixture exhibited a higher average rut depth than the 30 percent Thiopave design layer, as expected. However, no statistical difference was seen between the rutting behavior of the 40 percent Thiopave design and rich bottom mixtures for manual rut depths (one-way ANOVA p-value = 0.57 > critical p-value = 0.05). All of the Thiopave mixtures, including the rich bottom mixtures, showed less rutting susceptibility than the control mixture in the APA. This behavior was expected given the performance of the dynamic modulus and flow number testing as well as the performance of other Thiopave mixes in literature.

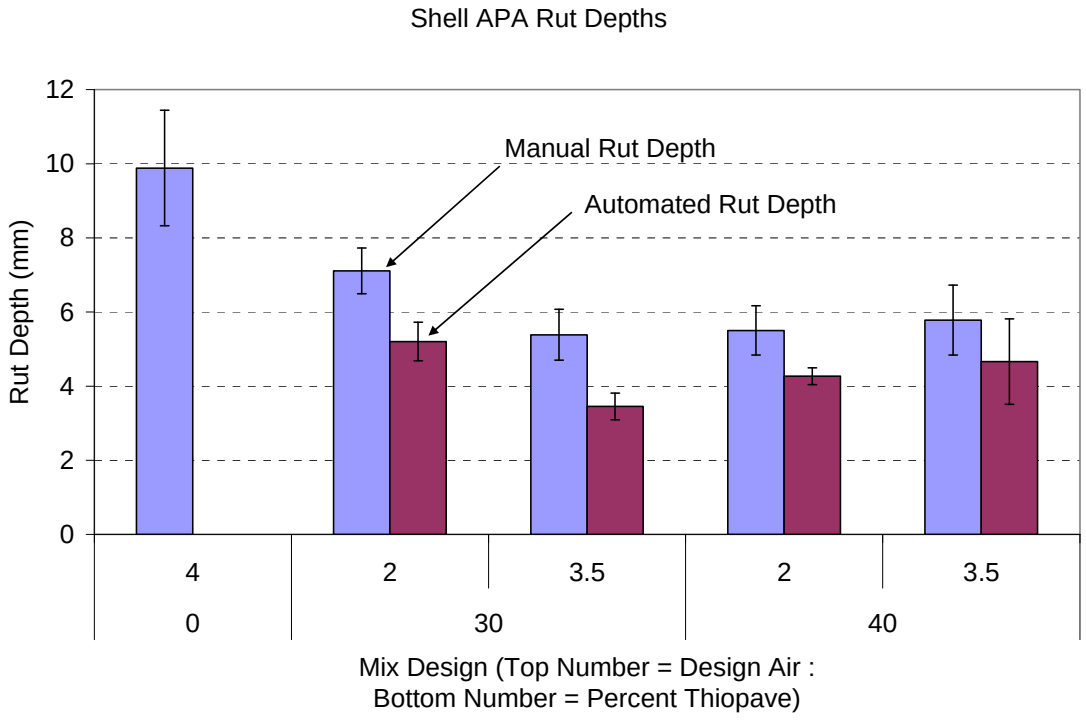

FIGURE 5.13 Manual Sample Rut Depths versus Percent Thiopave.

5.2.5 Hamburg Wheel Tracking Testing Results

Rutting and moisture susceptibility testing was also performed using the Hamburg Wheel-Tracking device. This testing was performed in accordance with AASHTO T 324 and more detail regarding the testing procedure and analysis of results is discussed in Section 4.3.5.

Figure 5.14 summarizes the results of the Hamburg Wheel-Tracking testing. This plot summarizes the average values and variability (plus and minus one standard deviation) of the steady-state rutting rate and stripping inflection points for the five mix designs tested. Definitions of these quantities are given in Section 4.3.5. For the design layer mixes (0%, 30% and 40% Thiopave), four replicates of each mixture were tested. For the rich bottom mix, three replicates were used. A complete database of all Hamburg data analysis results can be found in Table F.1 of Appendix F.

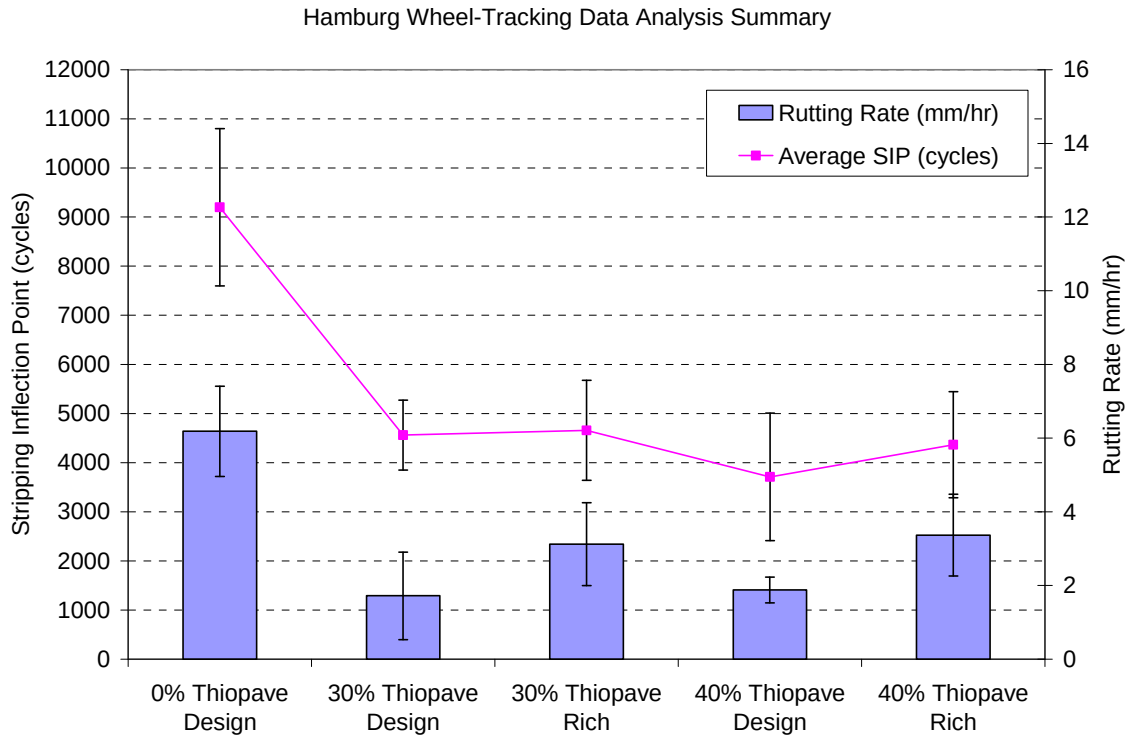

Figure 5.14 Hamburg Wheel-Tracking Data Analysis Summary

Figure 5.14 shows that the control mix had a much higher rutting rate than all the mixtures containing the Thiopave material. There was no visible difference between the average rutting rates for the 30% Thiopave design layer and the 40% Thiopave design layer. There were also no visible differences between the 30% Thiopave rich bottom layer and the 40% Thiopave rich bottom layer. It was evident that the Thiopave design layers had a lower average rutting rate than those of the Thiopave rich bottom layers. This was expected given the higher design binder content of those mixtures. These rutting data also compare well with the rut testing results from the APA and AMPT, given the dramatic difference in deformation resistance between the Thiopave mixtures and the PG 67-22 control mixture.

The data from the Hamburg device is also useful in that it gives a measure of the moisture sensitivity of the different mixtures. For the purposes of reporting a numerical average, a sample that did not show any evidence of stripping was assigned a stripping inflection point of 10,000 cycles (the maximum number of cycles allowed by the test). The average and variability of the stripping inflection points for the five mix designs are also shown in Figure 5.14. It can be seen that there is a large disconnect between the average stripping inflection point of the control mixture versus those of the Thiopave mixtures. There does not appear to be a significant difference in the stripping behavior of the four different Thiopave mixtures (average stripping inflection points falling between 3700 and 4700 cycles). While the control mix typically didn't exhibit an obvious stripping inflection point, it did rut at a significantly higher rate than the Thiopave mixtures. While the Thiopave mixtures did show signs of moisture related damage in the Hamburg device, it should be noted that these specimens showed significantly less rutting than the control mixture. Photographs of a set of tested Hamburg specimens from each mix design are shown in Figure 5.15. Based on visual inspection, the mixture appeared more brittle as the amount of Thiopave in the mixture was increased. This can be seen in the additional fracturing of the specimen surrounding the rutting path in the Thiopave mixes while little additional fracturing can be seen in the control mixture.

FIGURE 5.15 Tested Hamburg Wheel Tracking Specimens.

Given the results of the other laboratory testing (higher TSR values and higher rutting values for the control mixture), the results of this testing serve to validate the fact that the control mixture is much more susceptible to rutting than the Thiopave mixtures. The moisture susceptibility results from TSR testing after 14 days of curing also seem to agree well . The Thiopave mixtures show signs of moisture induced damage from both test methods.

5.2.6 Bending Beam Fatigue Test Results

The fatigue life of each of the five mixes was quantified using the bending beam fatigue testing apparatus. The mixes were tested in accordance with ASTM D7460 at three different strain levels with two replicates per strain level. Full details regarding the bending beam testing methodology can be found in Section 4.3.6.

A detailed summary of the bending beam fatigue test results is presented in Table F.1 in Appendix F. The data in this table include the specimen air voids, strain level, and cycles required for failure of the specimen. Despite adherence to the specification and tight control of specimen air voids, dimensions, and beam orientation, significant variability could still be seen in the duplicate results for a given mixture at a given strain level. This variability was especially evident for testing performed at the lowest strain level (200 microstrain). According to ASTM D7460 failure of the specimen is defined as the maximum point on a plot of Normalized Modulus × Cycles versus number of cycles (see Section 4.3.6). As discussed in Section 4.3.6, the test was terminated when the beam stiffness was reduced to 30 percent of the initial stiffness. This allowed the determination of the number of cycles to failure according to ASTM D 7460 and at 50 percent of the initial stiffness according to AASHTO T 321, and both sets of the results are presented in Appendix F.

Figures 5.16 and 5.17 compare the fatigue cracking resistance of the five mixtures determined in accordance with ASTM D 7460 and based on AASHTO T 321, respectively. A power model was used to fit the results for each of the five mixtures. A summary of the model coefficients and R^2 values is given in Table 5.6. Both of the figures show similar relative relationships between the mixtures.

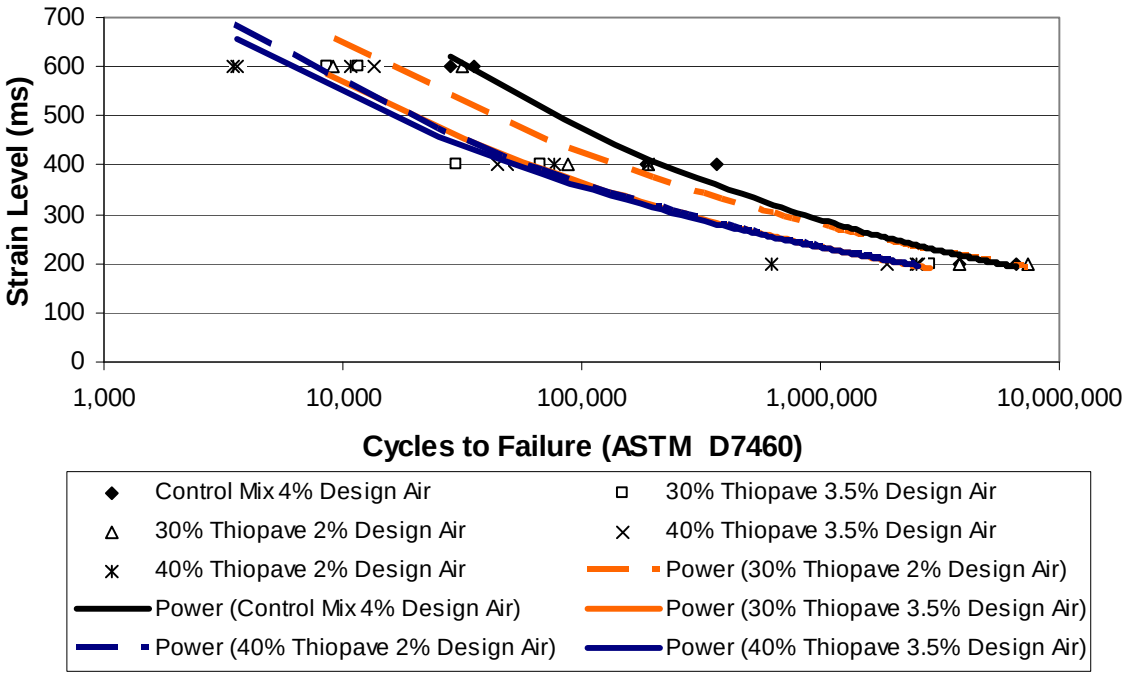

FIGURE 5.16 Comparison of Fatigue Resistance (ASTM D7460) for Five Mixtures.

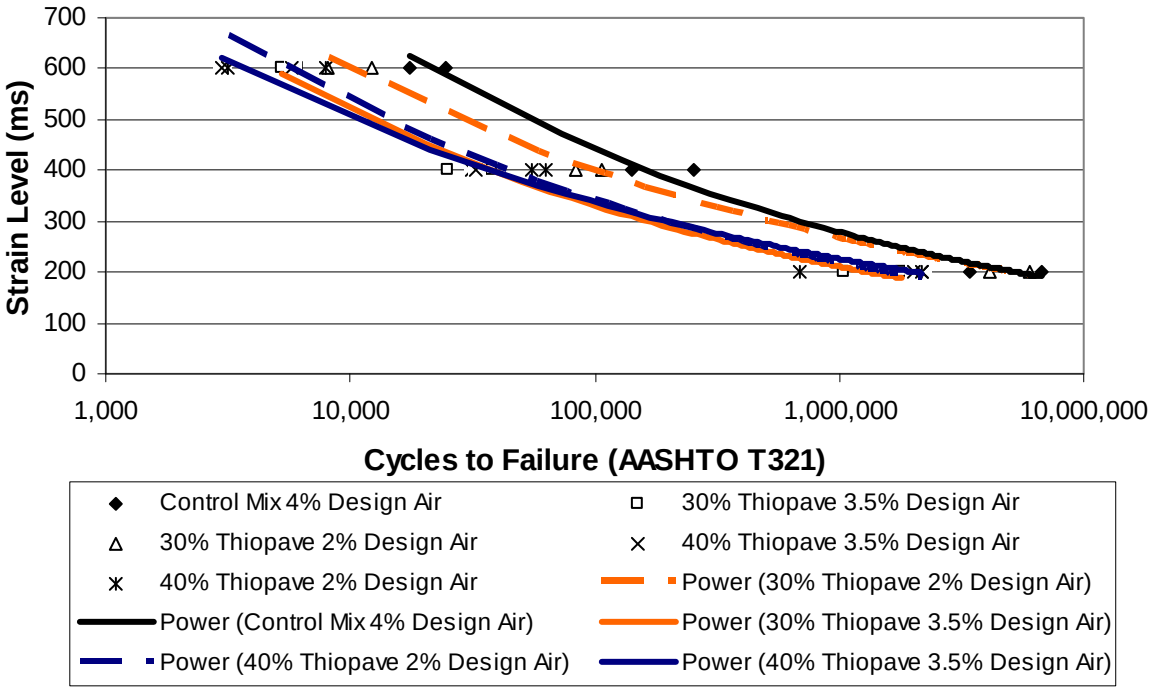

FIGURE 5.17 Comparison of Fatigue Resistance (AASHTO T 321) for Five Mixtures.

TABLE 5.6 Fatigue Curve Fitting Coefficients (Power Model Form)

Thiopave (%)	Design Voids (%)	ASTM D7460			AASHTO T321		
		α_1	α_2	R^2	α_1	α_2	R^2
0	4	5610.8	-0.215	0.982	4414.7	-0.199	0.984
30	3.5	3366.8	-0.193	0.975	3143.7	-0.196	0.990
30	2	3491.4	-0.183	0.963	3007.1	-0.176	0.995
40	3.5	2966.4	-0.184	0.972	2496.7	-0.174	0.993
40	2	3210.8	-0.190	0.890	3179.5	-0.194	0.957

By examining the model coefficients in Table 5.6, there was a significant difference between the magnitude of the intercept (α_1) and slope (α_2) terms between the control mixture and the Thiopave mixtures. The α_1 term for the control mixture was 1.5 to 2 times greater than that of those for the Thiopave mixtures. The α_2 term for the control mixture was also significantly different from those of the Thiopave mixtures. The R^2 values for each of the mixes are above 0.89, showing a good model fit for the dataset.

Table 5.7 shows the percentage difference between the average fatigue life of the control mixture and the average fatigue life of the Thiopave mixtures at the three strain levels tested in this study, using the failure criteria defined by the ASTM method. This information helps evaluate important aspects of the material behavior shown in Figure 5.16 as follows:

- At the high strain level of 600 microstrain, the control mixture exhibited the longest fatigue life. The average fatigue life of the control mixtures was between 36 and 78 percent longer than that of the Thiopave mixture tested. The 30 percent Thiopave mix with 2 percent air voids had the longest fatigue life among the Thiopave mixes at this high strain level.
- At 400 microstrain, the average fatigue life of the control mixture was 82 to 83 percent longer than the 30 and 40 Thiopave mixes with 3.5 percent design air voids, respectively. The control mixture had an average 50 and 52 percent longer fatigue life than the Thiopave mixtures with 2 percent design air voids.
- At the strain level of 200 microstrain, the control mixture had a significantly longer fatigue life to three of the Thiopave mixtures (30 and 40 percent Thiopave mixes with 3.5 percent design air voids, and 40 percent Thiopave mix with 2 percent design air voids). Each of these Thiopave mixtures had an average fatigue life between 54 and 70 percent shorter than that of the control mixture. However, the 30 percent Thiopave mix with 2 percent design air voids exhibited an average fatigue life approximately 8 percent longer than that of the control mixture.
- The results suggested that the 30 percent Thiopave mix with 2 percent design air voids was the superior performing Thiopave mixture in fatigue across the whole range of strain levels, but most notably at the low strain levels.

TABLE 5.7 Percentage Difference of Average Cycles to Failure for Thiopave Mixtures versus Control Mixture

Thiopave (%)	Design Air Voids	Strain Level		
		200 ms	400 ms	600 ms
30	3.5	-54%	-82%	-68%
30	2	8%	-50%	-36%
40	3.5	-57%	-83%	-73%
40	2	-70%	-52%	-78%

Table 5.8 shows the 95 percent one-sided lower prediction of endurance limit for each of the five mixes tested in this study based on the number of cycles to failure determined in accordance with ASTM D 7460 and AASHTO T 321. The procedure for estimating the endurance limit was developed under NCHRP 9-38 (see Section 4.3.6). Based on the results shown in Table 5.8, the 30 percent Thiopave mix with 2 percent design air voids had the highest predicted endurance limit among the five mixes tested in this study (according to the AASHTO failure criteria). The control mixture and the 40 % Thiopave design layer had the second highest endurance limit according to the AASHTO failure criteria. For the ASTM failure criteria, the control mix and the 30% rich bottom mix exhibited an equivalent endurance limit.

TABLE 5.8 Predicted Endurance Limits

Thiopave (%)	Design Voids (%)	Endurance Limit (Microstrain)*	
		ASTM D 7460	AASHTO T 321
Control	4	99	102
30	3.5	83	79
30	2	98	119
40	3.5	84	98
40	2	60	69

Note: * 95% one-sided lower prediction limit

5.2.7 Thermal Stress-Restrained Specimen Testing Results

The low temperature cracking resistance of each of the five mix designs was quantified using thermal stress-restrained specimen testing. The mixes were tested in accordance with AASHTO TP10 with three replicates per mix to determine the stress level and temperature at which low temperature cracking occurred. More details regarding the TSRST testing methodology can be found in Section 4.3.7. Table 5.9 shows a summary of TSRST testing results, including sample air voids, sample dimensions, fracture stress, and fracture temperature (temperature at which low temperature cracking occurred).

TABLE 5.9 Summary of TSRST Results

Thiopave (%)	Design Air Voids (%)	Sample ID	Sample Air Voids (%)	Sample Length (mm)	Sample Height (mm)	Sample Width (mm)	Fracture Stress (psi)	Fracture Temperature (oC)
0	4	75	6.3	255.21	50.8	51.86	367	-19.6
0	4	42	7.3	252.38	49.91	51.65	367	-20.5
0	4	72	6.9	254.95	52.48	53.53	313	-21.4
30	3.5	44	7.5	253.15	51.03	50.51	420	-18
30	3.5	45	7.2	254.41	51.25	50.39	366	-17.2
30	3.5	46	7.3	251.81	50.85	52.2	454	-22.6
40	3.5	81	7.4	253.72	51.81	53.19	435	-21.6
40	3.5	62	7.5	252.07	52.27	52.95	374	-17.5
40	3.5	79	7.0	253.13	51.92	52.8	480	-21.1
30	2	89	7.3	248	52.61	50.31	368	-22.6
30	2	95	6.2	250.98	50.95	50.96	386	-22.4
30	2	101	6.1	254.8	51.42	51.12	389	-20.7
40	2	92	5.7	249.045	51.424	50.116	373	-21.4
40	2	93	6	248.94	49.932	49.97	435	-20.7
40	2	102	6.1	254.68	51.89	50.96	477	-24.1

Table 5.10 shows the average and coefficient of variation (COV) of the fracture stress and fracture temperature for the five mixtures that underwent TSRST testing. There appeared to be an increase in the average fracture stress of the specimens with an increase in percent Thiopave.

However, one-way ANOVA testing of these data sets showed there was no statistical difference in the means of the data sets (p-value = 0.157). The average values of fracture temperature for the five mix designs fell between -19.3°C and -22.1°C. A one-way ANOVA test proved that there was no statistical difference in the average of these means (p-value = 0.382). Therefore, it can be said that the addition of the Thiopave material had no tangible impact on the low temperature cracking susceptibility of the control asphalt mixture. This result was expected given similar performance of other studies in literature. Table 5.11 shows the ANOVA results for fracture stress, and Table 5.12 shows the ANOVA results for fracture temperature.

TABLE 5.10 Statistics of TSRST Results

Mix ID	Statistic	Fracture Stress (psi)	Fracture Temperature (oC)
0% Thiopave 4% Design Air	Average	349.0	-20.5
	COV	8.9	4.4
30% Thiopave 3.5% Design Air	Average	413.3	-19.3
	COV	10.7	15.1
40% Thiopave 3.5% Design Air	Average	429.7	-20.1
	COV	12.4	11.1
30% Thiopave 2% Design Air	Average	381	-21.9
	COV	3.0	4.8
40% Thiopave 2% Design Air	Average	428.3	-22.1
	COV	12.2	8.1

TABLE 5.11 One-Way ANOVA Results for TSRST Fracture Stress

Source of Variation	SS	df	MS	F	P-value	F crit
Between Groups	14466.9333	4	3616.733	2.093502	0.156564	3.47805
Within Groups	17276	10	1727.6			
Total	31742.9333	14				

TABLE 5.12 One-Way ANOVA Results for TSRST Fracture Temperature

Source of Variation	SS	df	MS	F	P-value	F crit
Between Groups	17.356	4	4.339	1.165145	0.382348	3.47805
Within Groups	37.24	10	3.724			
Total	54.596	14				

5.3 Summary

This section presents the results of the laboratory testing conducted in this study and can be summarized as follows:

- Five mixes were evaluated in this study, including the control mix with 4 percent design air voids, 30 percent Thiopave mixes with 3.5 and 2 percent design air voids, and 40 percent Thiopave mixes with 3.5 and 2 percent design air voids.
- The Thiopave mixtures had higher TSRs, but lower conditioned and unconditioned splitting tensile strength results than the control mix when tested without being allowed to cure for 14 days. This was likely a consequence of not allowing the Thiopave mixtures to cure for two weeks prior to testing. TSR testing (with and without a freeze-thaw cycle) showed a reduction in the TSR value for the Thiopave-modified mixes after they had been allowed to cure for 14 days. It is recommended additional studies be performed to see which anti-stripping additives or technologies could best counter this effect.
- The Thiopave modified mixes had higher E* results for all combinations of test temperatures and frequencies than the control mix. There was a distinct separation between the master curve for the control and those of the Thiopave mixes.
- Based on the flow number test results, three of the Thiopave modified mixes exhibited the highest resistance to rutting. These mixes were the 30 percent Thiopave mix with 3.5 percent design air voids, the 30 percent Thiopave mix with 2 percent design air voids, and the 40 percent Thiopave mix with 3.5 percent design air voids. The control mix had the lowest rutting resistance with the 40 percent Thiopave mix with 2 percent design air voids having the second lowest.
- The APA results confirmed the observations based on the flow number test results—the control mix had higher APA rut depths than the 30 and 40 percent Thiopave mixes with 3.5 percent air voids. The 30 percent Thiopave mix with 2 percent design air voids showed more rutting susceptibility than the 30 percent Thiopave with 3.5 percent design air voids, but less rut susceptibility than the control mixture. Both the 40 percent Thiopave mixes showed similar rutting susceptibility, which was less than that of the control mix.
- The 30 and 40 percent Thiopave mixes showed better rutting resistance than the control mixture, but exhibited signs of moisture damage in the Hamburg test.
- Based on the BBF test results, the control mix had a longer fatigue life at 600 and 400 microstrain than the Thiopave mixes. However, the 30 percent Thiopave mix with 2 percent design air voids exhibited a fatigue life approximately 8 percent longer than that of the control mixture at 200 microstrain.
- The 30 percent Thiopave mix with 2 percent design air voids had the highest predicted endurance limit among the five mixes tested in this study according to AASHTO definition of failure. The control mixture and the 40 percent Thiopave mix with 3.5 percent design air voids had the second largest endurance limit according to the AASHTO failure criteria. Based on the ASTM failure criteria, the control mixture and the 30 percent Thiopave mixture with 2 percent design air voids exhibited virtually equivalent endurance limits.
- Based on the TSRST results, the addition of the Thiopave material had no tangible impact on the low temperature cracking susceptibility of the asphalt mixture. The average values of fracture temperature for the five mix designs fell within the range of -19.3^{o}C and -22.1^{o}C.

6. STRUCTURAL ANALYSIS AND DESIGN

6.1 Introduction

It is anticipated that two pavement test sections will be constructed utilizing the Thiopave material in the 2009 Test Track structural experiment. While the full-scale testing will provide invaluable data regarding constructability, seasonal effects, temperature fluctuations, aging and damage, there was a need to conduct a preliminary structural analysis to evaluate how the Thiopave material "performs" in a theoretical M-E framework. This analysis will enable the following:

1. Demonstrate how the Thiopave material may be modeled within common design analysis tools including the Mechanistic-Empirical Pavement Design Guide (MEPDG) and PerRoad.
2. Provide a theoretical basis of comparison between a control section, to be built in the 2009 structural study, and a variety of Thiopave experimental sections.
3. Provide a theoretical expectation as to how the experimental sections may respond and perform relative to control sections in the 2009 full-scale study.

The structural analysis investigation made use of the dynamic modulus (E*) data measured specifically for this project. Additional data gathered as part of the 2006 structural study were used where appropriate as will be described below. Data sets were developed to conduct MEPDG (version 1.0) analyses of a control section and eight hypothetical Thiopave test sections. The PerRoad program (version 3.3) was used to evaluate these nine sections and also develop complimentary sets of nine perpetual pavement cross sections. The following subsections detail this investigation.

6.2 MEPDG Investigation

The MEPDG, developed under NCHRP 1-37A (*8*) and further refined under NCHRP 1-40D, represents a major advance in the design of pavement structures over the existing predominant method used by many states (*9*). The MEPDG, pictured in Figure 6.1, utilizes mechanistic-empirical concepts to relate mechanistic material properties and pavement responses to empirical observations of performance. The MEPDG requires inputs in four major categories that include:

- General project information
- Traffic
- Climate
- Structural

From these inputs, the MEPDG makes predictions regarding specific modes of pavement distress that include bottom-up fatigue cracking, rutting, thermal cracking, top-down cracking and ride quality (i.e., International Roughness Index (IRI)).

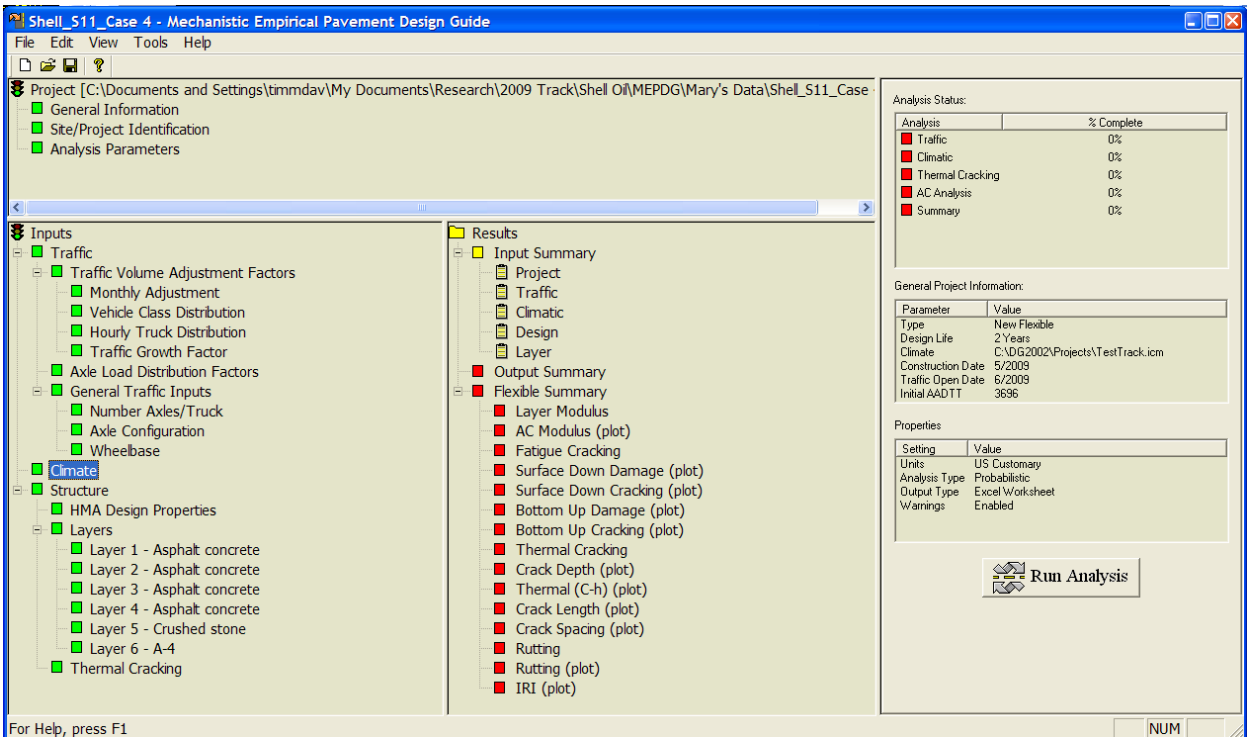

FIGURE 6.1 MEPDG Main Screen.

6.2.1 General Project Information

All the MEPDG inputs were selected to closely represent the Test Track, both in terms of historical data, and what is expected to occur in 2009. To that end, with respect to general project information, a two-year analysis was selected with the Base/Subgrade construction specified to occur in March 2009 and the HMA construction in May 2009. Traffic was specified to begin in June 2009. The sections were evaluated in terms of bottom-up fatigue cracking, top-down fatigue cracking and total pavement rutting using the default, built-in, MEPDG transfer functions. Though a reliability level of 90% was included in the analysis, all the results presented below are referenced to the 50th percentile.

As mentioned above, a total of nine pavement cross sections were considered in this investigation. Figure 6.2 illustrates the cross sections and materials used for each case. Each section consisted of three lifts of 2 inches/lift with a 1 inch wearing course. All sections were paved on a dense graded aggregate base that has been used extensively at the Test Track and by ALDOT for general highway construction. All sections were simulated on top of the "Test Track Soil" which is a material available on site and has been used extensively through eight years of research at the Test Track.

The control section in Figure 6.2 most closely replicates section S11 currently in place at the Test Track. It is anticipated that this cross section will be used as the control for the Thiopave experiment in addition to another structural investigation examining other technologies. The Thiopave sections replicate the control by exchanging the binder in layers of conventional

material with the Thiopave-modified binder. For example, Case 1 replaces the bottom three lifts with mixtures using 30% Thiopave designed to 2% air voids. Case 2 is identical, except using mixtures designed at 3.5% air voids. Cases 3 and 4 are direct companions to Cases 1 and 2, with the PG 76-22 wearing course binder replaced with Thiopave-modified PG 67-22 binder. Cases 5 through 8 replicate Cases 1 through 4, substituting 40% Thiopave for the 30% Thiopave. More details regarding these materials and their properties are provided in the following subsections.

FIGURE 6.2 Pavement Cross Sections.

6.2.2 Traffic

Traffic characterization within the MEPDG is very detailed and requires repetitions of particular axle types in specific weight ranges known as load spectra. While the MEPDG contains default load spectra that can be used for routine design, the traffic at the Test Track is very unique in that triple trailer vehicles apply the loads rather than a mixed distribution of traffic. Therefore, the Test Track fleet had to be converted into representative load spectra for the MEPDG.

Figure 6.3 shows one of the five triple tractor-trailer combinations used at the Test Track. All the tractor-trailer combinations have roughly equivalent gross-vehicle weights. The tandem axles, among all the vehicles weigh approximately 42,000 lb. Similarly, all the single axles, among all the trucks, weigh 21,000 lb/axle. The steer axles, however, required two different weight categories since one tractor is roughly 2,000 lb lighter than the other tractors. As shown in the figure, 20% (one of the five trucks) was represented with 10 kip, while the other 80% (four of the five trucks) were represented with 12 kips. It should be noted that the MEPDG makes no

distinction between single (dual tire) and steer (single tire) axles. Therefore, within the MEPDG, the steer axles were simulated as if they had dual tires.

FIGURE 6.3 Test Track Vehicle.

On average, five trucks operate at 45 mph approximately 16 hours per day during the two year testing cycle. Using historical trucking data from the 2006 Test Track, the average daily volume was established at 1,848 truck passes per day in the design direction. The hourly distribution is shown in Figure 6.4. The hourly fluctuations reflect driver breaks, maintenance and refueling stops throughout the day.

6.2.3 *Climate*

The MEPDG contains a sophisticated climate model called the enhanced integrated climate model (EICM) for computing thermal gradients and moisture contents within the pavement every six minutes throughout the simulation. While the model is sophisticated, all that is required of the designer is to select a relevant weather station from a comprehensive database. For these simulations, the closest predefined weather station located in Montgomery, Alabama was selected. Also, since the entire Test Track is built on a substantial embankment, the water table was set relatively deep (60 feet).

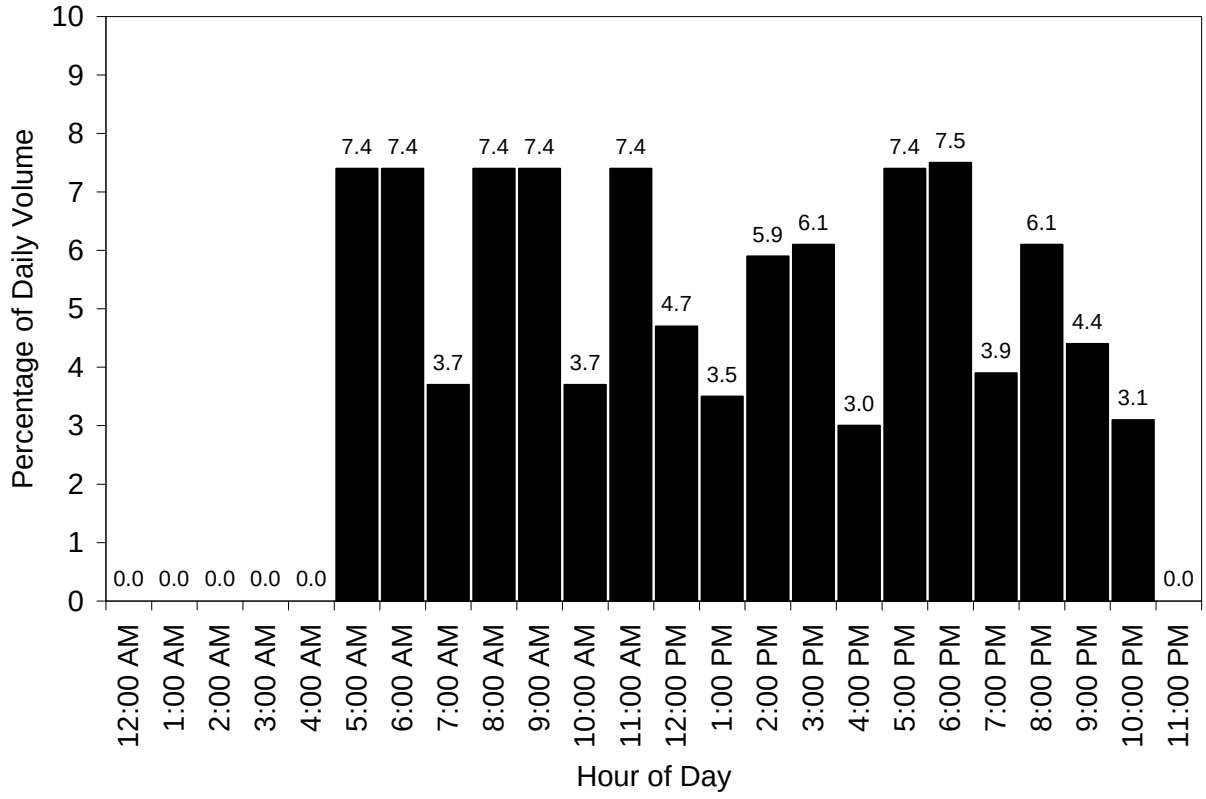

FIGURE 6.4 Hourly Traffic Distribution.

6.2.4 Subgrade Soil Properties

The subgrade material at the Test Track can be classified as an AASHTO A-4 soil (*10*). Within the MEPDG, this material type was selected and a representative modulus was selected based upon laboratory triaxial testing (*10*). Although the laboratory testing established non-linear stress-sensitivity models for this material, the MEPDG is not currently calibrated to use this type of information. Therefore, a representative value had to be selected. This was accomplished by determining the in situ stress state from dynamic pavement response measurements made during the 2006 experiment in Section S11 and determining a representative modulus from this stress state.

To determine the representative stress state, vertical stress measurements made during the course of the 2006 study were plotted over time to establish a weighted average vertical pressure. Figure 6.5 shows these vertical pressure measurements made over the course of one year. The seasonal trend is evident as the vertical pressures increase in the warmer months when the HMA is softer. These data were combined into a weighted average vertical stress that took into account the relative frequency of each axle type; 14.3% steer axles, 14.3% tandem axles and 71.4% single axles, respectively. The weighted average vertical stress was added to the geostatic stresses computed from the unit weights and thicknesses of the overlying materials to arrive at a total average vertical stress, σ_1. Horizontal stresses, σ_3, were computed by multiplying the

vertical stress by a horizontal earth pressure coefficient of 0.3572 (*10*). These two stresses were then used in the following equations to estimate a representative subgrade soil modulus:

$$M_r = k_1 p_a * \left(\frac{\theta}{p_a}\right)^{k_2} * \left(\frac{\sigma_d}{p_a}\right)^{k_3} \quad (6.1)$$

where:

M_r = resilient modulus, psi
k_1 = 1095.43 (*10*)
k_2 = 0.5930 (*10*)
k_3 = -0.4727 (*10*)
p_a = atmospheric pressure = 14.6 psi
θ = bulk stress = $\sigma_1 + 2*\sigma_3$
σ_d = deviator stress = $\sigma_1 - \sigma_3$

The subgrade soil modulus resulting from this procedure was 28,872 psi. Poisson's ratio was assumed to be 0.45. The final set of information for this material entered into the MEPDG was the gradation shown in Table 6.1.

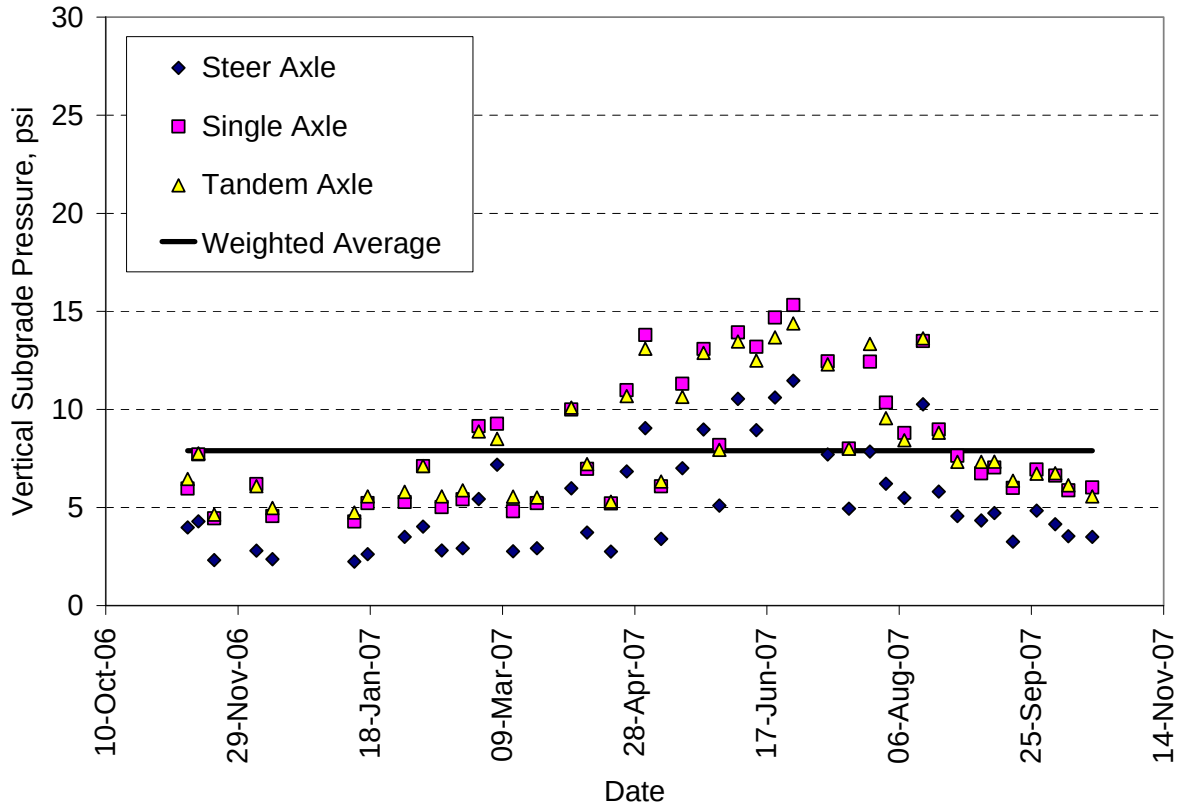

FIGURE 6.5 Vertical Stress Measurements in Subgrade (Section S11).

TABLE 6.1 Subgrade Soil Gradation

Sieve Size	Percent Passing
1 1/2"	100
1"	83
3/4"	81
1/2"	78
3/8"	75
#4	71
#8	68
#16	66
#30	64
#50	61
#100	56
#200	48.0

6.2.5 Granular Base Properties

An identical procedure as that outlined in Section 6.2.4 was followed in establishing the granular base properties for the MEPDG. The vertical stress measurements are shown in Figure 6.6 and the governing non-linear resilient modulus equation was (*10*):

$$M_r = k_1 p_a * \left(\frac{\theta}{p_a}\right)^{k_2} * \left(\frac{\sigma_d}{p_a}\right)^{k_3} \quad (6.2)$$

where:

M_r = resilient modulus, psi
k_1 = 581.08 (*10*)
k_2 = 0.8529 (*10*)
k_3 = -0.1870 (*10*)
p_a = atmospheric pressure = 14.6 psi
θ = bulk stress = $\sigma_1 + 2*\sigma_3$
σ_d = deviator stress = $\sigma_1 - \sigma_3$

The resulting aggregate base modulus was 12,530 psi with an assumed Poisson ratio of 0.40. The gradation information entered into the MEPDG is shown in Table 6.2. It is important to note that the aggregate base modulus was found to be lower than the subgrade soil modulus. While this is atypical, it is consistent with other studies at the Test Track comparing these two materials (*10*, *11*).

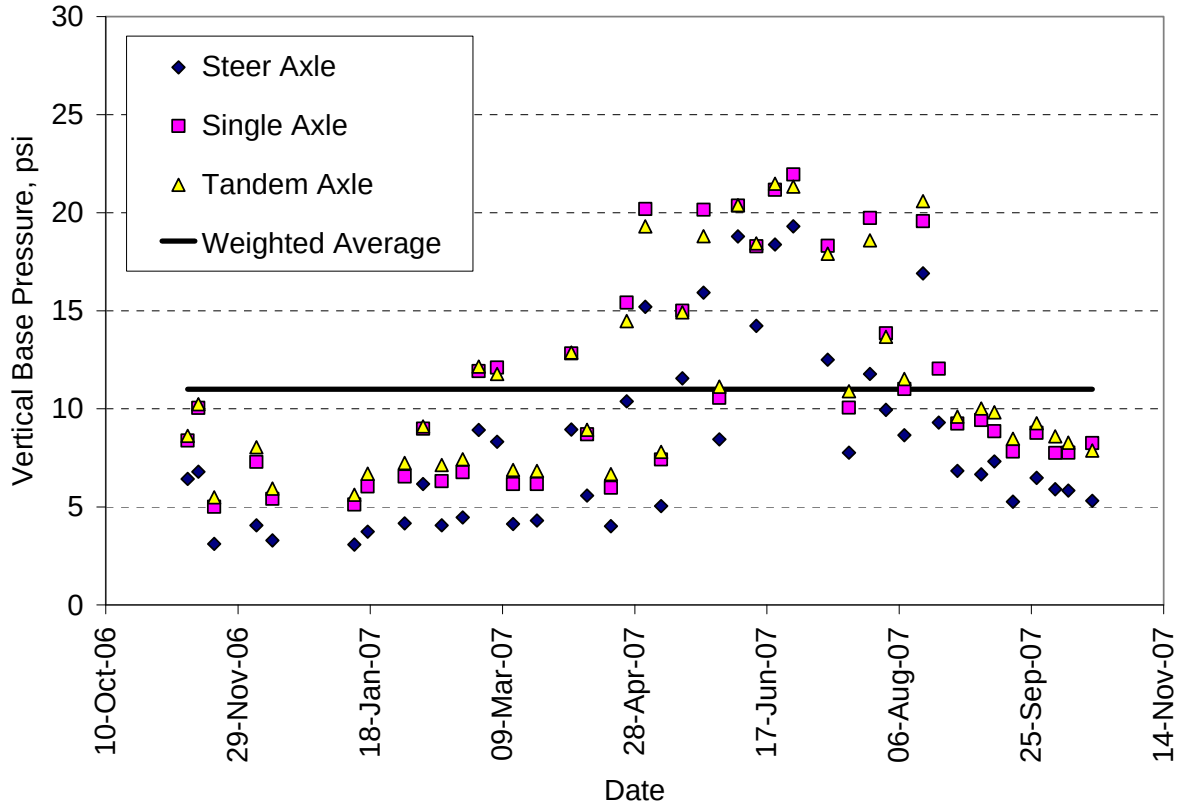

FIGURE 6.6 Vertical Stress Measurements in Base Aggregate Base (Section S11).

TABLE 6.2 Aggregate Base Gradation

Sieve Size	Percent Passing
1 1/2"	100
1"	95
3/4"	88
1/2"	83
3/8"	78
#4	57
#8	47
#16	39
#30	31
#50	23
#100	15
#200	10.2

6.2.6 HMA Materials

The HMA materials were characterized according to MEPDG Level 1 input criteria. These criteria included measured dynamic modulus of the mixtures at various temperatures and frequencies, dynamic shear modulus of the Rolling thin-film oven (RTFO) aged binder at three temperatures and an assortment of general properties of the mixtures. Entering the appropriate data into the MEPDG was somewhat challenging and is described in the following subsections.

6.2.6.1 HMA Dynamic Modulus (E*)

The E* data of the various mixtures were presented in Section 5.1 of this report. These data required some manipulation prior to entering into the MEPDG because of some special requirements of the MEPDG. First, the MEPDG requires the minimum test temperature to be between -12.2 and -6.6ºC (10 and 20ºF). The coldest test temperature for this project was 4.4ºC (40ºF) and was selected for ease of testing and that pavement temperatures in central Alabama rarely fall below 4.4ºC (40ºF). Second, the maximum test temperature must be between 51.6 and 57.2ºC (125 and 135ºF) in the MEPDG. The warmest temperature tested was 37.7ºC (100ºF) and was selected because warmer temperatures can become very difficult to generate meaningful results. Third, the MEPDG does not allow E* data in excess of 5,000,000 psi. Since this project was using the Thiopave material, which was meant to stiffen the virgin binder and ultimately the mixture, it was expected that the resulting E* would exceed 5,000,000 psi for some combinations of temperature and loading frequency. Given all these limitations, the E* data required special treatment to be entered into the MEPDG which then created a master curve for each of the mixtures.

Since E* data were generated at 4.4, 21.1, and 37.7ºC (40, 70 and 100ºF), it was decided to extrapolate the data, by using non-linear regression, to reach -9.4ºC (15ºF) and 54.4ºC (130ºF). The raw data were used to generate regression equations having the form:

$$E^* = a \cdot b^{Temperature} \cdot Frequency^{c} \tag{6.3}$$

where:

E* = mixture dynamic modulus, psi
Temperature = test temperature, F
Frequency = test frequency, Hz
a,b,c = regression constants

In general, the regression results were deemed sufficiently accurate for this study ($R^2 \geq 0.98$). Figure 6.7 plots the E* data generated from the regression equations versus the measured E* data while Table 6.3 tabulates the regression coefficients and corresponding R^2 values.

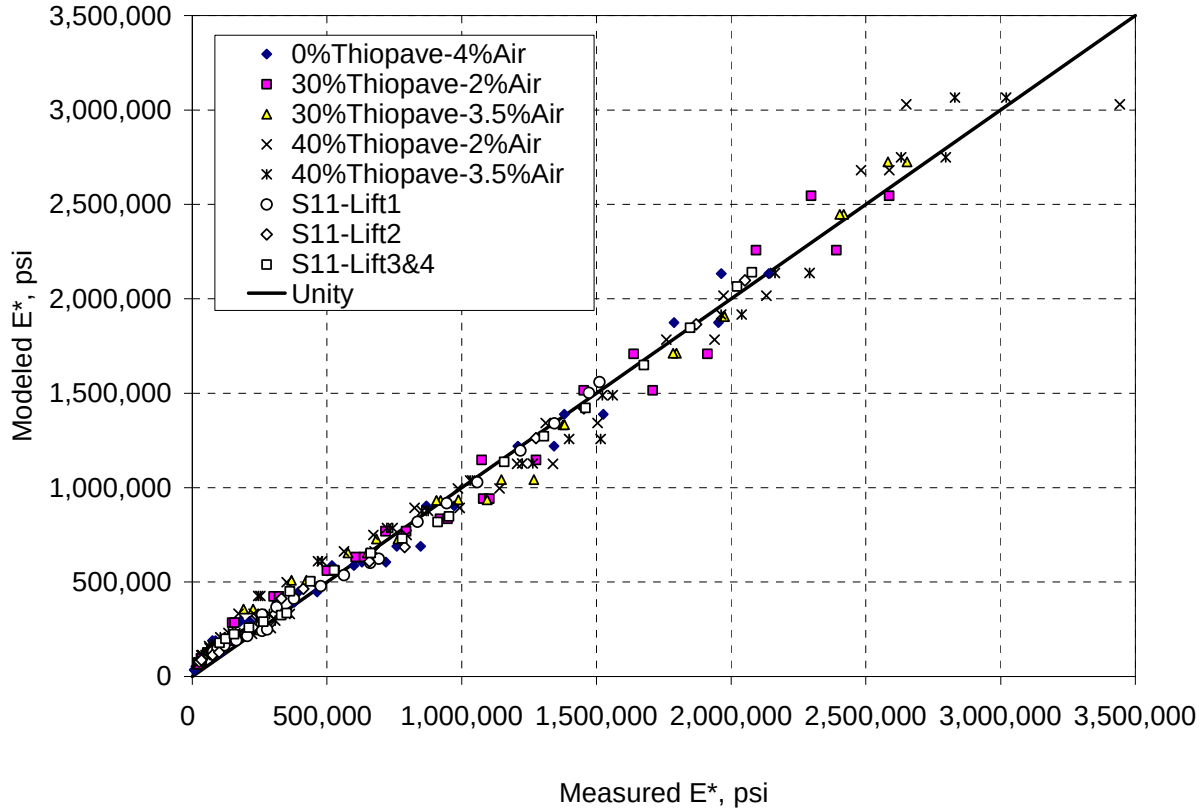

FIGURE 6.7 Predicted vs. Measured E* Data.

TABLE 6.3 E* Regression Coefficients and R^2 Values

Mixture	a	b	c	R^2
0%Thiopave-4%Air	6,230,321	0.9631	0.1866	0.99
30%Thiopave-2%Air	6,394,857	0.9675	0.1732	0.98
30%Thiopave-3.5%Air	6,830,164	0.9685	0.1553	0.99
40%Thiopave-2%Air	7,510,446	0.9676	0.1769	0.98
40%Thiopave-3.5%Air	6,978,065	0.9708	0.1568	0.99
S11-Lift1	3,112,030	0.9699	0.1646	0.99
S11-Lift3&4	4,370,389	0.9696	0.1619	0.99

Ideally, only measured E* data would be entered into the MEPDG. However, due to the limitations related to temperatures noted above, it was necessary to use the regression equations to extrapolate to more extreme temperatures. To meet the requirements of the MEPDG and still enter as much measured data as possible, the input data sets were a combination of extrapolated and measured data. The regression equations were used to generate E* data at the lowest and highest temperatures while the measured data were kept for the intermediate temperatures as documented in Tables 6.4 through 6.10. In cases where the measured and extrapolated data were contradictory (e.g., the extrapolated E* at the highest temperature was higher than the measured

E* at the next highest temperature), the appropriate measured data were eliminated from the input data set entered into the MEPDG. This was the case for the E* data measured at 37.7ºC (100°F) in Tables 6.4 through 6.8. This allowed the MEPDG to successfully create a master curve. It should be noted that the proposed lift 2 for the control section contains a different binder (PG 67-22) than that used in S11 (PG 76-22). Therefore, when developing the control cross-section, the 0% Thiopave at 4% air voids was used for this lift since it contains PG 67-22 as the base binder. Also, the Thiopave mixtures were tested at 5 and 10 Hz frequencies. In some cases, however, E* exceeded 5,000,000 psi and had to be left out of the MEPDG input.

TABLE 6.4 MEPDG E*(psi) Input Data – 0% Thiopave – 4% Air

	Frequency, Hz					Measured or
Temperature, C	0.01	0.1	0.5	1	5	Predicted?
-9.4	1,500,556	2,306,071	3,113,972	3,543,995	4,785,587	Predicted
4.4	558,903	920,047	1,275,534	1,452,916	1,870,117	Measured
21.1	80,394	195,511	346,568	428,369	674,208	Measured
54.4	19,851	30,507	41,195	46,884	63,310	Predicted

TABLE 6.5 MEPDG E*(psi) Input Data – 30% Thiopave – 2% Air

	Frequency, Hz				Measured or
Temperature, C	0.01	0.1	0.5	1	Predicted?
-9.4	1,754,249	2,613,740	3,453,852	3,894,336	Predicted
4.4	755,719	1,175,168	1,581,129	1,775,479	Measured
21.1	152,725	312,484	514,304	622,574	Measured
54.4	39,148	58,329	77,077	86,907	Predicted

TABLE 6.6 MEPDG E*(psi) Input Data – 30% Thiopave – 3.5% Air

	Frequency, Hz				Measured or
Temperature, C	0.01	0.1	0.5	1	Predicted?
-9.4	2,068,460	2,957,315	3,796,759	4,228,128	Predicted
4.4	913,738	1,378,511	1,790,708	1,973,166	Measured
21.1	207,839	395,663	613,365	723,738	Measured
54.4	52,337	74,827	96,067	106,982	Predicted

TABLE 6.7 MEPDG E*(psi) Input Data – 40% Thiopave – 2% Air

	Frequency, Hz				Measured or
Temperature, C	0.01	0.1	0.5	1	Predicted?
-9.4	2,029,537	3,049,643	4,053,809	4,582,486	Predicted
4.4	908,661	1,408,026	1,848,724	2,051,196	Measured
21.1	199,572	394,358	620,254	733,818	Measured
54.4	45,962	69,064	91,805	103,778	Predicted

TABLE 6.8 MEPDG E*(psi) Input Data – 40% Thiopave – 3.5% Air

	Frequency, Hz				Measured or
Temperature, C	0.01	0.1	0.5	1	Predicted?
-9.4	2,173,151	3,117,774	4,012,468	4,473,006	Predicted
4.4	1,035,569	1,541,316	2,000,360	2,226,329	Measured
21.1	248,740	474,056	732,876	863,845	Measured
54.4	71,843	103,072	132,650	147,875	Predicted

TABLE 6.9 MEPDG E*(psi) Input Data – S11 – Lift 1

	Frequency, Hz						Measured or
Temperature, C	0.5	1	5	10	20	25	Predicted?
-9.4	1,756,400	1,968,603	2,565,513	2,875,471	3,222,877	3,343,416	Predicted
4.4	835,804	944,340	1,218,220	1,344,113	1,472,278	1,511,486	Measured
21.1	259,521	313,185	476,981	563,375	660,985	691,975	Measured
37.7	77,489	94,120	163,573	205,132	259,472	277,941	Measured
54.4	52,460	58,798	76,627	85,885	96,261	99,862	Predicted

TABLE 6.10 MEPDG E*(psi) Input Data – S11 – Lift 3 and 4

	Frequency, Hz						Measured or
Temperature, C	0.5	1	5	10	20	25	Predicted?
-9.4	2,458,627	2,750,572	3,569,202	3,993,019	4,467,161	4,631,474	Predicted
4.4	1,157,594	1,304,856	1,676,636	1,848,167	2,021,584	2,076,940	Measured
21.1	362,400	438,207	662,193	779,674	910,981	953,139	Measured
37.7	101,226	123,137	210,643	263,823	330,154	351,426	Measured
54.4	70,623	79,009	102,524	114,698	128,317	133,037	Predicted

6.2.6.2 Binder Shear Modulus and Phase Angle (G* and δ)

There was no G* testing done specifically for this project since G* and phase angle cannot be accurately measured for the Thiopave-modified PG 67-22 because of the specific-gravity difference between sulfur and asphalt. However, G* had been completed on the RTFO-aged binders used in the S11 test section in the 2006 Test Track following test method AASHTO T 315. These data were used as primary G* inputs to the MEPDG. It is important to recognize that though the G* data are required for input, they are not used by the MEPDG in constructing the master curve when E* data have been provided. They are used for aging computations, but in this study aging is not a significant issue since the field sections are subjected to only two years of testing. Therefore, the G* data can largely be viewed as placeholders and were entered into the simulations according to the virgin binder used in each lift. Tables 6.11 and 6.12 list the G* and phase angle (δ) data for the PG 76 and 67-22 binders, respectively.

TABLE 6.11 PG 76-22 Shear Modulus and Phase Angle

Temperature, C	G*, Pa	Phase Angle (degrees)
21.1	1,881,000	57.98
37.7	134,200	60.55
54.4	22,420	58.39

TABLE 6.12 PG 67-22 Shear Modulus and Phase Angle

Temperature, C	G*, Pa	Phase Angle (degrees)
21.1	2,156,000	55.80
37.7	241,800	61.59
54.4	26,710	70.67

6.2.6.3 General Mixture Properties

The MEPDG requires a number of general mixture properties in addition to the specific E* and G* data described above. These inputs included:

- The master curve reference temperature which was left as the default 70^{o}F.
- The as-built effective volumetric binder content which was set to match the as-built values for Section S11. This was done on a lift-by-lift basis and was held constant between the non-Thiopave and Thiopave-modified mixtures. The pertinent values are listed in Table 6.13.
- The as-built air void content which was also set to match the as-built lifts in Section S11. These data are also listed in Table 6.13.
- The as-built unit weight of each lift. Like the above two inputs, these were also based on S11 data and were consistent between non-Thiopave and Thiopave mixtures. The values are listed in Table 6.13.
- Poisson ratio was set to 0.35 for all mixtures.
- Thermal conductivity was set to the default 0.67 BTU/hr/ft/^{o}F for all mixtures.
- Heat capacity was set to the default 0.23 BTU/lb/^{o}F for all mixtures.

TABLE 6.13 As-Built Properties of Mixtures

S11 Lift	Effective Volumetric Asphalt Content, %	Air Voids, %	Unit Weight, pcf
1	11.29	6.76	143.36
2	9.78	5.79	150.38
3	7.67	7.44	148.37
4	7.05	8.24	147.27

6.2.7 *MEPDG Results and Discussion*

Two sets of analyses were conducted with the MEPDG. The first was meant to simulate, as closely as possible, the existing section S11 so a quantitative assessment of the MEPDG could be made using existing performance data. The second analysis simulated the proposed nine cross sections shown in Figure 6.2. These two analyses are described below.

6.2.7.1 Analysis of Existing Section S11

The relevant data described above were entered into the MEPDG and simulated for Section S11. It is important to note that the as-built thicknesses were used rather than design thicknesses in this evaluation. The MEPDG generated plots of rutting, bottom-up fatigue cracking and top-down cracking for each distress. These were compared against actual measurements of these distresses.

Figure 6.8 shows the comparison between the measured rutting and the simulated rutting using the MEPDG. The S11 measurements were made using the NCAT ARAN van while the MEPDG predictions represent the 50^{th} percentile rut depths. While there is a definable offset between the two curves, the general trend is captured in that rut depth accumulation accelerates during warmer months and slows during cooler months. Furthermore, one could argue that predictions within 3-4 mm of measured, given the number of assumptions made in this analysis, is sufficiently accurate. Finally, calibration of the default transfer function for rutting could bring these two curves more in alignment. Therefore, the rut depth predictions can be characterized as reasonably accurate.

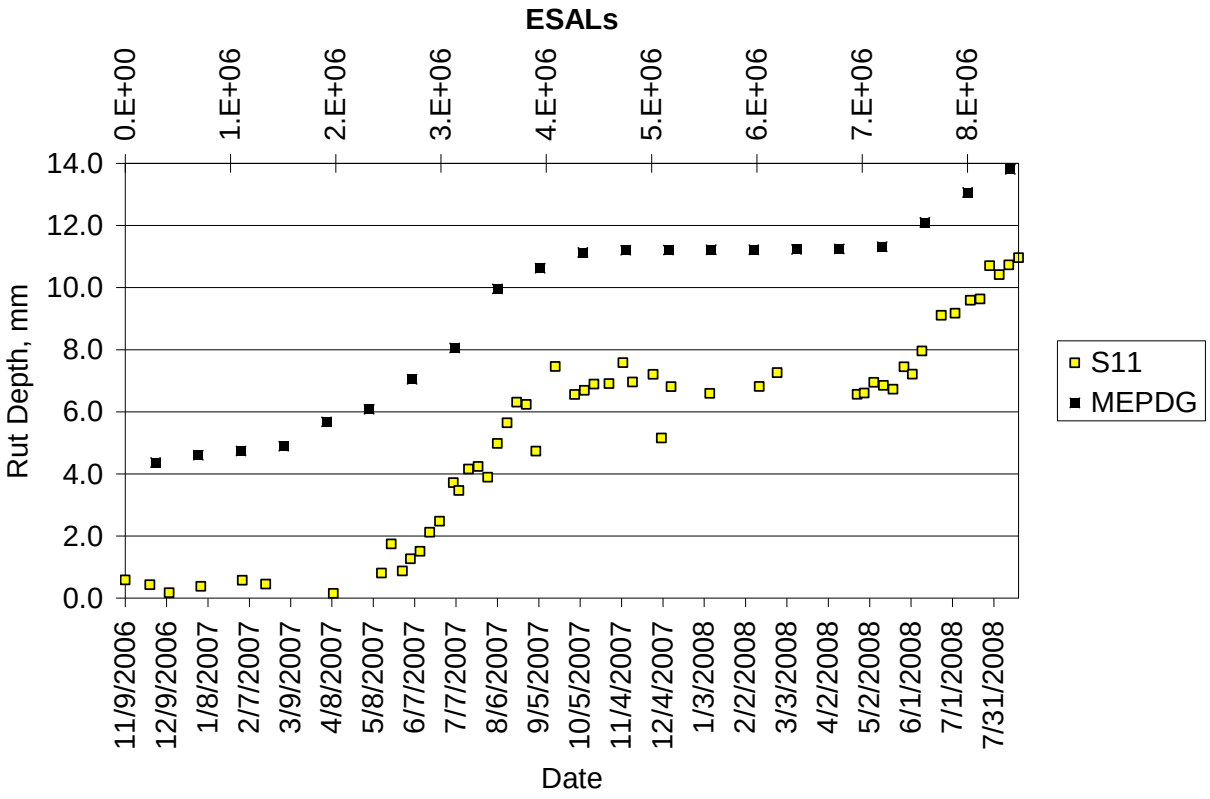

FIGURE 6.8 Measured and Simulated Rut Depths for Section S11.

Figure 6.9 illustrates the bottom-up crack progression in Section S11. The cracks were mapped on a weekly basis, with these three graphs representing snapshots in time. Each graph represents the central 150 ft of the test section with traffic moving right to left. The vertical axis represents the offset from the pavement centerline with the upper portion of each graph representing the outside wheelpath and the lower portion representing the inside wheelpath. It is important to note that cracking did not initiate until 5.6 million ESAL, but once it began, progressed quite rapidly.

Figure 6.10 compares the measured crack progression to the MEPDG prediction. Clearly, they follow different paths toward a similar result in June, 2008. The most concerning aspect is that the MEPDG predicts seasonal damage accumulation while the observed accumulation occurred rapidly once it initiated. Also, the MEPDG is showing a slowing of crack accumulation toward the end of the simulation while the observed cracking appears to be continuing to accumulate at a increasing rate. This is a fundamental issue with the MEPDG that cannot be fixed by merely changing calibration coefficients of the transfer function. Therefore, though the MEPDG may be valuable for this study in examining relative amounts of cracking between sections, it is difficult to have confidence in its ability to accurately predict actual amounts of cracking.

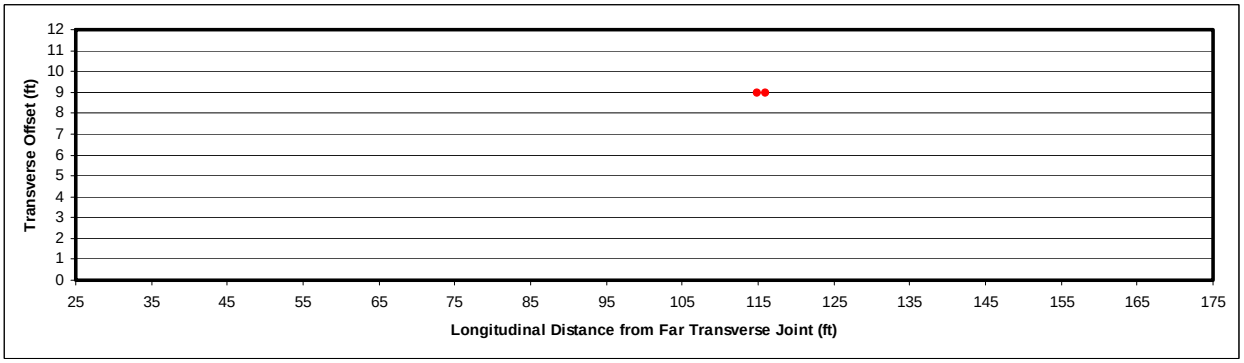

(a) 1/28/2008 @ 5.6 million ESAL and 0% of Lane Area Cracked

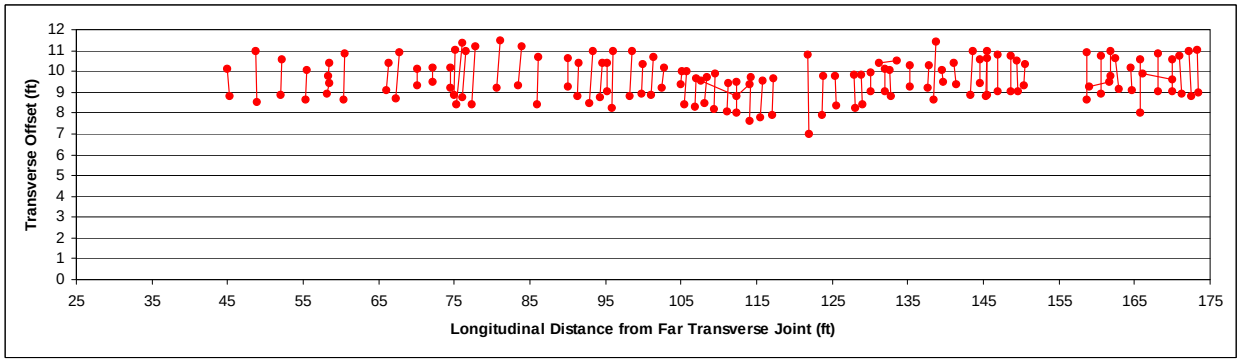

(b) 7/21/2008 @ 8.0 million ESAL and 24.5% of Lane Area Cracked

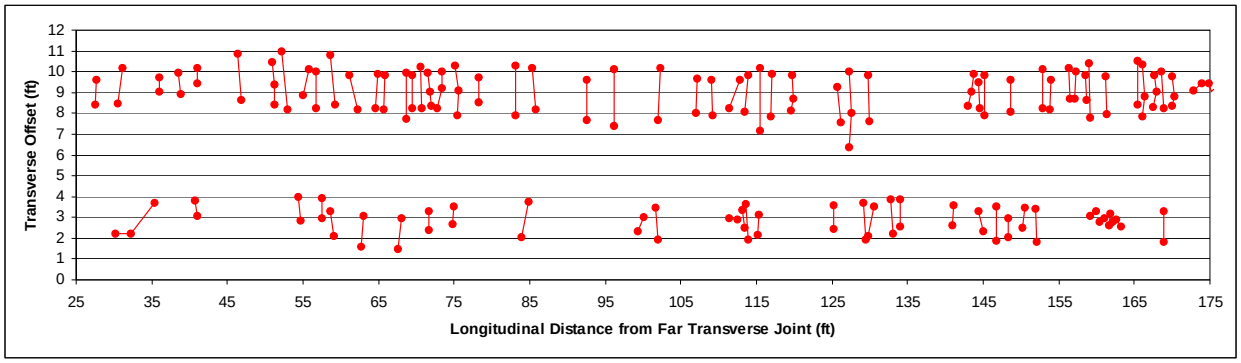

(a) 8/11/2008 @ 8.4 million ESAL and 36.2% of Lane Area Cracked

FIGURE 6.9 Fatigue Crack Progression in S11.

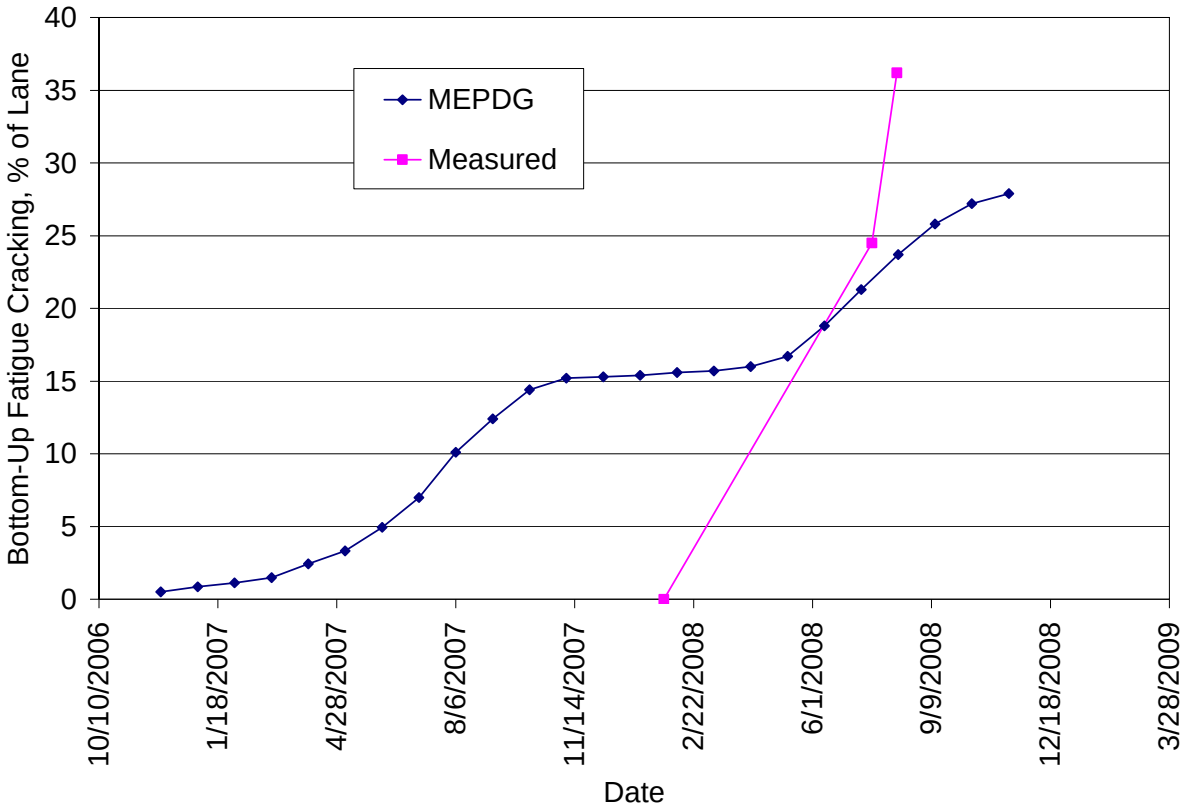

FIGURE 6.10 Measured and Simulated Fatigue Crack Progression in S11.

The final output evaluated was top-down cracking. No top-down cracking has been observed in Section S11. However, the MEPDG predicted it to reach 4,000 ft/mile by the end of the two-year cycle. Given this disparity, it was decided to discontinue top-down cracking from further consideration.

6.2.7.2 MEPDG Control and Thiopave Investigation

Nine sections were evaluated with the MEPDG. For convenience, Figure 6.11 illustrates the HMA lifts used in each section. The top lift of each cross section is 1 inch thick with the underlying layers comprising 2 inches per lift.

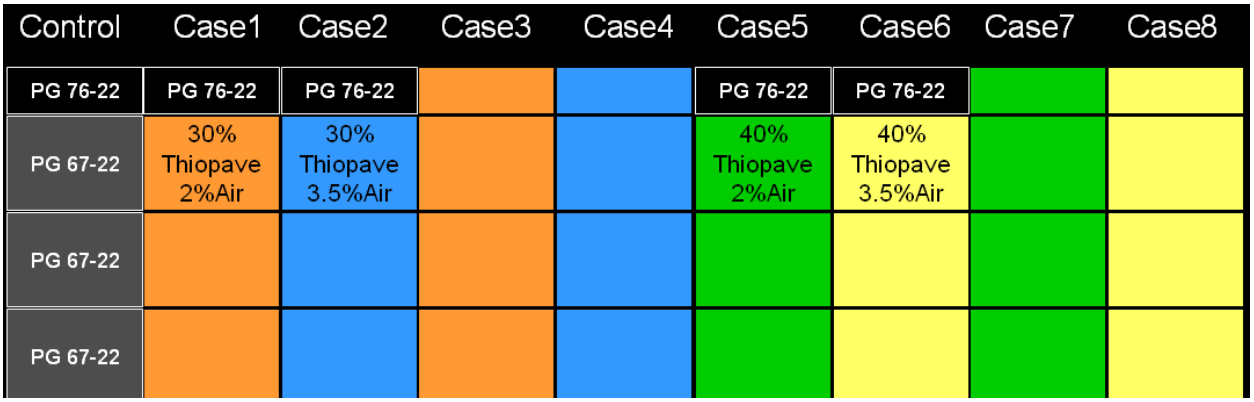

FIGURE 6.11 Pavement Cross Sections – HMA Lifts Only.

Figure 6.12 compares the MEPDG rutting prediction for each test section. Sections with the control mixture in the surface lift are shaded. As expected, due to the differences in E*, the control section is expected to develop the greatest amount of rutting with the Thiopave sections performing better in this respect. As more Thiopave is included in the pavement cross section, either through greater percentages or more layers, the rutting tended to decrease, though not appreciably. Also, the effect of the design air void content is evident where rutting is slightly reduced for mixtures with higher air voids and corresponding lower asphalt contents. Using 0.5 inches as a rutting threshold, the MEPDG predicts that the control section would fail while any of the Thiopave cross sections would perform satisfactorily over the two-year research cycle.

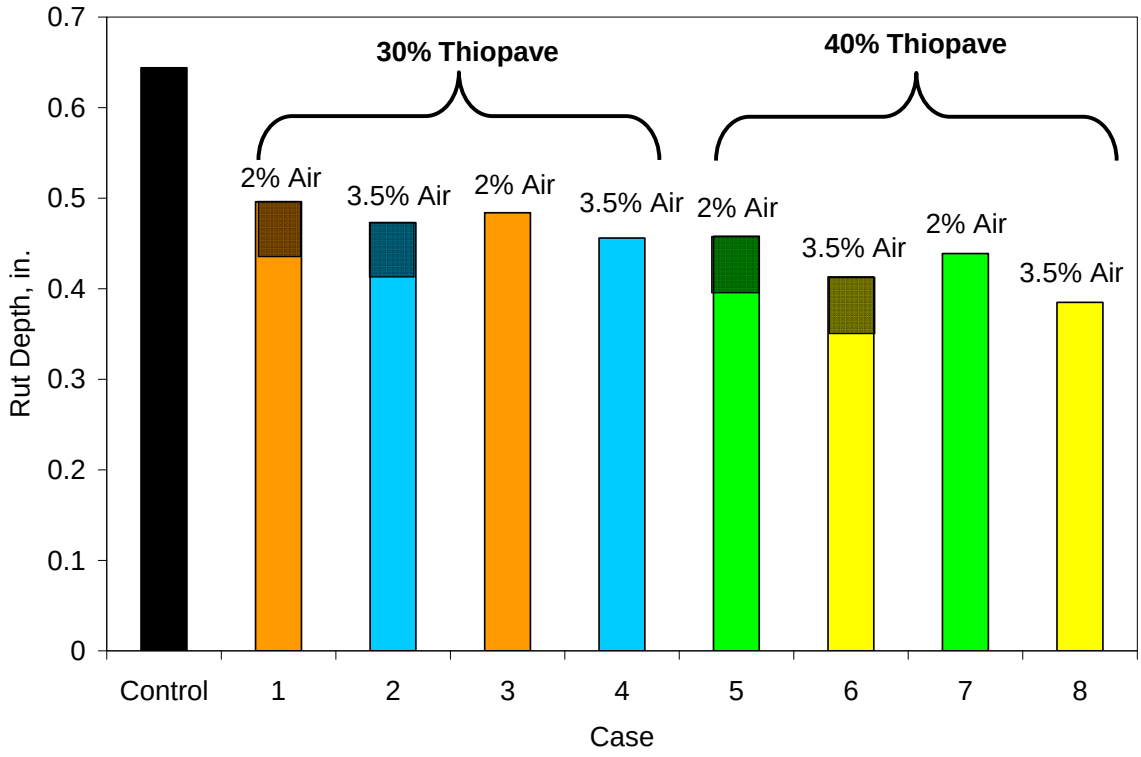

FIGURE 6.12 MEPDG Rutting Comparison.

Figure 6.13 compares the expected fatigue performance across all the cross sections. Again, there was a notable improvement in the Thiopave-modified sections. There also appeared to be greater differences among the Thiopave sections themselves with improved fatigue performance noted when additional Thiopave layers or Thiopave contents were included. As before with rutting, the higher air void content designs tended to show improved fatigue performance. Using 25% of lane area cracked as the design threshold, the MEPDG predicts the control section to clearly fail, while all but the first two Thiopave sections are expected to perform satisfactorily.

Though top-down cracking was not evaluated in this investigation due to the perceived inaccuracies of the MEPDG, it is important to note that a stiff upper lift of HMA could contribute to poor top-down cracking performance. Thus, even though the 40% Thiopave section at 3.5% air with all lifts modified appears to be superior for both fatigue and rutting, it is not recommended to use this section since top-down cracking could be a problem.

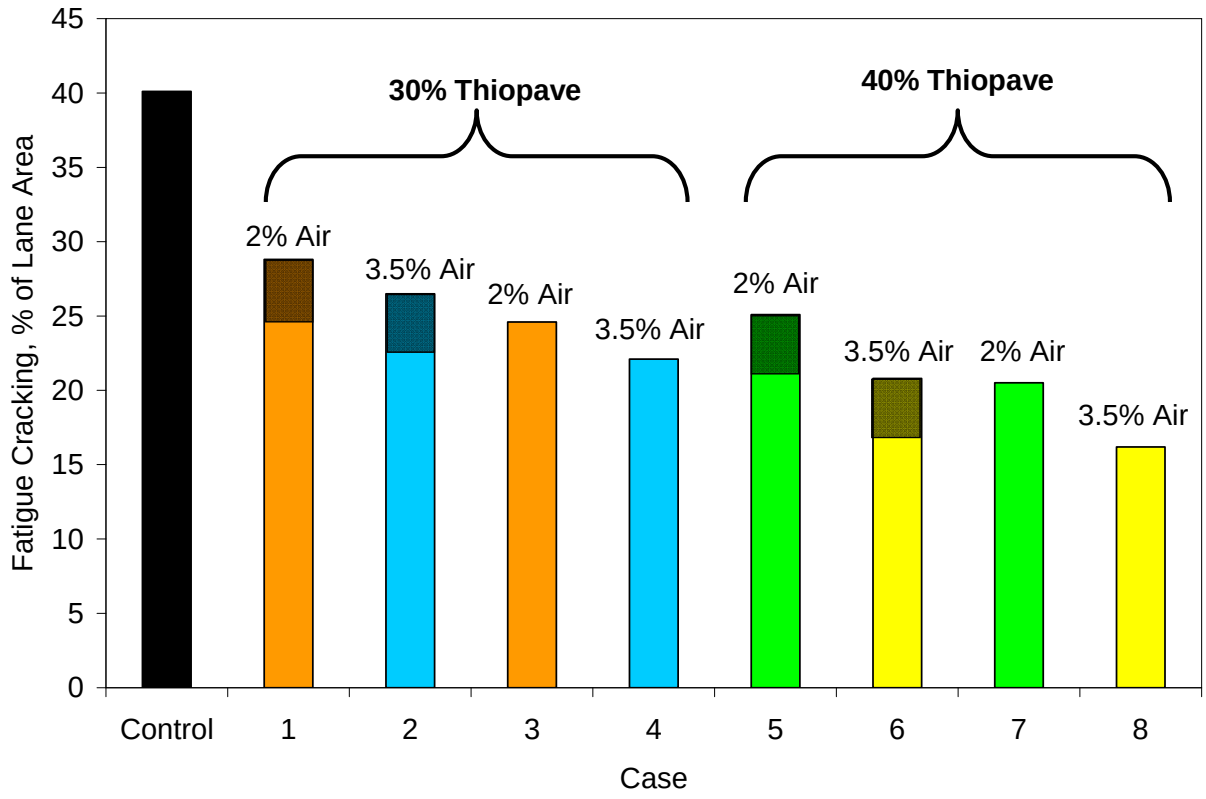

FIGURE 6.13 MEPDG Fatigue Cracking Comparison.

6.2.8 MEPDG Summary

Several key observations can be taken from the MEPDG investigation that include:

- Substantial data manipulation required to simulate test cases.
- Depending on materials, Thiopave appears to have potential to significantly improve performance relative to the control section for rutting and fatigue cracking. Differences were

more significant in fatigue cracking which were likely due to the increase in dynamic moduli between cases.
- Longitudinal top-down cracking predictions made by the MEPDG appear inaccurate.

6.3 PerRoad Investigation

The computer program, PerRoad was used in this investigation for three sets of analyses. The first was to evaluate the nine 7 inch cross-sections discussed above. The second was to develop perpetual pavement cross sections for each of the nine sets of cross-sections using 100 με as an endurance limit. The third analysis utilized 295 με as a less conservative endurance limit. PerRoad was a valuable tool in this investigation since it couples mechanistic analysis with Monte Carlo simulation in determining distributions of strain levels at critical locations in the pavement structure (*12*). The program, requisite inputs, outputs and discussion are presented in the sub-sections below.

6.3.1 Traffic

The main traffic input window in PerRoad is shown in Figure 6.14. In the "General Traffic Data" section of this input window, the only data used for computation is "Axle Groups/Day" which is typically computed from the other inputs. However, for this investigation, it was entered directly based on historical volume data at the Test Track. The relative percentages of each axle type were based directly on the truck configuration. As noted previously, each tractor trailer combination has a steer axle, a drive tandem and a set of five single axles. The relative percentages were 12.5% steer (1/8), 25% tandem (2/8) and 62.5% (5/8). The tandem axles were treated as two axles since studies of measured longitudinal strain at the Test Track had previously shown these axles to cause independent strain events (*13,14*).

The relative axle weight percentages were entered into the program according to the weights in Figure 6-3. It should be noted that the steer axles could be modeled directly in PerRoad whereas they were grouped with the other single axles in the MEPDG. Tire pressures were set at 100 psi for this analysis, consistent with the MEPDG analysis.

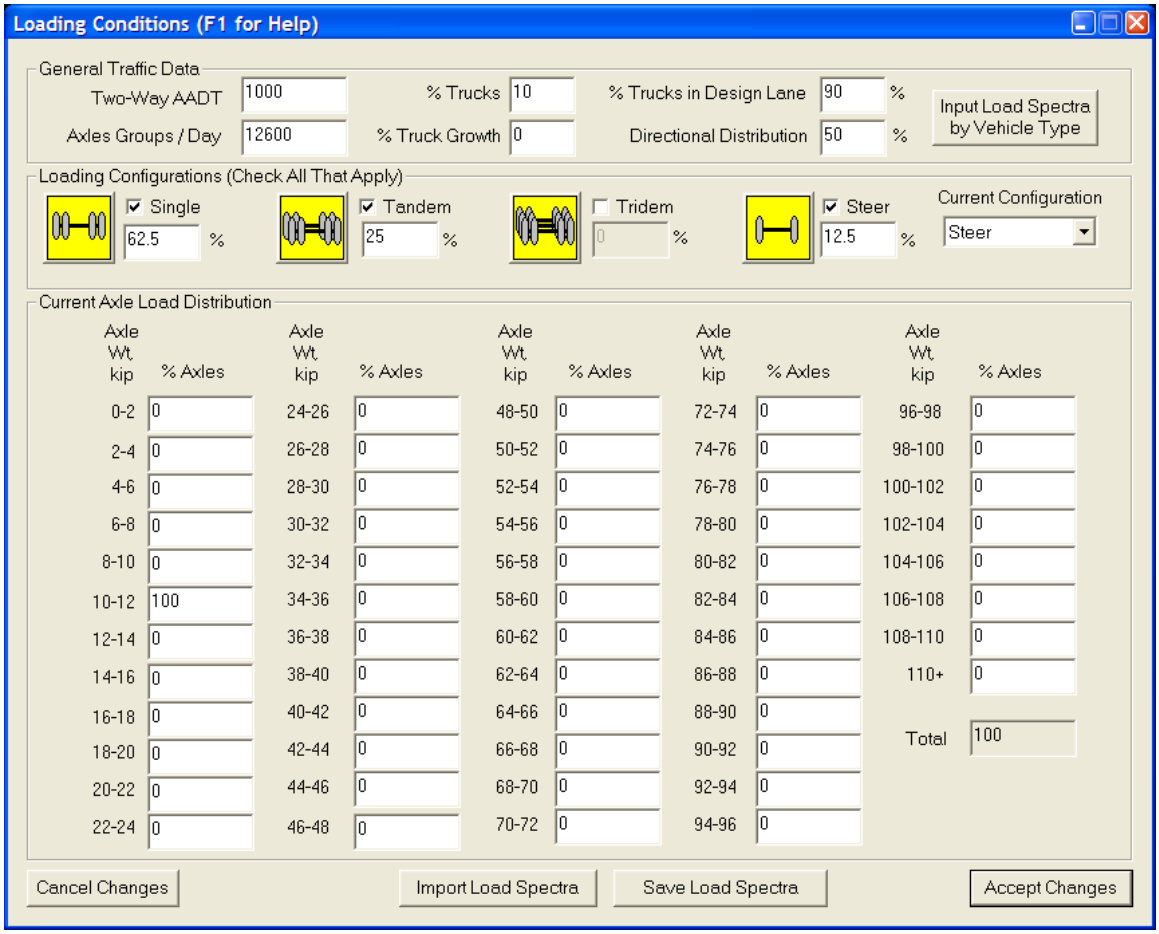

Figure 6.14 PerRoad Traffic Input Window.

6.3.2 Subgrade and Aggregate Base Properties

The average modulus of the subgrade and aggregate base was determined in the manner described above in the MEPDG analysis section. However, PerRoad can simulate the variability of the pavement layer moduli which was incorporated in this analysis. Data collected during the 2003 NCAT Test Track (*11*) on these materials indicated a lognormal distribution for modulus. The aggregate base coefficient of variation (COV) was set at 34% while the subgrade was set at 16.4%. The Poisson ratio was set at 0.40 for the aggregate base and 0.45 for the subgrade soil. Finally, the aggregate base thickness was set at an average of 6 inches normally distributed with a coefficient of variation of 14.8%. This level of variability was based on 12 surveyed depth locations from Section S11.

6.3.3 HMA Properties

Unlike the MEPDG that can handle a large number of pavement layers, and in fact subdivides layers entered by the designer into sublayers, PerRoad can only accommodate 5 pavement layers. Therefore, it was necessary to group two hot mix layers together to arrive at 5 total layers. Figure 6.15 illustrates the pavement cross sections analyzed by PerRoad. Basically, lifts three

and four from the previous analysis were grouped into one layer in this analysis. Since they are the same materials, this was not deemed problematic.

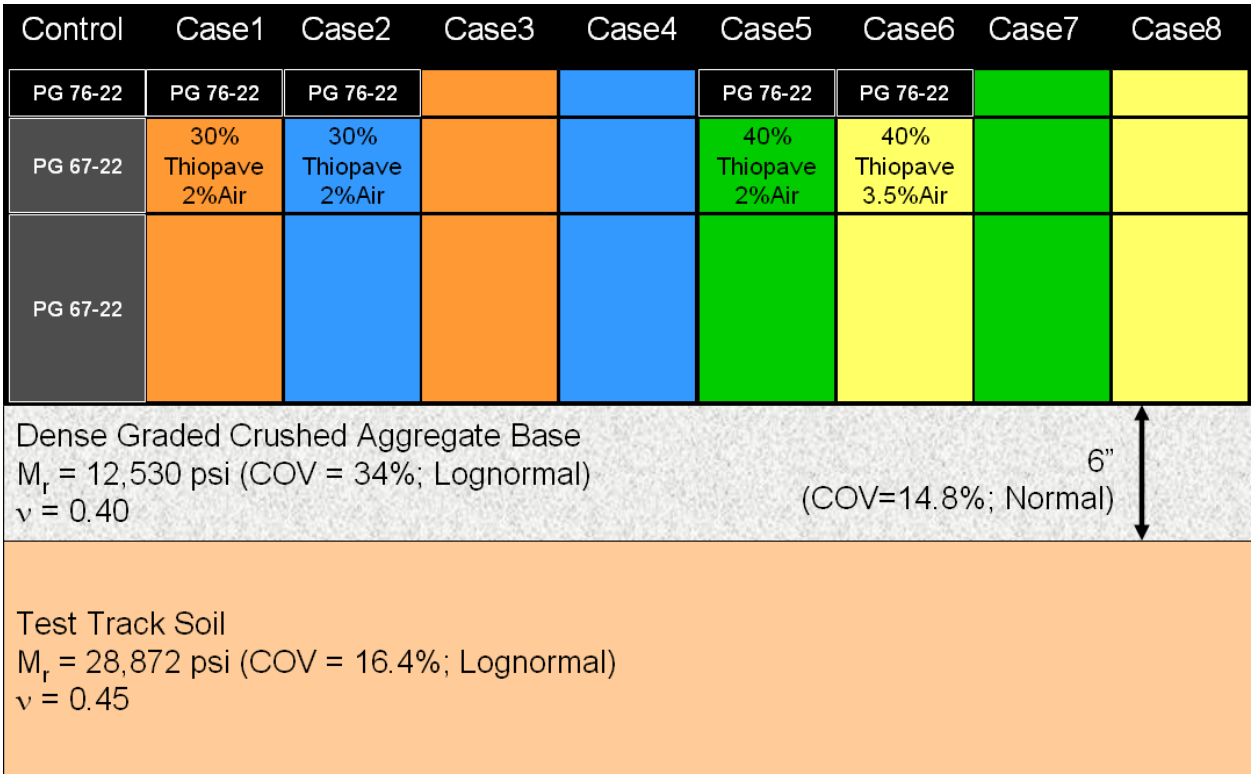

FIGURE 6.15 PerRoad Cross Sections.

For this analysis, measured pavement temperatures from the 2006 Test Track were used to establish the HMA moduli (E*). Temperature probes embedded at the top, middle and bottom of the HMA in Section S11 were used to generate hourly average in situ temperatures from November 10, 2006 through November 10, 2007. Mid-lift temperatures were then interpolated to represent the midpoint of Lifts 1, 2 and 3 shown in Figure 6.15. Figure 6.16 illustrates these temperatures where the seasonal trend is clearly evident.

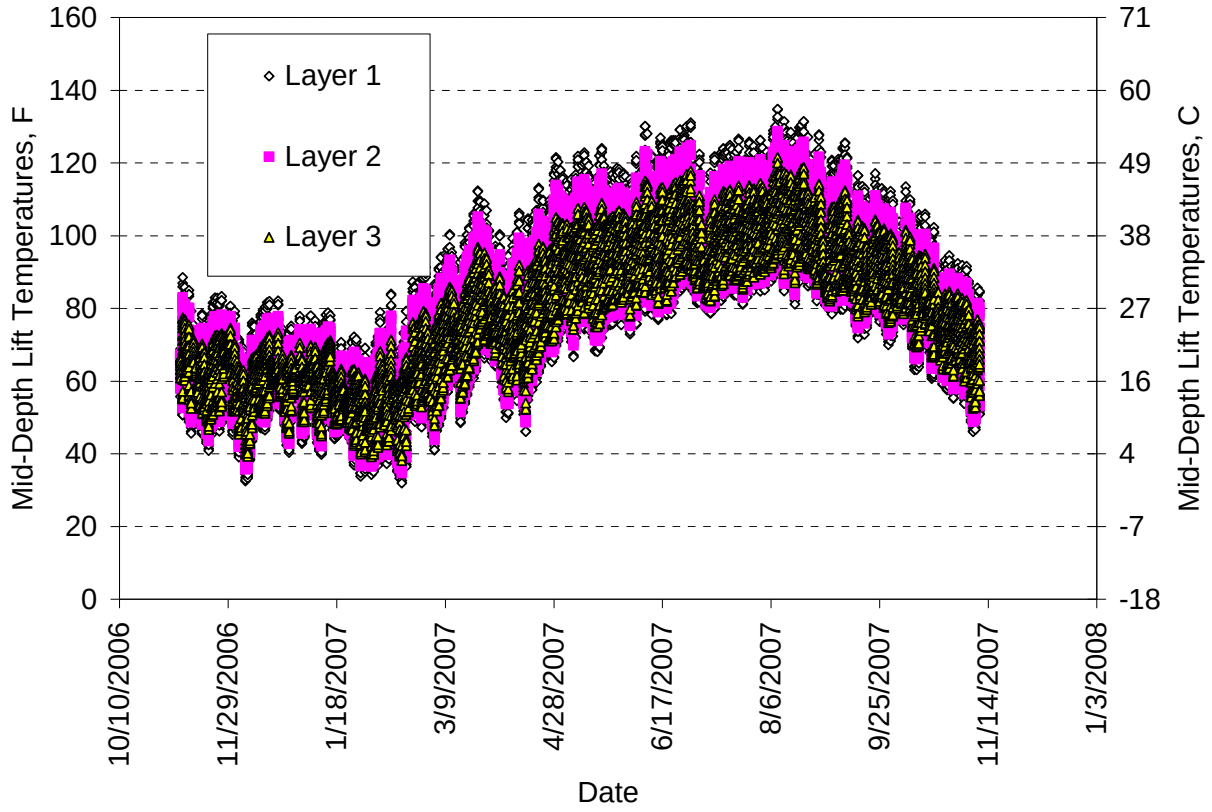

FIGURE 6.16 In Situ Measured Temperatures.

PerRoad can simulate five distinct seasons represented by an average modulus in that season. To accommodate this level of detail, the temperature data compiled in Figure 6.16 were converted into E* data using the previously developed equation (Equation 6.3) for each mixture. The coefficients for each mixture were listed in Table 6.3. The frequency was set at 10 Hz for this conversion. Figure 6.17 illustrates the resulting layer moduli for the as-built layers in Section S11 where again the seasonal trends are clearly evident. These trends were observed for the other mixtures as well.

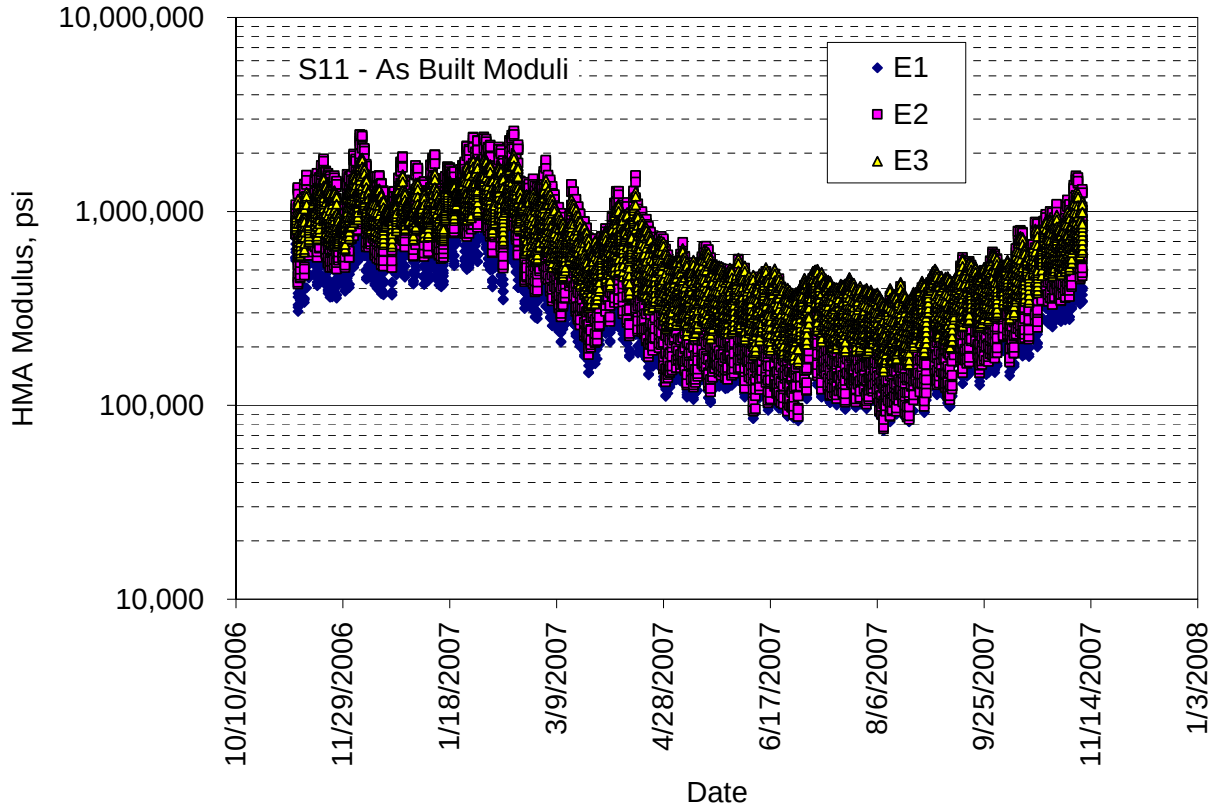

FIGURE 6.17 S11 – As Built HMA Moduli.

Since PerRoad can simulate five seasons, the layer moduli developed on an hourly basis were used to compute the 90th, 70th, 50th, 30th and 10th percentile values for each layer. These points represent the midpoint in each "season" as characterized by temperature. Figure 6.18 plots these "seasonal" values for the control case and one Thiopave cross section (Case 3). It is clear that the Thiopave moduli are significantly higher at each percentile when compared to the control mixtures. Additionally, a lognormal distribution was modeled around each seasonal value with a coefficient of variation equaling 26%. This value was consistent with previous measures of variability at the Test Track (*11*). Table 6.14 lists the seasonal input moduli for each cross-section derived by this method.

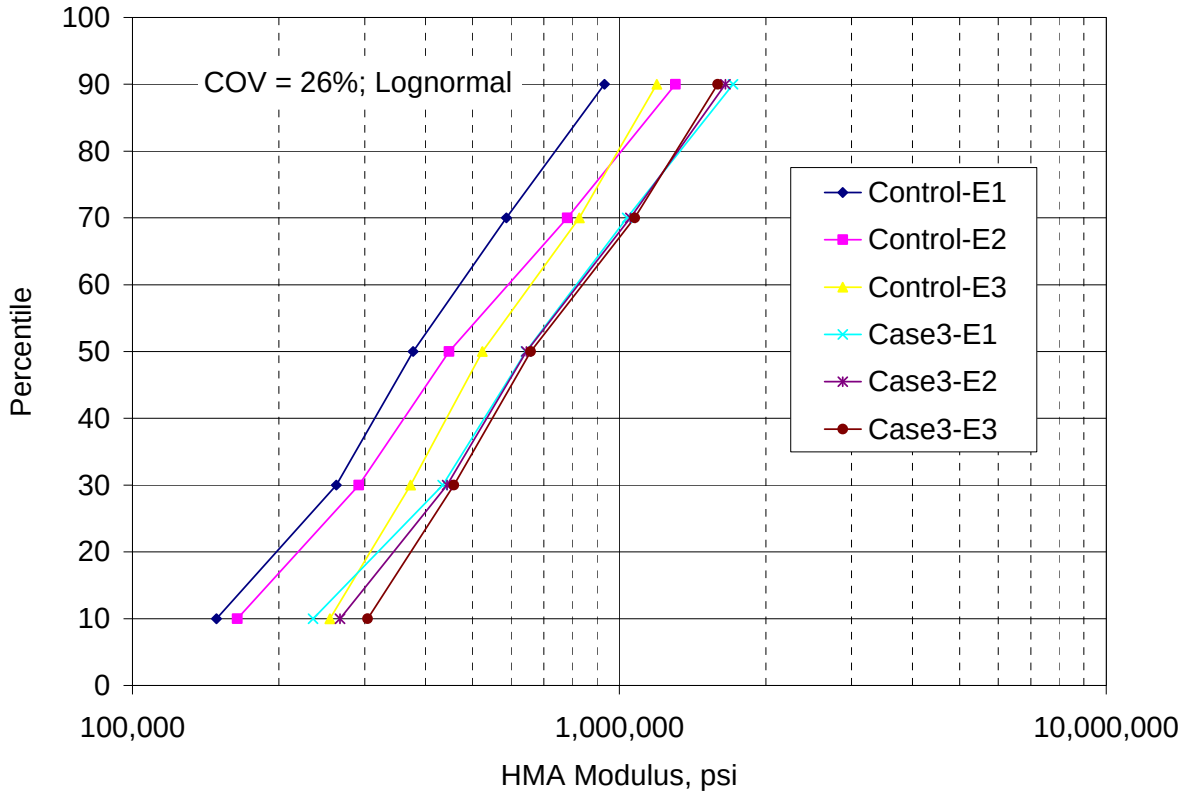

FIGURE 6.18 "Seasonal" Moduli for Control and Thiopave-Case 3.

TABLE 6.14 Seasonal HMA Moduli

		HMA Modulus, psi				
Section	**Lift**	**Season 1**	**Season 2**	**Season 3**	**Season 4**	**Season 5**
Control	1	932,239	586,439	377,224	262,172	148,898
	2	1,303,686	781,969	447,147	291,765	164,138
	3	1,194,333	827,586	523,298	372,703	254,450
Case 1	1	932,239	586,439	377,224	262,172	148,898
	2	1,650,931	1,053,370	644,446	442,775	267,031
	3	1,592,773	1,075,258	658,102	457,537	304,003
Case 2	1	932,239	586,439	377,224	262,172	148,898
	2	1,792,886	1,161,048	721,944	502,209	307,976
	3	1,731,777	1,184,369	736,733	518,390	349,119
Case 3	1	1,713,208	1,037,034	643,073	433,640	234,982
	2	1,650,931	1,053,370	644,446	442,775	267,031
	3	1,592,773	1,075,258	658,102	457,537	304,003
Case 4	1	1,858,244	1,143,633	720,458	492,186	272,159
	2	1,792,886	1,161,048	721,944	502,209	307,976
	3	1,731,777	1,184,369	736,733	518,390	349,119
Case 5	1	932,239	586,439	377,224	262,172	148,898
	2	1,968,738	1,258,329	771,303	530,704	320,685
	3	1,813,743	1,226,293	751,968	523,531	348,402
Case 6	1	932,239	586,439	377,224	262,172	148,898
	2	2,079,201	1,389,688	894,494	638,883	405,974
	3	2,013,405	1,415,553	911,472	657,949	456,031
Case 7	1	2,042,711	1,238,890	769,666	519,796	282,336
	2	1,968,738	1,258,329	771,303	530,704	320,685
	3	1,813,743	1,226,293	751,968	523,531	348,402
Case 8	1	2,149,391	1,370,349	892,786	627,051	362,001
	2	2,079,201	1,389,688	894,494	638,883	405,974
	3	2,013,405	1,415,553	911,472	657,949	456,031

6.3.4 Seven-Inch Cross Sections – Results and Discussion

Each of the cross sections was simulated in PerRoad from which cumulative strain distributions were generated. Strains were examined at the bottom of the asphalt layer (horizontal, tensile) and at the top of the subgrade (vertical, compressive), respectively. Figure 6.19 summarizes the HMA tensile strain data while Figure 6.20 contains the subgrade strain data. Both graphs show a marked gap between the control section and the Thiopave sections. To further quantify this gap, Figures 6.21 and 6.22 contain the 90th percentile strain data for the HMA and subgrade, respectively. It is interesting to note the relative similarities between Figures 6.21 (HMA strain)

and 6.13 (MEPDG fatigue) in addition to Figures 6.22 (Subgrade strain) and 6.12 (MEPDG rutting). In both sets of cases, it appears that Thiopave has a relatively similar influence in that fatigue and asphalt strain is more affected by the amount of lifts of Thiopave while rutting and subgrade strain is less affected by these factors. In this way, the MEPDG and PerRoad results were judged to be consistent. While these plots provide relative measures of pavement response, they will ultimately be used as a basis of comparison for the measured pavement sections when they are built.

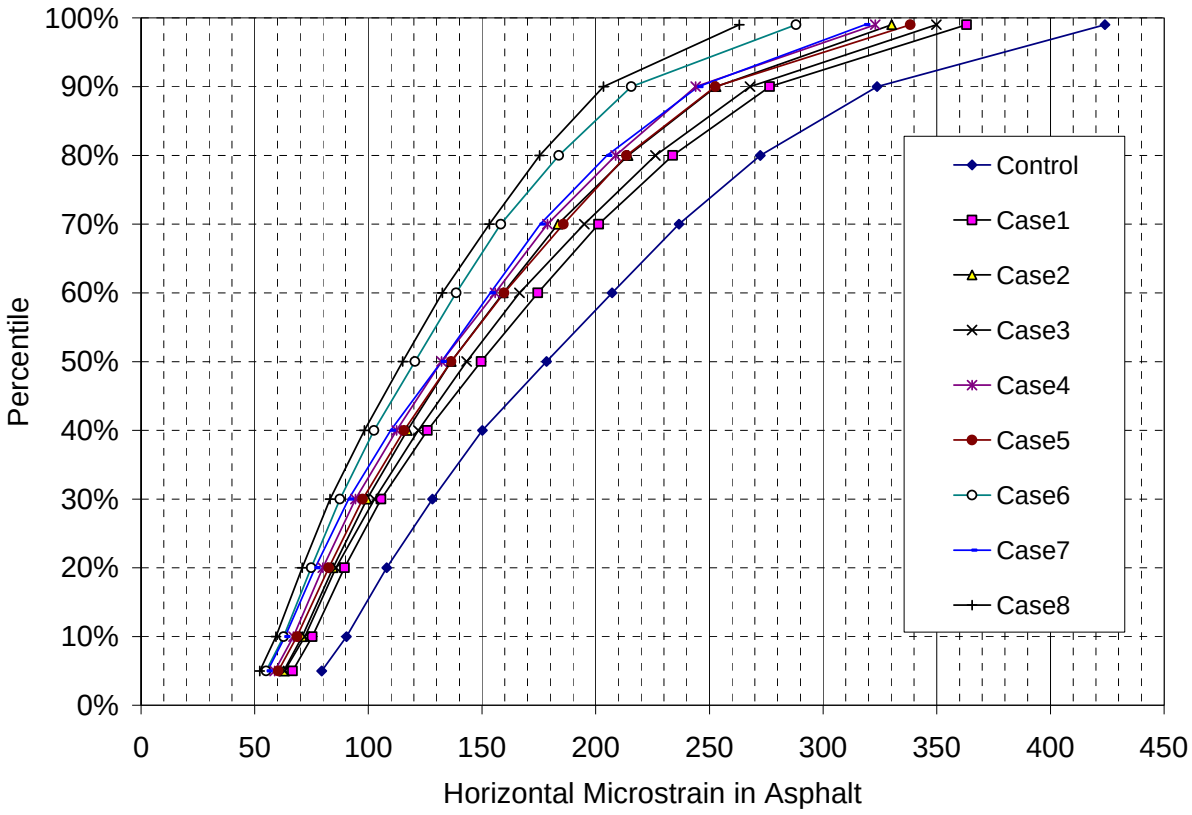

FIGURE 6.19 Horizontal Tensile Strain in HMA.

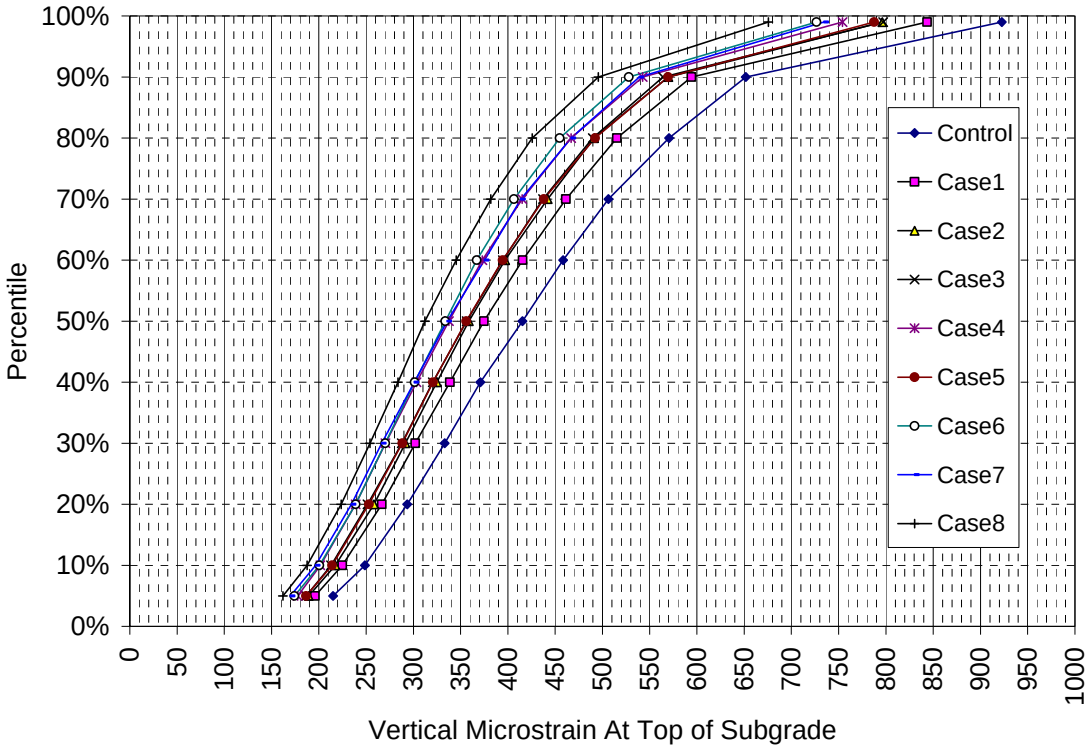

FIGURE 6.20 Vertical Compressive Strain in Subgrade.

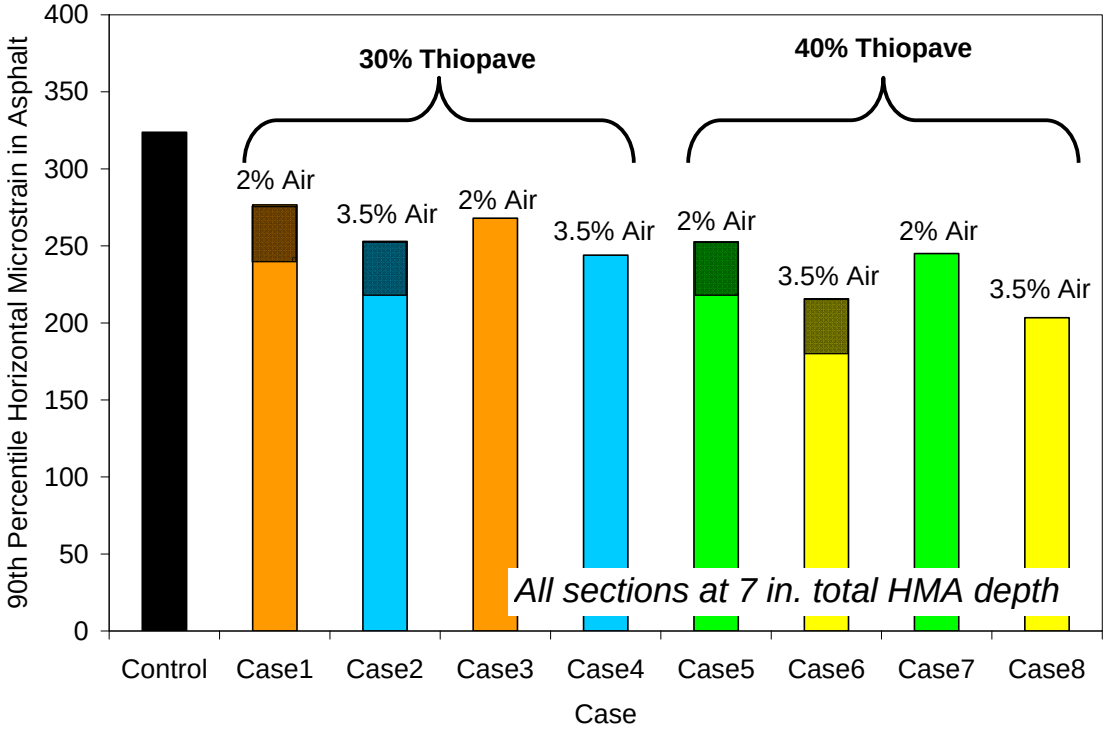

FIGURE 6.21 90th Percentile HMA Strain.

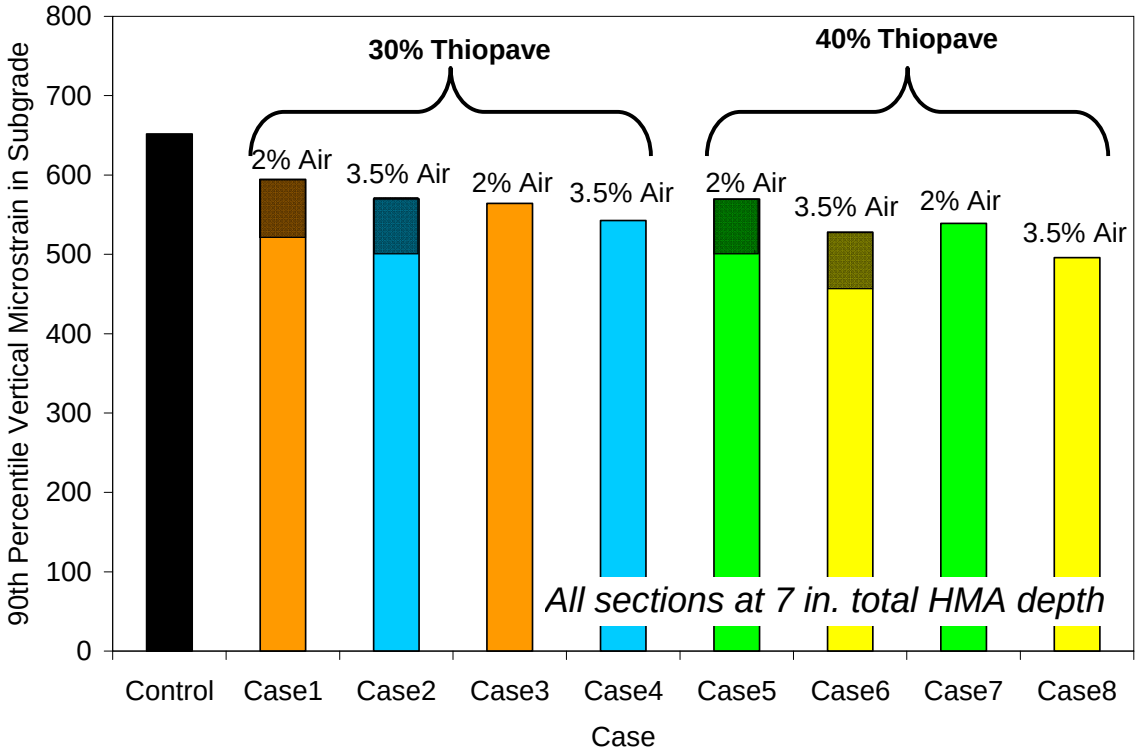

FIGURE 6.22 90th Percentile Subgrade Strain.

6.3.5 Perpetual Investigation – 100 με – Results and Discussion

In addition to the 7 inch sections analyzed above, perpetual pavement cross-sections were developed that were expected to eliminate bottom-up fatigue cracking. Currently, there is much debate about what strain level to use as a basis for design. This portion of the investigation designed the sections for 90% below 100 με. 100 με appears to be a conservative estimate of the endurance limit based on research in NCHRP 9-38. While the previous PerRoad analysis focused on equivalent thickness and the resulting strain distributions, this portion of the analysis varied the thickness of the bottom lift of HMA such that 90% of the tensile strains fell below 100 με.

Figure 6.23 shows the resulting asphalt strain distributions from the PerRoad structural design procedure. Figure 6.24 plots the total HMA thickness needed to achieve 90% below 100 με. The control section would need 9 inches of additional HMA, compared to the conventional MEPDG analysis using a 7 inch cross-section, to reach this target strain threshold while the Thiopave sections would require an additional 5 to 7 inches of HMA. This is a significant increase in the Thiopave sections, but also a significant savings versus the control section.

It is also important to examine the vertical strain data for these sections. These distributions are shown in Figure 6.25. A commonly used threshold for rutting is 200 με (*15*) which corresponds to the 80th percentile in these plots. Though this is less than the more stringent value of 90%

applied to the fatigue criteria, given previous performance of the unbound materials at Test Track, it is not expected that rutting in these layers will be a problem for these cross sections.

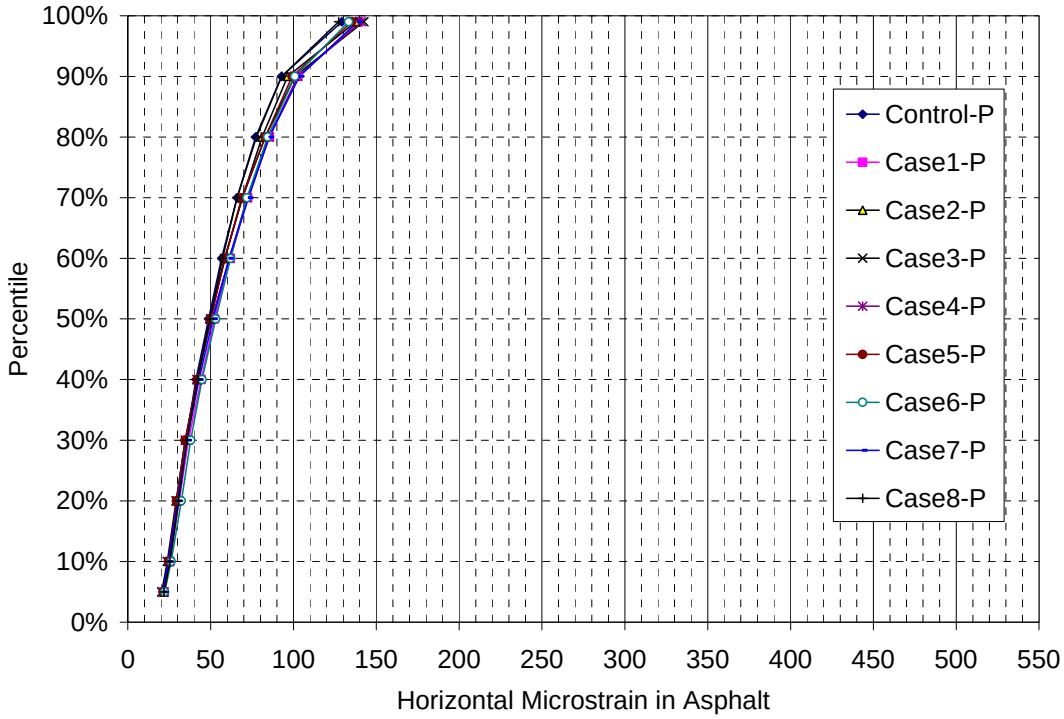

FIGURE 6.23 Strain Distributions Corresponding to 90% Below 100 με.

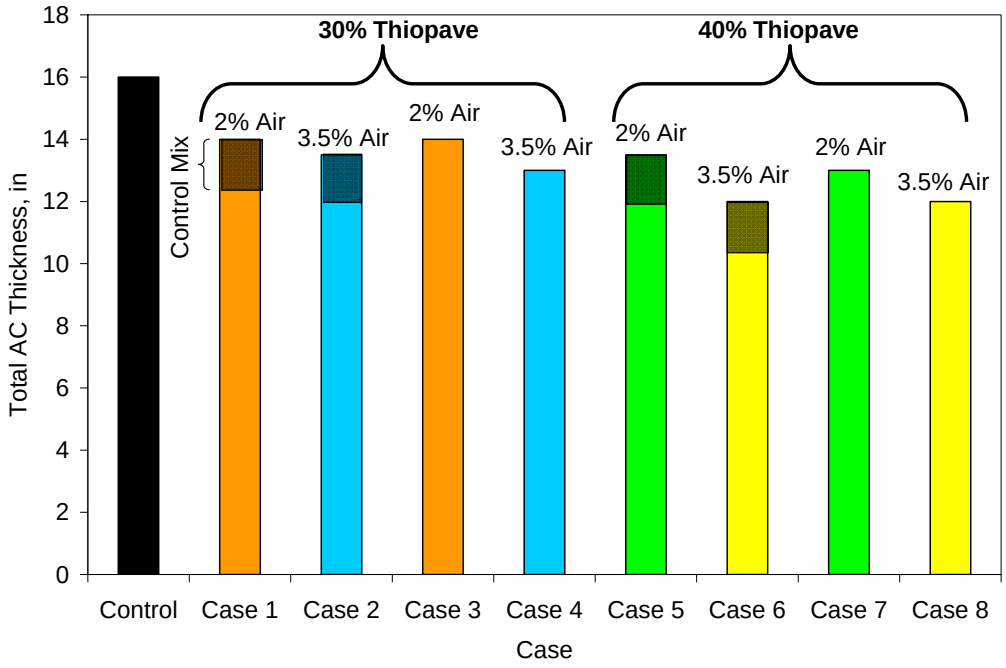

FIGURE 6.24 Total HMA Thickness Needed to Achieve 90% Below 100 με.

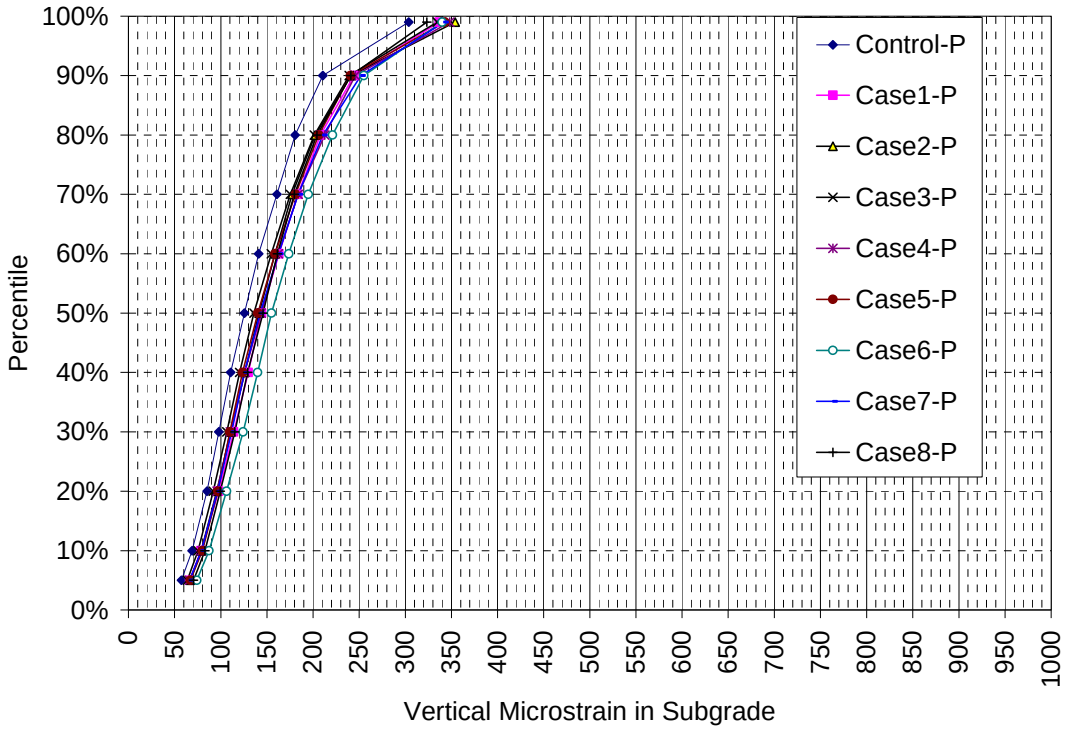

FIGURE 6.25 Vertical Strain Distributions for Perpetual Sections.

6.3.6 Perpetual Investigation – 295 με – Results and Discussion

The 100 με analysis was based upon thresholds developed in the laboratory. There is a common belief that the field threshold may be much higher than this value for a number of reasons that include:

- The laboratory test is conducted on a small specimen at a constant temperature, while in situ conditions include a continuous material and thermal cycling.
- The laboratory test is conducted at a single frequency with no rest periods. The opposite is true in the field.
- The laboratory test is conducted at either a constant strain or constant stress. This condition does not exist in the field where a range of stresses and strains are endured by the pavement.

Due to these and other reasons, it is reasonable to expect that the field threshold may be different than the lab threshold. Recent research by Willis *(16)* has established a recommended field-based strain distribution to preclude bottom-up fatigue cracking. This distribution, based upon testing at the Test Track, places the 90th percentile strain at 295 με. With Willis' distribution in mind, the third phase of the PerRoad analysis redesigned the nine sections to meet his recommended strain distribution.

Figure 6.26 shows the resulting total HMA thicknesses required to meet Willis' strain distribution. Note that the thicknesses are substantially thinner, as expected, than the 100 με requirement. Also, the control section is 0.5 inches thicker than the conventional MEPDG design, while the first three Thiopave sections already had reached "perpetual" status at 7 inches.

The remaining sections ranged between 5.5 and 6.5 inches. The 7.5 inch control section fits with previous studies at the Test Track where the optimal perpetual thickness is somewhere between 7 and 9 inches, with 9 inches likely on the conservative side (*16*). The stiffer materials found in the Thiopave, and the resulting lower strain values, naturally results in a thinner cross section.

The corresponding asphalt and subgrade strain distributions can be found in Figures 6.27 and 6.28, respectively. The biggest concern lies in the subgrade vertical strain distributions where the vertical strain exceeds the limit of 200 με approximately 95% of the time, for most cases. Subgrade deformation could be a problem in these sections despite the expected satisfactory fatigue performance.

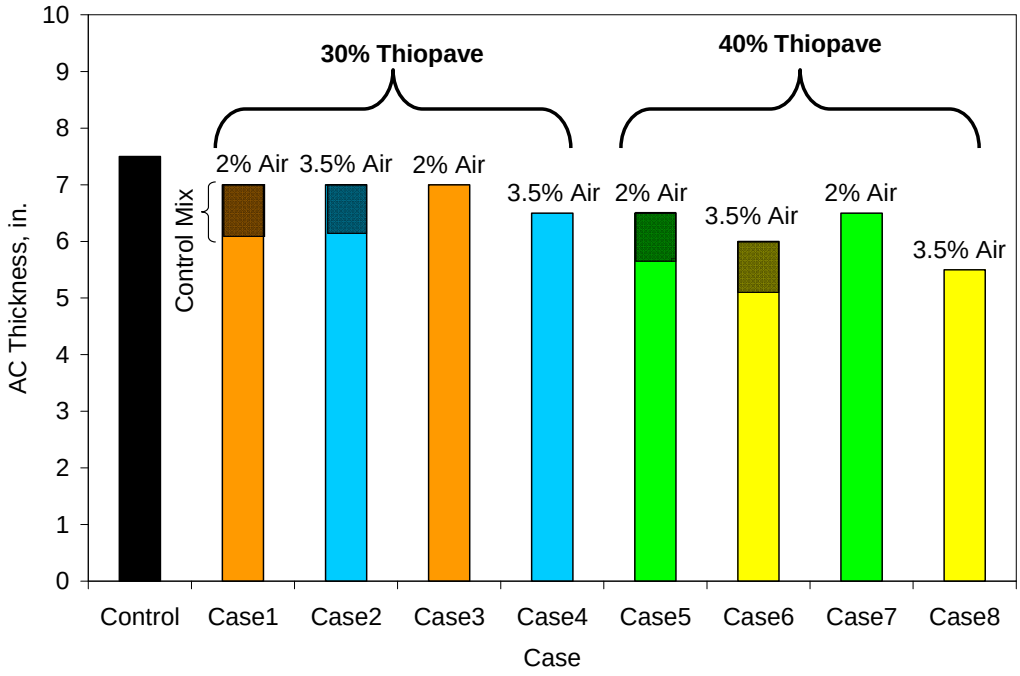

FIGURE 6.26 Total HMA Thickness Needed to Achieve 90% Below 295 με.

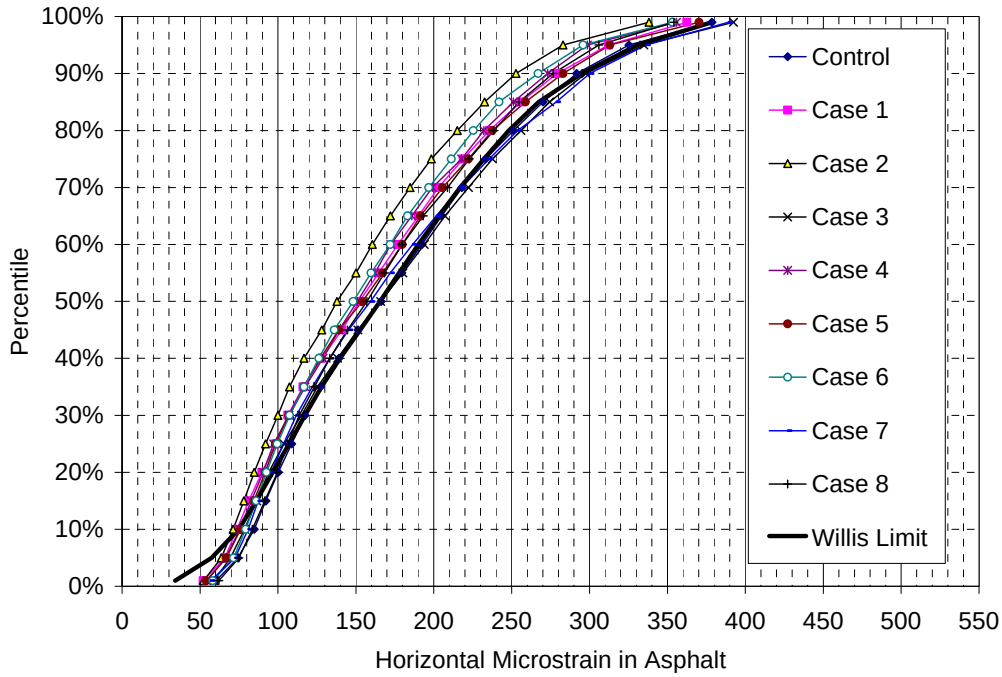

FIGURE 6.27 Asphalt Strain Distributions for 295 με Designs.

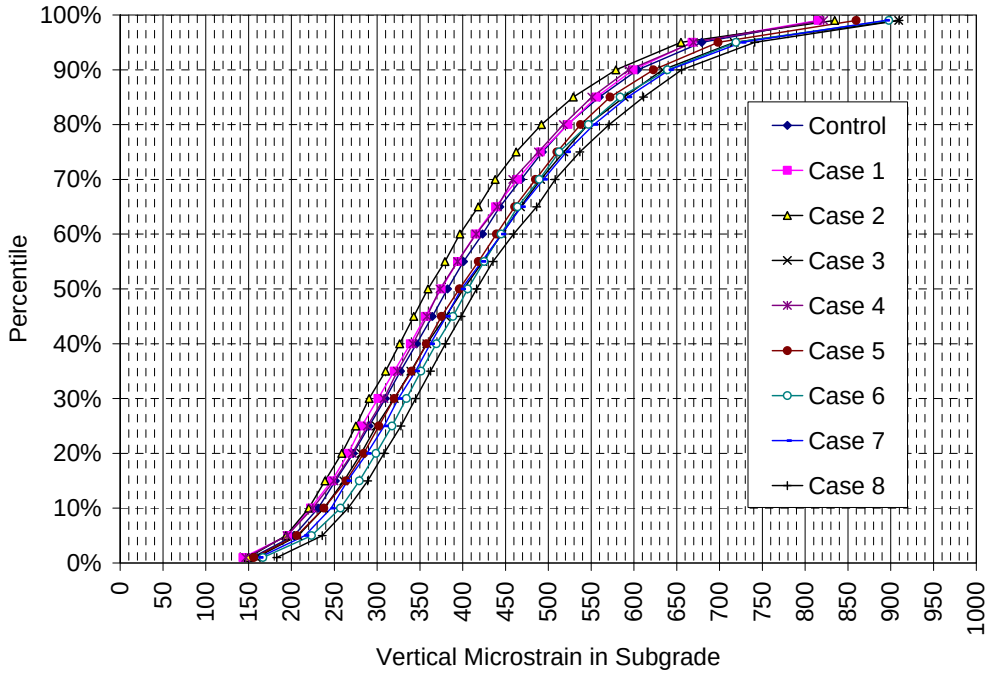

FIGURE 6.28 Subgrade Strain Distributions for 295 με Designs.

6.3.7 Perpetual Summary

This investigation consisted of three parts that examined the MEPDG cross-sections of 7 inches, the perpetual cross sections developed for an asphalt fatigue threshold of 100 με and finally

sections developed with a 295 με fatigue limit. The MEPDG investigation showed clear distinctions between the control and Thiopave sections and formed a basis of comparison for strain measurements that will be made when these sections are built. The 100 με fatigue threshold design substantially increased the design thicknesses, perhaps beyond what is practical and reasonable. Significant thickness reductions were noted, however, when comparing the control against the Thiopave sections. Finally, the 295 με fatigue threshold design resulted in a thicker control section (7.5 inches) and Thiopave sections either equaling or thinner than their 7-inch MEPDG counterparts. Caution must be exercised with these thin sections, however, as there could be vertical strain problems in the subgrade leading to permanent deformation problems.

7. CONCLUSIONS AND RECOMMENDATIONS

This study conducted the mix designs, evaluated the mechanistic and performance properties of the five mixtures—one control and four Thiopave-modified mixes—in the laboratory, and performed the theoretical structural pavement analysis to determine appropriate structural pavements for the field study in Phase II.

The following conclusions and recommendations are offered based on results of the laboratory study:

- The Thiopave mixtures had higher TSRs, but lower conditioned and unconditioned splitting tensile strength results than the control mix when tested without being allowed to cure for 14 days. This was likely a consequence of not allowing the Thiopave mixtures to cure for two weeks prior to testing. TSR testing showed a reduction in the TSR value for the Thiopave-modified mixes after they had been allowed to cure for 14 days. For two mixes (30 percent Thiopave mix with 2 percent design air voids and 40 percent Thiopave mix with 3.5 percent design air voids) used at the NCAT Pavement Test Track, mix design modifications or more additives will be explored with Thiopave to overcome this laboratory-measured moisture susceptibility limitation; a research plan is being planned.
- The control mix using a PG 67-22 binder exhibited lower E* results for all combinations of test temperatures and frequencies than the Thiopave mixes, especially at the high temperature and low frequency region, which means the Thiopave mixes would have higher rutting resistance.
- Based on the flow number, APA and Hamburg test results, all the Thiopave mixes had higher rutting resistance than the control mix. In general, the two Thiopave mixes with 3.5 percent design air voids exhibited the highest rutting resistance with the two Thiopave mixes with 2 percent design air voids having the second highest. The control mix showed the lowest rutting resistance among the five mixes evaluated in this study.
- The BBF test results showed that the control mix had a longer fatigue life at the 600 and 400 microstrain levels than all the Thiopave mixes. However, at the 200 microstrain level, the control mix exhibited a fatigue life that is shorter than that of the 30 percent Thiopave mix with 2 percent design air voids but higher than those of other Thiopave mixes.
- The 30 percent Thiopave mix with 2 percent design air voids had the highest endurance limit estimated according to the procedure proposed under NCHRP 9-38 (7). The control

mixture and the 40 percent Thiopave mix with 3.5 percent design air voids had the second highest endurance limit.
- Based on the TSRST results, the addition of the Thiopave material had no tangible impact on the low temperature cracking susceptibility of the asphalt mixture.
- Based on the results of the laboratory study, the 30 percent Thiopave mixture with 2 percent design air voids shows balanced rutting and fatigue cracking resistance that is better than that of the control mix. Thus, it is recommended that this Thiopave mix be used in Phase II study at the NCAT Pavement Test Track.

The following conclusions and recommendations are offered based on results of the structural pavement analyses:

- The MEPDG evaluation of Section S11 captured the rutting trend and accurately quantified the magnitude, though there was a slight offset between the MEPDG prediction and measured rut depth.
- The MEPDG evaluation of fatigue cracking in Section S11 did not accurately capture the development of fatigue cracking. However, the end result was reasonably accurate.
- The Thiopave sections were predicted by the MEPDG to have significant reductions in fatigue cracking and rutting compared to the control section. This effect tended to increase as more Thiopave lifts or more Thiopave material was used in a cross section.
- The PerRoad evaluation of the 7 inch cross sections indicated that significant reductions in tensile strains of the Thiopave section relative to the control section will likely be measured in the field.
- Perpetual pavement design using 100 με as the fatigue endurance limit resulted in seemingly over-conservative designs, though there was a 2 to 4 inch savings when comparing the Thiopave sections against the control.
- Perpetual designs using the 295 με "Willis Limit" for the fatigue threshold were more realistic. The Thiopave effect was a reduced pavement thickness on the order of 0.5 to 1.5 inches. There was concern, however, that some sections could be so thin that the base and/or subgrade could become overstressed, leading to rutting. Therefore, further investigation of the vertical stress/strain responses is warranted.
- Based on the structural analysis findings, it is recommended that 7 and 9 inch Thiopave cross sections be evaluated in the 2009 Test Track. The 7 inch cross-section may be perpetual and allow for many comparisons against the other materials in the structural experiment beyond the control section. Due to vertical stress/strain concerns, a section less than 7 inches is not recommended, so 9 inches is the logical alternative choice. This will allow for performance comparisons between the 7 and 9 inch sections in addition to comparing against section N3 which is also 9 inches and will be left in place for the 2009 investigation.

REFERENCES

1. Strickland, D., J. Colange, M. Martin, and I. Deme. *Performance Properties of Sulphur Extended Asphalt Mixtures with Modified Sulphur Pellets*. ISAP, 2008..
2. THIOPAVE Technical Information. Website: http://www.shell.ca/home/content/ca-en/shell_for_businesses/asphalt/Thiopave/Thiopave_technical.html. Accessed February 12, 2008.
3. Deme, I., and B. Kennedy. *Use of Sulfur in Asphalt Pavements.* Presented at the 5th International Symposium on Pavement Surface Characteristics, Roads and Airfields, Toronto, 2004.
4. Shell. *Shell THIOPAVE – Miscellaneous Lab Properties.* Powerpoint Presentation.
5. Bonaquist, R. *Refining the Simple Performance Tester for Use in Routine Practice*. NCHRP Report 614, TRB, Washington, D.C., 2008.
6. Biligiri, K.P., Kaloush, K.E., Mamlouk, M.S., and Witczak, M.W. Rational Modeling of Tertiary Flow for Asphalt Mixtures. *Journal of the Transportation Research Board: Transportation Research Record No. 2001*, 2007, pp. 63-72.
7. Prowell, B., et al. Endurance Limit of Hot Mix Asphalt Mixtures to Prevent Fatigue Cracking in Flexible Pavements. Draft Final Report for NCHRP 9-38, NCAT, Alabama, 2009.
8. Eres Consultants Division, Guide For Mechanistic-Empirical Pavement Design of New and Rehabilitated Pavement Structures. Final Report, NCHRP 1-37A, 2004.
9. American Association of State Highway and Transportation Officials, AASHTO Guide for Design of Pavement Structures, Washington, D.C., 1993.
10. Taylor, A.J., "Mechanistic Characterization of Resilient Moduli for Unbound Pavement Layer Materials," M.S. Thesis, Auburn University, 2008.
11. Timm, D.H. and A.L. Priest, "Material Properties of the 2003 NCAT Test Track Structural Study," Report No. 06-01, National Center for Asphalt Technology, Auburn University, 2006.
12. Timm, D.H. and D.E. Newcomb, "Perpetual Pavement Design for Flexible Pavements in the U.S.," International Journal of Pavement Engineering, Vol. 7, No. 2, June 2006, pp. 111-119.
13. Timm, D.H. and A.L. Priest, "Flexible Pavement Fatigue Cracking and Measured Strain Response at the NCAT Test Track," Proceedings of the 87th Annual Transportation Research Board, Washington, D.C., 2008.
14. Priest, A.L. and D.H. Timm, "Methodology and Calibration of Fatigue Transfer Functions for Mechanistic-Empirical Flexible Pavement Design," Report No. 06-03, National Center for Asphalt Technology, Auburn University, 2006.
15. Monismith, C.L. and F. Long (1999). Overlay Design for Cracked and Seated Portland Cement Concrete (PCC) Pavement – Interstate Route 710. Technical Memorandum TM UCB PRC 99-3, Pavement Research Center, Institute for Transportation Studies, University of California, Berkeley.
16. Willis, J.R., "Field-Based Strain Thresholds for Flexible Perpetual Pavement Design," PhD. Dissertation, Auburn University, 2008.

APPENDIX A Test Results for Mix Designs

TABLE A.1 Test Results for Mix Design (per Shell Design Spreadsheet)

Thiopave (%)	Thiopave + Bitumen (%)	Equivalent Binder (%)	Gmb	Gmm	Air Voids (%)	VMA	VFA	Dust Proportion
0	N/A	4.00	2.403	2.596	7.4	15.7	52.7	1.10
0	N/A	4.50	2.415	2.576	6.3	15.7	60.3	0.97
0	N/A	5.00	2.443	2.556	4.4	15.2	71.0	0.86
0	N/A	5.50	2.453	2.543	3.5	15.1	76.8	0.79
30	4.95	4.30	2.483	2.602	4.6	13.8	66.8	0.89
30	5.52	4.80	2.493	2.590	3.8	14.0	73.1	0.80
30	6.09	5.30	2.516	2.564	1.9	13.7	86.2	0.70
30	6.66	5.80	2.517	2.554	1.5	14.2	89.7	0.65
40	5.82	4.80	2.480	2.593	4.4	14.7	70.3	0.75
40	6.42	5.30	2.505	2.573	2.6	14.3	81.7	0.66
40	7.02	5.80	2.514	2.562	1.9	14.6	87.3	0.61

APPENDIX B TSR Testing Results

TABLE B.1 Test Results for TSR Testing (ALDOT Method – Less than 14 days of Curing)

Thiopave (%)	Design Air (%)	ID	Conditioning	Sample Air Voids (%)	Saturation (%)	Failure Load (lb)	Splitting Tensile Strength (psi)	TSR
0	4	1	Conditioned	6.9	66.6	4600	132.49	0.99
0	4	3	Conditioned	6.9	64.8	4350	125.29	
0	4	6	Conditioned	6.3	62.2	4800	138.25	
0	4	2	Unconditioned	6.4	N/A	5200	149.77	
0	4	4	Unconditioned	7.2	N/A	4450	128.17	
0	4	7	Unconditioned	7.0	N/A	4200	120.97	
30	4	2	Conditioned	7.0	63.8	3550	102.25	1.04
30	4	3	Conditioned	7.4	61.4	3050	87.85	
30	4	4	Conditioned	6.7	61.7	3650	105.13	
30	4	1	Unconditioned	7.2	N/A	3350	96.49	
30	4	6	Unconditioned	6.6	N/A	3400	97.93	
30	4	7	Unconditioned	7.3	N/A	3100	89.29	
40	4	1	Conditioned	7.3	63.3	3400	97.93	1.16
40	4	3	Conditioned	6.3	61.3	3850	110.89	
40	4	6	Conditioned	6.6	59.7	3650	105.13	
40	4	2	Unconditioned	7.3	N/A	3550	102.25	
40	4	4	Unconditioned	7.2	N/A	2850	82.09	
40	4	9	Unconditioned	6.3	N/A	3015	86.84	

TABLE B.2 Test Results for TSR Testing (ALDOT Method – With 14 days of Curing)

Thiopave (%)	Design Air (%)	ID	Conditioning	Sample Air Voids (%)	Saturation (%)	Failure Load (lb)	Splitting Tensile Strength (psi)	TSR
30	4	111	Conditioned	7.3	56.2	2350	68.65	0.60
30	4	112	Conditioned	7.1	54.7	2550	74.29	
30	4	113	Conditioned	7.0	58.6	2610	76.04	
30	4	81	Unconditioned	7.1	N/A	4150	120.28	
30	4	85	Unconditioned	7.1	N/A	4400	127.26	
30	4	86	Unconditioned	7.0	N/A	4100	118.72	
40	4	114	Conditioned	7.5	60.6	2550	74.49	0.67
40	4	115	Conditioned	7.6	60.9	2700	78.66	
40	4	116	Conditioned	7.7	57.7	2450	71.26	
40	4	68	Unconditioned	7.4	N/A	3440	99.69	
40	4	69	Unconditioned	6.9	N/A	3960	115.23	
40	4	73	Unconditioned	6.8	N/A	4140	119.94	

TABLE B.3 Test Results for TSR Testing (AASHTO Method – With 14 days of Curing)

Thiopave (%)	Design Air (%)	ID	Conditioning	Sample Air Voids (%)	Saturation (%)	Failure Load (lb)	Splitting Tensile Strength (psi)	TSR
0	4	1	Conditioned	6.5	73.8	4100	120.18	0.87
0	4	3	Conditioned	7.1	71.6	3850	111.72	
0	4	6	Conditioned	6.4	73.9	3900	113.17	
0	4	2	Unconditioned	6.4	N/A	5200	149.77	
0	4	4	Unconditioned	7.2	N/A	4450	128.17	
0	4	7	Unconditioned	7.0	N/A	4200	120.97	
30	4	2	Conditioned	6.7	73.3	3300	95.68	0.71
30	4	3	Conditioned	7.2	70.6	2700	78.13	
30	4	4	Conditioned	7.0	70.1	2950	85.56	
30	4	1	Unconditioned	7.1	N/A	4150	120.28	
30	4	6	Unconditioned	7.1	N/A	4400	127.26	
30	4	7	Unconditioned	7.0	N/A	4100	118.72	
40	4	1	Conditioned	7.0	77.3	3080	89.32	0.73
40	4	3	Conditioned	7.1	73.6	2740	79.49	
40	4	6	Conditioned	7.2	72.4	2620	76.03	
40	4	2	Unconditioned	7.4	N/A	3440	99.69	
40	4	4	Unconditioned	6.9	N/A	3960	115.23	
40	4	9	Unconditioned	6.8	N/A	4140	119.94	

APPENDIX C Dynamic Modulus Test Results

TABLE C.1 Test Results of Dynamic Modulus Testing

Thiopave (%)	Design Air Voids	Curing Time (days)	Sample ID	Test Temperature (^{o}F)	Test Frequency (Hz)	E* (ksi)	Phase Angle (deg)
0	4	2	19	69.98	25	907.9	23.87
0	4	2	19	69.98	10	724.0	26.65
0	4	2	19	69.98	5	603.6	28.35
0	4	2	19	69.98	1	368.8	32.16
0	4	2	19	69.98	0.5	294.7	33.05
0	4	2	19	69.98	0.1	163.5	35.08
0	4	2	19	69.98	0.01	67.7	34.92
0	4	2	20	69.98	25	918.7	25.59
0	4	2	20	69.98	10	713.4	27.77
0	4	2	20	69.98	5	589.9	29.2
0	4	2	20	69.98	1	354.6	32.95
0	4	2	20	69.98	0.5	279.9	33.51
0	4	2	20	69.98	0.1	154.0	34.71
0	4	2	20	69.98	0.01	67.1	34.13
30	3.5	2	23	69.98	25	1386.1	25.27
30	3.5	2	23	69.98	10	1026.4	25.05
30	3.5	2	23	69.98	5	856.0	26.52
30	3.5	2	23	69.98	1	554.5	29.88
30	3.5	2	23	69.98	0.5	453.4	30.45
30	3.5	2	23	69.98	0.1	276.6	31.73
30	3.5	2	23	69.98	0.01	139.4	30.74
30	3.5	2	24	69.98	25	987.1	24.24
30	3.5	2	24	69.98	10	777.4	26.88
30	3.5	2	24	69.98	5	645.4	28.54
30	3.5	2	24	69.98	1	400.9	31.7
30	3.5	2	24	69.98	0.5	320.1	32.1
30	3.5	2	24	69.98	0.1	186.2	32.42
30	3.5	2	24	69.98	0.01	92.8	31.12
30	2	2	25	69.98	25	826.4	24.89
30	2	2	25	69.98	10	639.3	27.61
30	2	2	25	69.98	5	523.4	29.24
30	2	2	25	69.98	1	315.7	32.48
30	2	2	25	69.98	0.5	249.5	33.03
30	2	2	25	69.98	0.1	141.3	33.59
30	2	2	25	69.98	0.01	142.8	46.77
30	2	2	27	69.98	25	925.2	25.12
30	2	2	27	69.98	10	715.9	27.88
30	2	2	27	69.98	5	588.9	29.33
30	2	2	27	69.98	1	354.9	32.36
30	2	2	27	69.98	0.5	279.6	32.6
30	2	2	27	69.98	0.1	159.1	32.68

Thiopave (%)	Design Air Voids	Curing Time (days)	Sample ID	Test Temperature (^{o}F)	Test Frequency (Hz)	E* (ksi)	Phase Angle (deg)
30	2	2	27	69.98	0.01	75.0	30.66
40	3.5	2	34	69.98	25	1120.3	21.15
40	3.5	2	34	69.98	10	904.0	24.19
40	3.5	2	34	69.98	5	760.9	26.02
40	3.5	2	34	69.98	1	492.0	29.59
40	3.5	2	34	69.98	0.5	402.5	30.39
40	3.5	2	34	69.98	0.1	246.7	31.15
40	3.5	2	34	69.98	0.01	130.9	29.6
40	3.5	2	35	69.98	25	1241.5	19.47
40	3.5	2	35	69.98	10	1009.9	22.26
40	3.5	2	35	69.98	5	859.1	23.95
40	3.5	2	35	69.98	1	577.1	27.35
40	3.5	2	35	69.98	0.5	475.4	28.27
40	3.5	2	35	69.98	0.1	304.6	29.56
40	3.5	2	35	69.98	0.01	168.8	28.66
40	2	2	37	69.98	25	1187.1	23.42
40	2	2	37	69.98	10	924.0	25.85
40	2	2	37	69.98	5	769.7	27.46
40	2	2	37	69.98	1	487.6	30.85
40	2	2	37	69.98	0.5	392.0	31.43
40	2	2	37	69.98	0.1	235.4	31.65
40	2	2	37	69.98	0.01	118.0	30.04
40	2	2	39	69.98	25	1061.4	28.76
40	2	2	39	69.98	10	769.4	27.08
40	2	2	39	69.98	5	635.4	28.72
40	2	2	39	69.98	1	392.5	32.04
40	2	2	39	69.98	0.5	314.4	32.51
40	2	2	39	69.98	0.1	184.2	32.72
40	2	2	39	69.98	0.01	91.3	30.36
0	4	17	2	69.98	25	1049.1	22.89
0	4	17	2	69.98	10	818.7	25.44
0	4	17	2	69.98	5	678.5	26.94
0	4	17	2	69.98	1	421.3	30.91
0	4	17	2	69.98	0.5	335.9	31.93
0	4	17	2	69.98	0.1	190.3	33.99
0	4	17	2	69.98	0.01	79.8	34.07
0	4	23	2	39.92	10	2139.5	12.52
0	4	23	2	39.92	5	1952.6	13.59
0	4	23	2	39.92	1	1525.5	16.47
0	4	23	2	39.92	0.5	1342.8	17.83
0	4	23	2	39.92	0.1	971.6	21.68
0	4	23	2	39.92	0.01	599.7	26.23
0	4	24	2	69.98	10	847.7	25.05
0	4	24	2	69.98	5	718.4	26.16
0	4	24	2	69.98	1	463.0	29.87
0	4	24	2	69.98	0.5	378.7	30.51

Thiopave (%)	Design Air Voids	Curing Time (days)	Sample ID	Test Temperature (^{o}F)	Test Frequency (Hz)	E* (ksi)	Phase Angle (deg)
0	4	24	2	69.98	0.1	212.8	32.42
0	4	24	2	69.98	0.01	86.3	33.13
0	4	25	2	114.98	10	106.4	43.45
0	4	25	2	114.98	5	76.9	40.19
0	4	25	2	114.98	1	34.9	39.06
0	4	25	2	114.98	0.5	26.6	36.84
0	4	25	2	114.98	0.1	14.8	33.74
0	4	25	2	114.98	0.01	8.1	30.5
0	4	15	11	69.98	25	913.7	23.69
0	4	15	11	69.98	10	728.7	26.14
0	4	15	11	69.98	5	602.6	27.81
0	4	15	11	69.98	1	369.6	31.48
0	4	15	11	69.98	0.5	293.7	32.38
0	4	15	11	69.98	0.1	163.7	33.81
0	4	15	11	69.98	0.01	65.0	33.28
0	4	21	11	39.92	10	1963.4	13.89
0	4	21	11	39.92	5	1787.6	14.37
0	4	21	11	39.92	1	1380.3	17.4
0	4	21	11	39.92	0.5	1208.3	18.77
0	4	21	11	39.92	0.1	868.5	22.45
0	4	21	11	39.92	0.01	518.1	26.77
0	4	22	11	69.98	10	759.3	26.57
0	4	22	11	69.98	5	630.0	27.1
0	4	22	11	69.98	1	393.8	29.95
0	4	22	11	69.98	0.5	314.4	30.48
0	4	22	11	69.98	0.1	178.3	31.62
0	4	22	11	69.98	0.01	74.5	31.27
0	4	23	11	114.98	10	93.5	44.96
0	4	23	11	114.98	5	73.5	39.93
0	4	23	11	114.98	1	33.2	38.3
0	4	23	11	114.98	0.5	24.8	36.12
0	4	23	11	114.98	0.1	14.1	33.06
0	4	23	11	114.98	0.01	7.4	31.62
30	3.5	17	13	69.98	25	2124.5	23.67
30	3.5	17	13	69.98	10	1294.0	19.78
30	3.5	17	13	69.98	5	1104.3	21.69
30	3.5	17	13	69.98	1	759.6	25.26
30	3.5	17	13	69.98	0.5	636.3	26.07
30	3.5	17	13	69.98	0.1	419.2	27.92
30	3.5	17	13	69.98	0.01	229.2	27.66
30	3.5	23	13	39.92	10	2652.5	9.81
30	3.5	23	13	39.92	5	2417.2	11.08
30	3.5	23	13	39.92	1	1970.5	13.34
30	3.5	23	13	39.92	0.5	1796.6	14.26
30	3.5	23	13	39.92	0.1	1375.8	17.85
30	3.5	23	13	39.92	0.01	921.7	22.07

Thiopave (%)	Design Air Voids	Curing Time (days)	Sample ID	Test Temperature (^{o}F)	Test Frequency (Hz)	E* (ksi)	Phase Angle (deg)
30	3.5	24	13	69.98	10	1267.9	20.21
30	3.5	24	13	69.98	5	1094.9	21.71
30	3.5	24	13	69.98	1	764.1	24.94
30	3.5	24	13	69.98	0.5	649.3	25.69
30	3.5	24	13	69.98	0.1	423.2	27.57
30	3.5	24	13	69.98	0.01	225.7	27.61
30	3.5	25	13	114.98	10	246.9	35.33
30	3.5	25	13	114.98	5	194.1	32.83
30	3.5	25	13	114.98	1	111.8	31.21
30	3.5	25	13	114.98	0.5	85.8	30.24
30	3.5	25	13	114.98	0.1	57.2	27.89
30	3.5	25	13	114.98	0.01	37.0	25.19
30	3.5	15	14	69.98	25	1493.7	18.52
30	3.5	15	14	69.98	10	1192.8	20.81
30	3.5	15	14	69.98	5	998.0	22.91
30	3.5	15	14	69.98	1	679.8	26.99
30	3.5	15	14	69.98	0.5	567.5	28.34
30	3.5	15	14	69.98	0.1	364.8	30.44
30	3.5	15	14	69.98	0.01	195.2	30.08
30	3.5	21	14	39.92	10	2582.0	10.09
30	3.5	21	14	39.92	5	2403.1	10.82
30	3.5	21	14	39.92	1	1975.8	12.75
30	3.5	21	14	39.92	0.5	1784.8	13.67
30	3.5	21	14	39.92	0.1	1381.2	16.55
30	3.5	21	14	39.92	0.01	905.8	21.61
30	3.5	22	14	69.98	10	1147.7	21.52
30	3.5	22	14	69.98	5	987.7	23.14
30	3.5	22	14	69.98	1	683.4	26.71
30	3.5	22	14	69.98	0.5	577.4	27.6
30	3.5	22	14	69.98	0.1	368.1	29.84
30	3.5	22	14	69.98	0.01	190.0	29.52
30	3.5	23	14	114.98	10	206.4	38.59
30	3.5	23	14	114.98	5	166.6	35.46
30	3.5	23	14	114.98	1	90.5	33.69
30	3.5	23	14	114.98	0.5	69.5	32.65
30	3.5	23	14	114.98	0.1	44.4	30.74
30	3.5	23	14	114.98	0.01	28.9	25.99
30	2	15	5	69.98	25	1377.4	20.76
30	2	15	5	69.98	10	1102.9	23.39
30	2	15	5	69.98	5	923.0	25.18
30	2	15	5	69.98	1	603.4	28.65
30	2	15	5	69.98	0.5	490.7	29.42
30	2	15	5	69.98	0.1	302.3	30.75
30	2	15	5	69.98	0.01	156.9	29.87
30	2	23	5	39.92	10	2296.1	11.77
30	2	23	5	39.92	5	2092.6	12.69

Thiopave (%)	Design Air Voids	Curing Time (days)	Sample ID	Test Temperature (^{o}F)	Test Frequency (Hz)	E* (ksi)	Phase Angle (deg)
30	2	23	5	39.92	1	1638.5	15.71
30	2	23	5	39.92	0.5	1453.1	17.12
30	2	23	5	39.92	0.1	1074.3	20.96
30	2	23	5	39.92	0.01	717.6	24.08
30	2	24	5	69.98	10	1080.0	23.4
30	2	24	5	69.98	5	919.8	24.67
30	2	24	5	69.98	1	607.4	28.04
30	2	24	5	69.98	0.5	500.1	28.77
30	2	24	5	69.98	0.1	302.1	30.25
30	2	24	5	69.98	0.01	148.4	29.55
30	2	25	5	114.98	10	189.6	38.53
30	2	25	5	114.98	5	145.5	37.89
30	2	25	5	114.98	1	71.5	36.98
30	2	25	5	114.98	0.5	55.8	34.95
30	2	25	5	114.98	0.1	32.5	32.23
30	2	25	5	114.98	0.01	18.8	28.66
30	2	15	6	69.98	25	1359.0	19.93
30	2	15	6	69.98	10	1089.1	22.7
30	2	15	6	69.98	5	911.9	24.6
30	2	15	6	69.98	1	602.5	28.18
30	2	15	6	69.98	0.5	496.9	28.98
30	2	15	6	69.98	0.1	309.8	30.62
30	2	15	6	69.98	0.01	160.0	30.45
30	2	23	6	39.92	10	2586.9	11.62
30	2	23	6	39.92	5	2391.1	12.67
30	2	23	6	39.92	1	1912.5	15.16
30	2	23	6	39.92	0.5	1709.1	16.41
30	2	23	6	39.92	0.1	1276.0	19.88
30	2	23	6	39.92	0.01	793.8	24.71
30	2	24	6	69.98	10	1103.0	22.79
30	2	24	6	69.98	5	947.5	24.31
30	2	24	6	69.98	1	637.7	27.88
30	2	24	6	69.98	0.5	528.5	28.68
30	2	24	6	69.98	0.1	322.9	30.65
30	2	24	6	69.98	0.01	157.1	29.95
30	2	25	6	114.98	10	180.3	43.36
30	2	25	6	114.98	5	139.3	37.17
30	2	25	6	114.98	1	73.7	35.26
30	2	25	6	114.98	0.5	58.2	33.5
30	2	25	6	114.98	0.1	36.1	31.63
30	2	25	6	114.98	0.01	22.9	29.05
40	3.5	15	7	69.98	25	1762.6	19.87
40	3.5	15	7	69.98	10	1412.1	20.99
40	3.5	15	7	69.98	5	1189.0	23.03
40	3.5	15	7	69.98	1	812.2	27.15
40	3.5	15	7	69.98	0.5	681.8	27.96

Thiopave (%)	Design Air Voids	Curing Time (days)	Sample ID	Test Temperature (^{o}F)	Test Frequency (Hz)	E* (ksi)	Phase Angle (deg)
40	3.5	15	7	69.98	0.1	441.1	29.63
40	3.5	15	7	69.98	0.01	239.2	29.3
40	3.5	18	8	69.98	25	1569.7	17
40	3.5	18	8	69.98	10	1312.3	19.42
40	3.5	18	8	69.98	5	1135.9	21.2
40	3.5	18	8	69.98	1	789.3	24.43
40	3.5	18	8	69.98	0.5	668.3	25.03
40	3.5	18	8	69.98	0.1	427.0	27.76
40	3.5	18	8	69.98	0.01	220.2	27.37
40	2	16	15	69.98	25	1418.2	19.54
40	2	16	15	69.98	10	1121.9	22.4
40	2	16	15	69.98	5	942.7	24.49
40	2	16	15	69.98	1	622.1	28.33
40	2	16	15	69.98	0.5	503.6	29.12
40	2	16	15	69.98	0.1	310.5	30.52
40	2	16	15	69.98	0.01	157.8	29.92
40	2	15	17	69.98	25	1587.1	17.71
40	2	15	17	69.98	10	1317.5	19.92
40	2	15	17	69.98	5	1128.7	21.99
40	2	15	17	69.98	1	772.9	26.02
40	2	15	17	69.98	0.5	647.3	26.89
40	2	15	17	69.98	0.1	414.7	28.74
40	2	15	17	69.98	0.01	217.8	28.42
40	3.5	56	7	39.92	10	2830.6	10.44
40	3.5	56	7	39.92	5	2630.4	11.11
40	3.5	56	7	39.92	1	2162.1	13.09
40	3.5	56	7	39.92	0.5	1962.2	14.13
40	3.5	56	7	39.92	0.1	1522.0	17.25
40	3.5	56	7	39.92	0.01	1031.5	21.91
40	3.5	56	8	39.92	10	3020.6	10.71
40	3.5	56	8	39.92	5	2796.3	11.96
40	3.5	56	8	39.92	1	2290.6	13.37
40	3.5	56	8	39.92	0.5	2038.5	14.56
40	3.5	56	8	39.92	0.1	1560.6	17.18
40	3.5	56	8	39.92	0.01	1039.6	21.98
40	3.5	57	7	69.98	10	1398.3	19.85
40	3.5	57	7	69.98	5	1224.6	21.17
40	3.5	57	7	69.98	1	852.4	25.12
40	3.5	57	7	69.98	0.5	722.4	25.95
40	3.5	57	7	69.98	0.1	466.7	28.3
40	3.5	57	7	69.98	0.01	244.5	28.79
40	3.5	57	8	69.98	10	1515.9	20.89
40	3.5	57	8	69.98	5	1263.6	22.34
40	3.5	57	8	69.98	1	875.3	25.75
40	3.5	57	8	69.98	0.5	743.3	26.28
40	3.5	57	8	69.98	0.1	481.4	28.04

Thiopave (%)	Design Air Voids	Curing Time (days)	Sample ID	Test Temperature (^{o}F)	Test Frequency (Hz)	E* (ksi)	Phase Angle (deg)
40	3.5	57	8	69.98	0.01	252.9	30.19
40	3.5	58	7	114.98	10	361.7	37.2
40	3.5	58	7	114.98	5	307.6	34.78
40	3.5	58	7	114.98	1	176.4	33.36
40	3.5	58	7	114.98	0.5	136.3	31.98
40	3.5	58	7	114.98	0.1	77.8	29.48
40	3.5	58	7	114.98	0.01	37.7	26.2
40	3.5	58	8	114.98	10	285.9	35.41
40	3.5	58	8	114.98	5	237.9	33.13
40	3.5	58	8	114.98	1	134.2	31.79
40	3.5	58	8	114.98	0.5	104.1	30.97
40	3.5	58	8	114.98	0.1	62.7	29.96
40	3.5	58	8	114.98	0.01	33.5	25.86
40	2	54	15	39.92	10	2650.0	15.07
40	2	54	15	39.92	5	2482.0	14.39
40	2	54	15	39.92	1	1971.8	16.1
40	2	54	15	39.92	0.5	1759.2	17.06
40	2	54	15	39.92	0.1	1311.6	20.16
40	2	54	15	39.92	0.01	824.8	24.55
40	2	53	17	39.92	10	3442.2	15.53
40	2	53	17	39.92	5	2586.7	11.31
40	2	53	17	39.92	1	2130.6	12.9
40	2	53	17	39.92	0.5	1938.3	14.02
40	2	53	17	39.92	0.1	1504.5	16.84
40	2	53	17	39.92	0.01	992.5	21.67
40	2	55	15	69.98	10	1205.1	24.66
40	2	55	15	69.98	5	986.1	23.91
40	2	55	15	69.98	1	672.0	27.12
40	2	55	15	69.98	0.5	563.2	27.69
40	2	55	15	69.98	0.1	350.6	29.83
40	2	55	15	69.98	0.01	171.6	30.04
40	2	54	17	69.98	10	1338.3	21.57
40	2	54	17	69.98	5	1140.4	22.05
40	2	54	17	69.98	1	795.7	25.37
40	2	54	17	69.98	0.5	677.3	26.09
40	2	54	17	69.98	0.1	438.2	28.55
40	2	54	17	69.98	0.01	227.6	29.34
40	2	56	15	114.98	10	248.3	37.42
40	2	56	15	114.98	5	169.3	35.6
40	2	56	15	114.98	1	85.2	35.32
40	2	56	15	114.98	0.5	63.9	34.08
40	2	56	15	114.98	0.1	36.3	32.23
40	2	56	15	114.98	0.01	18.7	28.28
40	2	55	17	114.98	10	291.4	36
40	2	55	17	114.98	5	222.1	34.14
40	2	55	17	114.98	1	117.5	33.9

Thiopave (%)	Design Air Voids	Curing Time (days)	Sample ID	Test Temperature (^{o}F)	Test Frequency (Hz)	E* (ksi)	Phase Angle (deg)
40	2	55	17	114.98	0.5	88.0	33.06
40	2	55	17	114.98	0.1	49.9	31.78
40	2	55	17	114.98	0.01	26.0	28.23

APPENDIX D Flow Number Test Results

TABLE D.1 Summary of Flow Number Test Results

%Thiopave	Design Air Voids	Specimen ID	Air Voids of Specimen	Flow Number - Power Model (Cycles)	Microstrain at Flow Point - Power Model	Flow Number-Francken Model (Cycles)	Microstrain at Flow Point - Francken Model
0	4	2	7.3	34	19933	41	22729
0	4	11	7.2	31	27629	35	29567
30	2	5	6.5	259	17674	336	20707
30	2	6	6.8	238	20763	298	23815
30	3.5	13	7.2	281	17784	385	21532
30	3.5	14	7.1	212	19359	318	24293
40	2	15	7.3	143	19298	188	23127
40	2	17	6.6	161	16643	262	22504
40	2	37	6.7	166	18134	176	18604
40	2	39	6.8	157	19818	159	19945
40	3.5	7	6.6	290	12128	593	18723
40	3.5	8	7	233	14317	417	20809
40	3.5	34	7.1	241	13755	287	14726
40	3.5	35	7.3	262	17339	244	16791

TABLE D.2 Average Flow Number Values (by Mix Design)

% Thiopave	Design Air Voids	Average Flow Number - Power Model (Cycles)	Average Flow Number - Francken Model (Cycles)
0	4	32	38
30	2	249	317
30	3.5	247	352
40	2	157	196
40	3.5	257	385

APPENDIX E Asphalt Pavement Analyzer Test Results

TABLE E.1 Summary of APA Test Results

%Thiopave	Sample ID	Air Voids (%)	Manual Rut Depth		Automated Rut Depth	
			Individual (mm)	Average (mm)	Individual (mm)	Average (mm)
0	1	7.2	8.79	9.89	N/A	N/A
0	7	6.8	8.67		N/A	
0	5	6.6	12.02		N/A	
0	3	7.0	10.06		N/A	
30	1	6.8	5.51	5.39	3.09	3.45
30	7	6.9	5.41		3.13	
30	3	7.3	5.83		3.76	
30	5	7.0	4.04		3.38	
30	6	7.1	5.91		4.01	
30	4	7.0	5.62		3.35	
40	5	7.1	5.43	5.78	3.45	4.66
40	7	6.8	5.31		4.08	
40	8	6.9	4.75		4.22	
40	4	6.9	5.28		4.02	
40	3	6.8	6.91		6.24	
40	6	7.2	7.01		5.97	
30	2	30	7.5	7.11	4.39	5.20
30	2	35	7.5		5.09	
30	2	36	7.5		4.99	
30	2	37	7.5		5.55	
30	2	38	7.6		5.91	
30	2	39	7.5		5.30	
40	2	26	6.8	5.50	4.428	4.27
40	2	29	7.4		4.343	
40	2	31	6.9		4.525	
40	2	32	7.5		3.979	
40	2	33	7.4		4.331	
40	2	34	7.0		4.006	

APPENDIX F Hamburg Wheel-Tracking Test Results

TABLE F.1 Summary of Hamburg Raw Data Analysis

Mix	Sample ID	Air Voids of Cut Sample (%)	Slope of Steady-State Rutting Curve (mm/cycle)	Rutting Rate (mm/hr)	Total Rut Depth (mm) (Based on Rate)	Stripping Inflection Point (cycles)
0% Thiopave Design	1A	8.4	0.002048	5.161	20.479	None
	1B	8.3				
0% Thiopave Design	2A	8.6	0.003145	7.925	31.448	None
	2B	5.8				
0% Thiopave Design	3A	8.7	0.002433	6.131	24.328	6800
	3B	7.0				
0% Thiopave Design	6A	8.2	0.002193	5.526	21.929	None
	6B	7.4				
30% Thiopave Design	1A	9.3	0.000540	1.361	5.400	3600
	1B	8.4				
30% Thiopave Design	2A	7.9	0.000300	0.756	3.000	4500
	2B	7.3				
30% Thiopave Design	9A	7.9	0.000520	1.310	5.200	4900
	9B	7.4				
30% Thiopave Design	10A	7.8	0.001370	3.452	13.699	5250
	10B	8.1				
40% Thiopave Design	1A	9.7	0.000680	1.714	6.800	4300
	1B	7.6				
40% Thiopave Design	2A	8.9	0.000593	1.494	5.930	5250
	2B	6.2				
40% Thiopave Design	11A	8.1	0.000800	2.016	7.999	2850
	11B	7.5				
40% Thiopave Design	12A	8.2	0.000910	2.293	9.099	2450
	12B	6.5				

30% Thiopave Rich	13A	6.8	0.00125	3.150	12.499	5550
	13B	7.3				
30% Thiopave Rich	15A	8.0	0.00168	4.234	16.799	3550
	15B	6.4				
30% Thiopave Rich	17A	7.1	0.000788	1.986	7.879	4875
	18A	7.9				
40% Thiopave Rich	14A	6.7	0.00114	2.873	11.399	3600
	20B	7.3				
40% Thiopave Rich	16A	7.4	0.00103	2.596	10.299	3900
	16B	6.8				
40% Thiopave Rich	19A	7.1	0.00184	4.637	18.399	5600
	19B	7.1				

APPENDIX G Bending Beam Fatigue Test Results

TABLE G.1 Summary of Bending Beam Fatigue Test Results

Thiopave (%)	Design Air Voids (%)	Sample ID	Sample Air Voids (%)	Strain Level (ms)	Cycles to Failure (ASTM D7460)	Cycles to Failure (AASHTO T321)
0	4	63	6.4	400	185,490	141,250
		64	6.6	400	364,470	254,090
		66	6.7	600	35,120	17,600
		34	6.4	600	28,500	24,540
		86	6.4	200	3,821,390	3,432,060
		99	7.1	200	6,606,930	6,674,890
30	3.5	74	7.5	400	29,890	24,990
		76	7.4	400	66,740	37,820
		25	7.9	600	11,680	5,200
		26	6.8	600	8,580	6,130
		27	7.7	200	1,944,860	1,810,410
		77	7.8	200	2,854,660	1,036,460
30	2	36	6.5	400	86,870	84,240
		37	6.6	400	190,540	106,330
		51	5.7	600	31,780	12,300
		52	6.4	600	9,130	8,030
		53	6.5	200	3,841,000	4,105,190
		54	6.8	200	7,432,090	6,025,590
40	3.5	59	7.3	400	48,720	31,540
		60	7.6	400	44,440	32,850
		47	6.3	600	3,610	2,970
		48	7.2	600	13,420	5,770
		49	7.1	200	2,563,820	2,187,760
		50	6.9	200	1,915,230	2,026,120
40	2	55	6.5	400	189,810	62,930
		57	6.5	400	76,440	54,950
		58	6.5	600	3,480	3,170
		68	6.3	600	10,710	7,950
		69	6.8	200	2,524,770	2,165,480
		70	6.4	200	628,540	683,910